STUDIES
IN THE MEASUREMENT, FORM AND INTERPRETATION
OF SOME ELECTRICAL PROPERTIES
OF NORMAL AND PATHOLOGICAL HUMAN SKIN
IN VIVO

A thesis submitted to the Faculty of Clinical Medicine
in the University of Oxford
for the degree of Doctor of Philosophy



Volume 2

David Charles Salter
Merton College
Easter 1981

PART IV: INTERPRETING THE MEASUREMENTS

Chapter 11. A REVIEW OF SOME INTERPRETATIONS OF THE LINEAR AND POSSIBLY ONLY SLOWLY TIME-VARIANT ELECTRICAL PROPERTIES OF SKIN

11.1 Introduction

We have seen in Sections 4.2 and 9.5, amongst others, that the skin obeys the Cole complex impedance equation

$$Z = R_\infty + \frac{R_o - R_\infty}{1 + (j\omega\tau_p)^{1-m}} \qquad (11.1.1)$$

However, it is likely that a great deal more clinical benefit could accrue from investigations of skin impedance if the reasons for this behaviour were understood. We might then be able to non-invasively obtain valuable physiological information from the values of the parameters of the Cole equation which best fitted the clinical data.

This Chapter is therefore concerned with reviewing and testing the various interpretations of the Cole equation which have appeared in the literature of skin electrophysiology. It then goes beyond these interpretations to review and test what are likely to be better hypotheses. The review as a whole is long and detailed because to my knowledge nothing like it has appeared before, and there is therefore a lot of ground to cover.

During the course of the Chapter it will be useful to recall from Section 4.2 that the Cole equation (11.1.1) corresponds to complex conductivities of the form

$$\sigma^* = \sigma_o + \frac{\sigma_o \left[1 - \frac{\sigma_o}{\sigma_\infty}\right](j\omega\tau_p)^{1-m}}{1 + \frac{\sigma_o}{\sigma_\infty}(j\omega\tau_p)^{1-m}} \qquad (11.1.2)$$

which as $\sigma_\infty/\sigma_o \to \infty$, corresponding to $R_\infty/R_o \to o$, tends to reduce to

$$\sigma^* = \sigma_o + \sigma_o (j\omega\tau_p)^{1-m} \qquad (11.1.3)$$

Bearing this in mind will be useful since the results obtained by investigators of physical systems other than skin have very often been expressed in forms like (11.1.2) or (11.1.3), and it may be helpful to point out explicitly how closely related these are to the Cole equation which we ourselves are concerned to interpret.

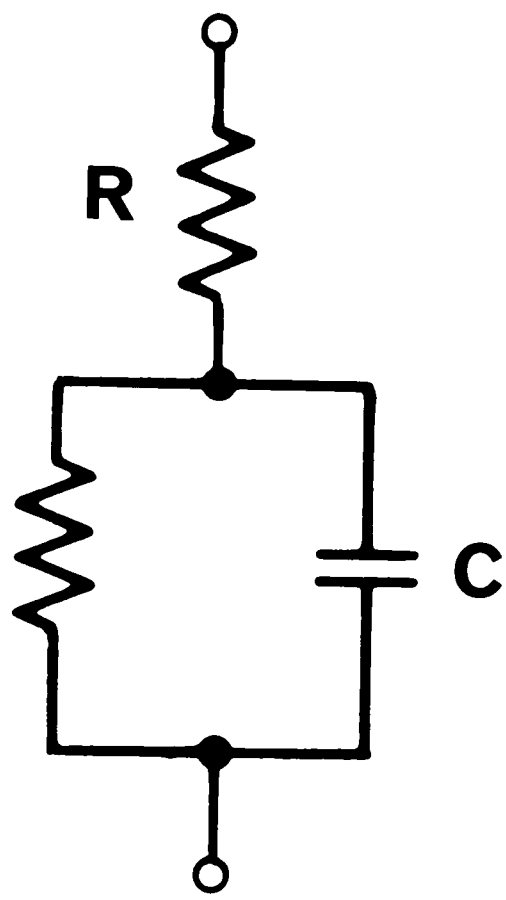


Fig. 11.2.I

11.2 The historical development of the small-signal equivalent circuits of human skin

At the beginning of this review of interpretations of the linear electrical behaviour of skin, it may be helpful to consider how the Cole equation which so well describes this behaviour, and also the equivalent circuits which model it, were developed. There are of course two alternative equivalent circuits with no intrinsic reason for choosing between them, and even in the early days it was relatively easy to deduce this much. However, the development of the particular circuits discussed in Section 4.2 as the two forms which best modelled the behaviour of skin was a process which took many years.

In 1907, Lapicque suggested the network of Fig. 11.2.I as an equivalent circuit for nerve membrane. Following the ideas of Nernst, (see e.g. Lucas, 1910; Cole, 1933b), the criterion for excitation was the achievement of a certain "threshold" potential difference across the capacitor C.

Philippson in 1921 said that a circuit such as that of Lapicque could also model the A.C. properties of various biological tissues, provided however that the capacitance C depended upon frequency ω according to

$$C = B\omega^{(\alpha-1)} \qquad (11.2.1)$$

where B and α are constants. (N.B. to maintain consistency of notation, the α here equals one minus the α used by Philippson.)

Eventually, in 1928, Gildemeister applied these ideas to human skin, saying that its A.C. properties could be modelled by the Lapicque circuit if $r \gg R$, and C was replaced by a complex impedance of constant phase angle between 0 and 90 degrees. This is an extension of Philippson's idea. Gildemeister construed the need for such a complex impedance in the equivalent circuit as evidence of electrochemical polarization phenomena

in the tissue. (Indeed such an impedance is usually referred to as a "polarization impedance" because it was first employed to represent such electrochemical phenomena.) He also plotted impedance loci of skin on the complex impedance plane, obtaining in each case a more or less straight line inclined at an angle of $(\alpha\pi/2)$ to the equivalent series resistance axis and intercepting this axis at a value of R.

Cole however stated (1928) that for arbitrary positive r and R, the impedance locus of the Lapicque-Gildemeister circuit describes a minor arc of a circle in the complex impedance plane, intercepting the equivalent series resistance axis at values of R and (R+r). Consequently in the case of infinite r, the chord length (R+r)-R is infinite and the arc becomes an inclined straight line, as found by Gildemeister. (Incidentally the m used by Cole equals $\tan\left[(1-\alpha)\frac{\pi}{2}\right]$ in the notation used here. For reasons which will become clear I follow other workers in using a different m defined by $m = 1-\alpha$.) In 1932 Cole published an analytic proof of his geometric assertion of 1928, and also demonstrated that the complex impedance loci of many biological tissues were indeed well approximated by minor arcs of circles. It is interesting in the present context however that Cole was inspired to do this work by the results Gildemeister had obtained for human skin, and he was correspondingly pleased to talk to me about how it all happened.

Figure 3b of a later paper by Cole (Cole, 1933a) presented the first picture of the Lapicque circuit incorporating the constant-phase-angle "polarization impedance" suggested by Gildemeister, and in 1934, conforming to the notation in the work of Fricke (1932), Cole gave analytic expression to this impedance as

$$z(\omega) = z_1(j\omega)^{-\alpha} \qquad (11.2.2)$$

where z_1 and α are constants, and $j = \sqrt{-1}$. However, the polarization impedance can be written much more elegantly as

$$z_p(\omega) = R_1(j\omega\tau)^{-\alpha} \qquad (11.2.3)$$

where R_1 is a constant which now has the units of impedance, i.e. ohms, and the product inside the brackets, which has to be raised to a non-integer power, is now dimensionless due to the introduction of the time constant (or relaxation time) τ. Equations (11.2.1), (11.2.2) and (11.2.3) are of course mutually compatible, as has been demonstrated elsewhere in a review of the rather confusing notation used in the literature of biological polarization impedance (see Salter, 1979, Section 5, or Section 3.8 of this thesis). Cole first published the improved expression (11.2.3) in 1937 (Cole and Jahn, 1937, p.268), and it is implicit in the form of the "Cole equation" (Cole, 1940, p.117), which gives the complex impedance of the finally resulting Lapicque-Gildemeister-Cole equivalent circuit for biological tissue. However, it was not until much later that this circuit and its alternative (cf. Cole, 1928) were published for the first time in detail (Salter, 1979, or see Section 4.2 of this thesis).

It is interesting that these studies of the complex impedance loci of biological tissues later provided the foundation for analysing the complex permittivity loci Cole's younger brother obtained for various dielectric materials. The loci when plotted on the complex permittivity plane were (to the Cole brothers' delight) well represented by minor arcs of circles, and so could immediately be described by the now world-famous Cole-Cole equation (Cole and Cole, 1941) which is an algebraic analogue of the earlier Cole equation describing biological impedances. Moreover, although the physics was different, the equivalent circuit for the dielectric case still involved a polarization impedance. Unfortunately however the attempt

to understand this fact in physical terms continues to this day, research adding all the time to the already enormous number of alternative hypotheses.

I mention these latter aspects just to show that insofar as dielectric theory contributes to the interpretation of skin impedance phenomena, it is only repaying an old debt!

11.3 Some analogous phenomenologies

11.3.a Non-Debye dielectric relaxation

The classical Debye dielectric (see e.g. Daniel,1967, Ch.2) is a system containing only one relaxation time and whose complex relative permittivity ε^*r obeys an equation of the form

$$\varepsilon_r^* = \varepsilon_\infty + \frac{\varepsilon_s - \varepsilon_\infty}{1 + j\omega\tau} \qquad (11.3.a.1)$$

which describes a semicircular locus on the complex permittivity plane.

This form of dielectric relaxation appears however to be the exception rather than the rule (Böttcher and Bordewijk, 1978, Section 62), and certainly most solids at least show dielectric relaxation behaviour which can be termed "non-Debye" in that the complex permittivity locus is not a semicircle.

In such cases the system is usually assumed to have more than one relaxation time, the various values of relaxation time being (simultaneously) present in the material according to some probability distribution known as the "distribution of relaxation times" (DRT), as was discussed in Section 3.7.

The various forms of non-Debye dielectric relaxation have recently been reviewed very comprehensively by Böttcher and Bordewijk (1978, Ch.IX) and the only type which is relevant to us at the moment is that introduced by Cole and Cole in 1941.

A "Cole-Cole dielectric" is one whose complex relative permittivity obeys an equation of the form

$$\varepsilon_r^* = \varepsilon_\infty + \frac{(\varepsilon_s - \varepsilon_\infty)}{1 + (j\omega\tau)^{1-\alpha}} \qquad (11.3.a.2)$$

which describes a locus on the complex permittivity plane which is a minor arc of a circle, becoming a Debye semicircle in the case of $\alpha = o$.

It may be noted that equation (11.3.a.2) is an algebraic analogue of the Cole complex impedance equation, and this is no accident, as was pointed out in Section 11.2. However, a system obeying (11.3.a.2) will NOT have a complex impedance obeying the Cole equation, and vice versa, as may be shown by considering equivalent circuits or directly by the use of an algebraic transformation, the one following being for a unit cube of material:

$$Z = \frac{1}{j\omega\varepsilon_o\varepsilon_r^*} \qquad (11.3.a.3)$$

The Cole-Cole dielectric is introduced here therefore merely as a phenomenological analogue, although if we knew something about the physical reasons for this particular form of non-Debye dielectric relaxation, it might by analogy give us some insight into the physical reasons for the Cole type of complex impedance behaviour. Sadly, however, despite no doubt hundreds of man-years of effort (not least by the Cole brothers themselves; cf. Cole, 1965), there is still no fundamental physical interpretation of Cole-Cole dielectric relaxation, although there are at least glimmerings of interpretation for some of the other forms of non-Debye dielectric relaxation.

11.3.b The work of Jonscher

In the latter part of the seventies the work of a group led by Professor A.K. Jonscher of Chelsea College, London, raised hopes amongst investigators of dielectric phenomenology that perhaps at last a single underlying mechanism for non-Debye relaxation could be found, since this was what was claimed in a long series of papers in "Nature" and other journals (see e.g. Jonscher, 1977).

These papers however were presumably rather hastily written because they contain so many conceptual naiveties. I put right some of the early ones by writing to "Nature" myself (Salter, 1978a), but unfortunately found that I had strained at a gnat and swallowed a camel by assuming that the Cole-Cole energy criterion (Salter, 1978a) which applies in the frequency domain still applies in the time domain, whereas of course it does not (c.f. Section 3.8). I am very grateful to Professor Brendan Scaife of Trinity College, Dublin, for bringing this to my attention, thus saving me from embarrassing myself in the Proceedings of the Royal Society.

Since that time Professor Scaife and I have kept a close watch on the publications from Professor Jonscher's group. They too later dropped the Cole-Cole energy criterion and quietly reverted to something like the old ideas of distributions of activation energy, buried within a rather esoteric model involving transitions between so-called "correlated states" defined in a certain way (cf. Ngai et al., 1979). States meeting the necessary criteria are claimed to be extremely common.

However, the theory insofar as it has been published to date (a pre-print of Jonscher, 1981), contains fundamental mathematical inconsistencies, as can be seen from the following.

Jonscher (1981, eqn.76) derives a function K(t) defined by

$$K(t) = \exp\{-n[\gamma + \ln(i\zeta t) + Ei(i\zeta t)]\} \qquad (11.3.b.1)$$

with n a constant, γ equal to Euler's constant, i equal to the square root of minus one, ζt a dimensionless number, and Ei the exponential integral function of complex argument. This K(t) is proportional to a hazard function in the sense of Salter (1978c, or see Appendix H) and indeed Jonscher proceeds to apply it in this sense.

Now, in the case of dielectric relaxation, a hazard function h(t) is related to the macroscopic decay function $\Phi(t)$, itself determined by the microscopic dipole correlation function $\phi(t)$, by the probability density function f(t) where (Salter, 1978c, or see Appendix H)

$$f(t) = h(t) \exp\left[-\int_0^t h(u)\,du\right] = -\frac{d\Phi(t)}{dt} \qquad (11.3.b.2)$$

and

$$\frac{\varepsilon_p^*(\omega) - \varepsilon_\infty}{\varepsilon_s - \varepsilon_\infty} = L[f(t)] \qquad (11.3.b.3)$$

where L denotes Laplace transformation. Jonscher's equations (81b) and (82) are equivalent to (11.3.b.2). However, if (11.3.b.2) and (11.3.b.3) are to make any sense the hazard function h(t) must be purely real, i.e. not complex, and yet Jonscher's h(t) can from (11.3.b.1) be written

$$K(t) = (i\zeta t)^{-n} \exp[-n(\gamma + Ei(i\zeta t))] \qquad (11.3.b.4)$$

and this leads to a complex hazard function, which is nonsense. However, most of Jonscher's subsequent equations do not apply the K(t) of (11.3.b.4) correctly anyway, and so the mathematical absurdity is not obvious.

Professor Scaife agrees with this assessment of the situation, and Professor Jonscher has said that he will ask Dr Ngai to investigate these complaints.

We should probably conclude then that far from providing an insight into non-Debye dielectric relaxation, the work of Professor Jonscher's group has only been useful for its classification of the behaviour of a wide range of materials. At least so far as I can tell from attendance at the last three years of relevant conferences, the entire community of specialists qualified to judge the theoretical side of this group's work remain unconvinced of its validity, and in general prefer to politely ignore Jonscher's "panacea approach" to the theory of irreversible processes.

11.3.c A Z-plane analogue of some work of Brot and Darmon

We have seen that there is at present little hope of gaining insight into the physical reasons for the Cole type of complex impedance behaviour from considering such few theories as do exist of the Cole-Cole type of complex permittivity behaviour.

There has however been significant progress in producing Cole-Cole dielectric behaviour in computer models of physical systems, and this approach can be copied in analogy to attempt to produce behaviour described by the Cole complex impedance equation.

In particular, Brot and Darmon (1970) carried out Monte Carlo calculations of the cooperative evolution of ordered and disordered configurations of 240 molecules of several hexasubstituted benzenes in response to applied electrical fields. Using this method they were able to predict Cole-Cole complex permittivity behaviour for 1,2,3-trichlorotrimethylbenzene, and this corresponded to what was observed experimentally.

The procedure was as follows. For a given temperature T, a particular initial configuration of the 240 molecules is set up (in the computer). Each molecule is assumed to have an initial orientation derived by N_i which is one of six possibilities ($1 \leq N_i \leq 6$), each producing a particular effective molecular dipole moment. Next the total Coulombic interaction energy of the block, E_i, is calculated for this configuration. Now a molecule J is chosen at random. For this molecule it is assumed that the activation energy for reorientation $\Delta E = (U - E_i)$ is always positive, with U equal to an arbitrary constant. Then a random number p between 0 and 1 is compared with $\exp [-(U - E_i)/kT]$ and if p is less than or equal to it, there is an opportunity to re-orient the molecule. A new orientation for the molecule J is then chosen at random from among the six possibilities and the new total energy of the block E_i' is calculated.

Thus each "successful" trial alters the conditions in the block under which later trials are made; this is therefore a model of a co-operative system having an "evolving time constant" in the sense of Salter (1978c, or see Appendix H).

By setting up a correspondence between physical quantities, it is now possible to see under what conditions a computer model of a Cole-type complex impedance could be produced.

These are as follows. For a given temperature T, a particular system of 240 "spatial domains" is set up (in the computer). Each domain is assumed to have an initial resistivity N_i which is one of (say) six possible values, for example depending upon the structure of each domain, because different structures may produce different mobilities for a particular charge carrier. Next the total entropy of the block, E_i, is calculated for these conditions. Now a domain J is chosen at random. For this domain it is assumed that the activation energy for resistivity change $\Delta E = (U - E_i)$ is always positive, with U equal to an arbitrary constant. Then a random number p between 0 and 1 is compared with $\exp [-(U-E_i)/KT]$ and if p is less than or equal to it, there is an opportunity to change the resistivity of the domain. A new resistivity for the domain J is then chosen at random from among the six possibilities and the new total entropy of the block E_i' is calculated. Note that a constant number of elements in the structure must locally alter that structure in a correlated way each time the structure does alter, if the Brot and Darmon analogy is to be preserved. *That is, if the principal effect of a Brot and Darmon molecule is to change the local resistivity rather than the local polarization each time it reorients, we transfer the circular arc locus directly from* ε^* *to* Z.

An analogy such as this offers an insight into what may be the mechanisms underlying the Cole-type complex impedance behaviour of the materials we consider in the next subsection, and also possibly of the skin.

170

11.3.d Solid ionic conductors

The concepts of inhomogeneity and "domains" of different resistivity are in fact very common in the literature describing the properties of materials which exhibit a complex impedance behaviour obeying the Cole equation.

One class of such materials is that of the vitreous or microcrystalline solid electrolytes. For example, glasses containing alkali metal oxides belong to this class, being solid ionic conductors, and their complex impedance properties have been reported by Ravaine and Souquet (1974) amongst others. Ravaine and Souquet (1974) in fact actually quote the Cole equation (with $R_\infty = 0$) and say that they believe it to be generally applicable to polycrystalline solid electrolytes.

Their paper has however been singled out from the mass of similar ones primarily because they formulated one of the least empirical theories of Cole-type complex impedance behaviour in solid electrolytes, that is, discounting the various publications of Jonscher. Nevertheless, the theory they propose is not useful for our purposes. A Cole-Cole DRT is indeed involved in their theory, but it is only involved arbitrarily, not derived from any fundamental physical hypotheses. Moreover, although they do not point this out, equation (6) of their theory in fact assumes that the material can be considered as a bundle of separate columns, each column being represented as a chain network of a series sequence of relaxing units, each relaxing unit being composed of a (variable) resistor in parallel with a capacitor. This arrangement is however unacceptable in that it ignores "sideways" interaction between the columns without there being any justification for doing so, since the resistor values are chosen ramdomly. (In the chain network models of skin to be considered in Section 11.5, the variable elements are chosen non-randomly, as a function

of distance, and it can be shown that this qualification does not then apply.) In fact Ravaine and Souquet should have proceeded to employ methods equivalent to those discussed in subsection 11.7.a, i.e. three-dimensional impedance matrices.

The work of Raistrick et al., (1976) may be consulted for an excellent phenomenological review of the Cole-type complex impedance behaviour of solid ionic conductors. They found at frequencies high enough (or temperatures low enough) for the electrode/material interface impedance not to dominate, that the behaviour of the bulk of various lithium silicates and aluminosilicates obeyed the Cole complex impedance equation.

Raistrick et al. point out however that there is still no fundamental theoretical interpretation of this behaviour, although they themselves considered that polarization phenomena at crystal grain boundaries were responsible. This idea is similar to that of "resistivity domains", and in fact related concepts have already been current for decades in the literature of skin electrophysiology (cf. subsection 12.6.d).

11.3.e Amorphous semiconductors

The simple type of energy band structure described in Section 3.9 arises in simple physical conditions which unfortunately are never found in the real world. Even the most perfect semiconductor crystal we can obtain is certain for thermodynamic reasons to have lattice defects, and also a surface. These produce discontinuities in the lattice and thereby complicate the energy band structure by adding to it so-called "localized states" with which individual electrons or holes may be associated for periods very much longer than that of a phonon vibration. If such states arise because of lattice defects at the crystal surface they are known as surface states (see e.g. Smith, 1978, p.219 ff).

These concepts are carried further in the theories which have been developed to describe the properties of amorphous semiconductors. Amorphous semiconductors are those with such great spatial inhomogeneities of composition and structure that they must be regarded as non-crystalline. Nevertheless, many concepts developed for crystalline semiconductors remain useful for amorphous ones (Mott and Davis, 1971), and it seems that the main effect of disorder in the material is to partially fill in the bandgap with localized states. If one can imagine disorder increasing from zero, what happens is that the band edges "grow" so-called "bandtails" of localized states, and these bandtails proceed to extend towards each other across the band gap. If the disorder continues to increase, the bandtails will eventually meet in the middle of the bandgap, and go on to overlap. (For a popular introduction to these ideas see e.g. Taylor, 1978, and for a more rigorous discussion see Mott and Davis, 1971.)

Pollak (1971) pointed out that the presence of a large density of localized states was an important feature of amorphous semiconductors such

as chalcogenide glasses, amorphous germanium and silicon, and disordered aggregates of organic and biological polymers, since the electrons or holes occupying the localized states profoundly affect the dielectric and conductive properties of such materials. Moreover, the complex conductivity of these materials, including proteins, is usually found to be of the by now familiar but still enigmatic form corresponding to the Cole complex impedance equation with $R_\infty = 0$, namely

$$\sigma^*(j\omega) = \sigma_1 + \sigma_2(j\omega\tau)^\alpha \qquad \text{(11.3.e.1)}$$
$$\text{cf.(11.1.3)}$$

(e.g. Elliott, 1977; Pethig, 1979, p.301 ff) and so theoreticians were led to consider that the occurrence of a large density of localized states and a complex conductivity of the form of (11.3.e.1) might well be related.

Now doped and compensated n-type crystalline silicon obeys (11.3.e.1) with alpha approximately equal to 0.8. Pollak and Geballe (1961) postulated that conduction in this material takes place by quantum-mechanical tunnelling between neighbouring donor impurity states, and produced a theory with exactly the frequency dependence required by experiment. This success led Austin and Mott (1969) to modify the theory for use with amorphous semiconductors by taking localized states close to the Fermi level to be analogous to the impurity states in the previous case. However this theory too can only predict values of alpha approximately equal to 0.8, which is too restricted to be widely applicable, and there are other objections to it as well (see e.g. Elliott, 1977). Fortunately though, as Lewis (1977) shows, the Austin-Mott theory describes only part of the spectrum of possibilities for conduction mechanisms involving localized states.

An alternative which he himself takes up, (as will be discussed later in Section 11.8) is to consider transitions between localized states not

near the Fermi level, i.e. states in those parts of the bandtails which are nearer the band edges (or mobility edges as they are often called in this context). The idea is that given the necessary energy by phonons, electrons or holes can be expected to escape from a localized state in the bandtail up into the band, where they can travel relatively freely in states which are delocalized, until they are trapped once again into a localized state, presumably part of the same bandtail but in some other part of the material. Such a process will be referred to as "multi-phonon-activated hopping", since it is indeed hopping in the proper sense of hopping OVER something, in this case a potential barrier of activation energy required to enter the band, and not tunnelling, which has however frequently been termed "hopping", to the confusion of many. It is of course possible nonetheless to combine the best of both worlds and to allow for the possibility that if a particular electron or hole does not in fact obtain from phonons enough energy to reach the band, it may still be able to move through the material by tunnelling through the potential barrier at a higher energy level (see e.g. Lewis, 1977, p.198).

Lewis has shown using these concepts that given a bandtail of a particular (and plausible) shape, not only can complex conductivities of the form (11.3.e.1) be expected, but also that alpha may take any of the values found experimentally. Consequently, since (as will be shown in Section 11.4), the conductive properties of skin can be considered to be determined by those of a semiconductive polymer aggregate of microcrystalline and amorphous keratins, it will be well worth seeing whether this type of theory developed in the literature of solid-state physics, can also help interpret something of the electrical behaviour of skin. The necessary investigation will be begun in Section 11.8.

11.3.f The problem of the origin and form of the DRT in skin

So far in this Section we have considered just a few of the physical systems which may contain hints towards the solution of the problem of why human skin obeys the Cole complex impedance equation. There are many other such physical systems however which did not seem as likely to be directly relevant and yet which provide seemingly endless grounds for further speculation.

This subsection is intended to raise a number of questions and points for consideration which we will proceed to deal with in greater detail in the remainder of this Chapter, during the course of trying to interpret why it is that the complex impedance of skin obeys the Cole equation.

The rigorous analysis of the conduction of electric current through a material as inhomogenous as human skin is a very difficult problem. What little theory exists to be used is very complicated (cf. Landauer, 1978), indeed becoming unwieldy even for biological systems much simpler than human skin (cf. Eisenberg et al., 1979), and non-existent for most tissues of practical interest (see e.g. Cole et al., 1969). Moreover, as Weinberg and Householder (1941) have shown, all attempts to extract detailed physical characteristics of biological tissues just from measurements of complex impedance are subject to fundamental mathematical restrictions.

Thus it should give some relief to meet the information reviewed in the next subsection, namely that the distinctive linear electrical behaviour of skin, that is, its obedience to the Cole complex impedance equation, is almost entirely due to the properties of the stratum corneum. We may therefore narrow our investigations somewhat.

The first question which must therefore be dealt with is that of whether or not it is the *structure* of the stratum corneum which is important in producing Cole-type complex impedance behaviour. Schanne and

Ruiz P.-Ceretti (1978, p.54), say that a powerful and general interpretation of obedience to the Cole equation is now available, by which they mean the existence of a suitable distribution of time constants of the relaxing units, usually assumed to be due to a distribution of cell sizes or shapes. This optimism however conflicts with their own conclusion on p.319, and certainly the variety of cell shapes and sizes in the corneum is much too small to explain the observed values of m. Similar disappointments have been reported by these authors themselves (p.342, 345) and by Fatt (1964, p.639), and others (K.S. Cole, personal communication, 1978).

It may however be the *layered arrangement of cells* in the corneum which is important, in combination for example with the gradient of hydration which is to be expected through these layers. This type of model is examined in Section 11.5.

The structure of the corneum may alternatively be important because it is made up of cellular sub-units, around which the phenomena of *surface conduction and counter-ion relaxation* may take place. This type of model is examined in Section 11.6.

The second question we must deal with is that of whether or not it is the structure *of the corneum cells themselves* which is important. For example, the fact that they are bounded by a cell membrane, altered though it is in the process of keratinization. This fact is not as trivial as might at first be assumed, because all natural membranes (but not artificial, e.g. black lipid, membranes, cf. Takashima and Schwan, 1974, p.52) behave like a polarization impedance in series with a resistance, and such membranes combined with additional conductance paths would therefore obey the Cole equation. This concept dates back at least as far as Cole (1928, 1932) and there is now a good deal of experimental evidence in favour of it (e.g. Cole and Jahn, 1937; Cole, 1968, p.7 and Fig.7; Taylor, 1977, p.303), even considering (K.S. Cole, personal communication, 1978) the

caveats of Schwan (1957, pps.165 - 188). There are various possible interpretations of it but here we will review only three.

Firstly, *roughness of the membrane surface* could produce these effects (Scheider, 1975), at least if the membrane were exposed to electrolyte solution, which in the tightly-packed corneum (cf. Hashimoto, 1971) does not seem to be a reasonable picture. Moreover, this mechanism can only produce particular fractional values of m.

Secondly, *gating currents* as discussed by Schwan (1957) might be a possible cause in living membranes, at least if the channels interacted or for some other reason did not obey Poisson statistics and thus act as single time constants. However, in the corneocyte membranes there are no gating currents, because the cells are dead.

A third possibility is that these effects are observed because of the fact that *natural cell membranes include "protein modules"*, whereas artificial lipid bilayers do not. Proteins tend to obey the amorphous semiconductor complex admittance (11.3.e.1), (see e.g. Pethig, 1979, p.301 ff), which implies that they can be modelled as a polarization impedance in parallel with a resistor, just as is needed to model the Cole equation with $R_\infty = 0$ (cf. Section 11.1), although more accurate measurements would probably require a non-zero R_∞ to be included too. The hydration of these proteins will bring the activation energy for conduction through these modules down to reasonable values even if no other effect does (cf. Pethig, 1979, Ch.9), and I think that this is probably the best interpretation of the "constant phase angle membrane". Soon after I thought of it, I had the opportunity to discuss the idea at length with Professor K.S. Cole while staying as his guest for four days in San Diego, and I am pleased to say that he thinks it is a good idea too!

Finally, in the case of the cells of the corneum we should remember that not just the membrane has protein in it but also the region inside the membrane which once was the cytoplasm. In fact the entire cell is unusually rich in proteins of the keratin family, with only a little room left for lipids and other substances such as water. Thus perhaps the skin obeys the Cole complex impedance equation because *the corneum is electrically equivalent to a sort of "proteinaceous syncytium" obeying (11.3.e.1), further shunted by the conductances of the skin appendages.*

In the Sections which follow, we shall examine this and our previous hypotheses in some detail.

11.4 The electrical conductance of the keratins of the corneum

11.4.a The importance of the corneum

Since the effect of the dermis and deeper layers is usually negligible, the electrical conductance of the skin may be approximated by the sum of the conductance of the epidermis and that of the skin appendages which pierce through it. Most investigators other than psychophysiologists are interested primarily in the epidermis, and would take steps (such as reducing the ambient temperature) to ensure that the conductance contribution of the appendages was minimised. In this circumstance the conductance of the skin will be almost entirely determined by the conductance of the epidermis, and it is easy to prove, for example by stripping the skin with adhesive tape (e.g. Lawler et al., 1960; Tregear, 1966, pps. 64, 65; Yamamoto and Yamamoto, 1976a, 1976b; and cf. Scheuplein, 1976a, 1976b) that the conductance of the epidermis is usually almost entirely determined by that of the stratum corneum, the least conductive epidermal layer. Consequently if we are to examine the factors influencing the conductance of the skin, it is reasonable to begin with those influencing the conductance of the group of proteins known as keratins, since as will be elaborated below, the corneum is almost entirely composed of such proteins.

11.4.b The keratins of the corneum

The bulk of the stratum corneum is made up of flattened cells adhering to each other by means of mucopolysaccarides, interdigitation and other factors (see e.g. Kligman, 1964, p.418 ff; Scheuplein, 1978, p.1683 ff). The cells are sometimes referred to as keratinocytes because when mature they are mainly composed of proteins of the keratin family. This family may be loosely defined as those proteins containing sulphur in the form of cystine and cysteine (Rothman, 1954, Ch.15). Adjacent molecules of cysteine tend to combine by cross-linking such that the -SH groups are oxidized to -S-S- groups and a strong disulphide bond is formed (for a diagram, see e.g. Rothman, 1954, p.368). Further information concerning the chemistry of the keratins can be found in the detailed review by Jarrett (1973, Ch.5) although the keratin family is large, and perhaps because of this the biochemical nature of the particular keratins of human stratum corneum does not appear to be very fully understood, even in the more recent research papers.

It is however well established that mature keratinocytes such as compose the corneum contain two main forms of keratin, a filamentous component embedded in an amorphous component (see e.g. Jarrett, 1973, p.147 ff; Scheuplein, 1978, p.1686, ff). It is also known that the membrane of the cell is thickened as the process of keratinization of the cell contents proceeds.

The cell contents are of importance to our consideration of the conductance properties of the stratum corneum because as will be seen in subsection 11.4.d, the best available evidence indicates that movement of electrical charge carriers occurs transcellularly through the partially hydrated matrix of intracellular keratins, rather than intercellularly through material which Scheuplien (1978, p.1728) describes as "largely lipid and an unattractive substrate for water-soluble substances".

11.4.c Hydration of the corneum keratins

Under normal (non-occluded) conditions more water will tend to diffuse out of the body through the skin than diffuses into the body through the skin. This net loss is known as the "trans-epidermal water loss" or TEWL (subsection 2.1.g; for a review see e.g. Grice, 1980), and it is associated with a gradient of water content across the corneum depending in magnitude on various factors (Scheuplein, 1978) including the permeability of the corneum itself, the diffusivity and water content of deeper layers, and also the relative humidity at the skin surface (cf. Goodman and Wolf, 1969). The water in the corneum diffuses within the matrix of intracellular keratin, apparently most easily within the amorphous component between the α-keratin filaments (Idson, 1973, p.199).

Some of this water is (temporarily) adsorbed by the keratin; indeed the corneum has a great affinity for water and can absorb at least three times its dry weight of it (Kligman, 1964, p.424; Scheuplein and Morgan, 1967). It would seem from the study of adsorption isotherms that water is adsorbed onto the keratin molecules in successive monolayers, the binding energy of adsorption becoming smaller as more layers are added. Nevertheless it is usually assumed that although the first monolayer is very strongly bound, further layers are held in place by much weaker (hydrogen) bonds of roughly equal strength, this assumption being made in order to justify the application of the relatively simple so-called BET isotherm theory. Unfortunately, however the BET theory should really be admitted to be too simple to adequately describe the water adsorption properties of human stratum corneum, and the general theory of adsorption should be used instead (see Pethig, 1979, p.119 ff). The necessary parameters are given in Table 11.4.c.A in Pethig's notation, by courtesy of Dr M. Leduc:

Table 11.4.c.A

Parameters of the General Isotherm			
Calculated from the results of:	Goodman & Wolf (1969)	Rieger & Deem (1974)	Leduc & Turek (1978)
h_m	0.136	0.151	0.210
C	0.516	0.534	0.453
b	0.960	0.877	0.758

11.4.d Electrical conduction in keratins and the effect of water

Baxter (1943) studied the D.C. electrical conductivity of wool keratin amongst other textiles, and found that it was a semiconductor with an activation energy of 1.34 eV at the particular hydration level he used. Since this value was closer to the activation energy for conduction in ice (1.27 eV) than to that for liquid water (0.44 eV), he concluded that conduction in wool keratin was likely to be via ice-like water, and developed a model for his results based upon tunnelling of electrons between adsorbed water molecules uniformly distributed in space throughout the material.

This concept was questioned however by King and Medley (1949a, 1949b), who made very careful electrolytic investigations of horn keratin and found that for water contents of 15% or more, the results indicated that the conduction mechanism was ionic, not electronic. They may in fact have been demonstrating protonic conduction through the ice-like water of Baxter. King and Medley (1949b) found as expected that the conductivity of the keratin increased with water content, and were able to accurately model their results using a modified Bjerrum theory based upon the assumption that an increase in the content of polar adsorbate would increase the dielectric constant of the keratin-water system (cf. King's earlier work: King, 1947). This increase in dielectric constant would in turn lower the effective ionic dissociation energy, and the resulting increase in the number of mobile ions would increase the conductivity.

A thorough review of more recent work on electrical conduction in proteins has been given in a monograph by Pethig (1979). In Chapter 9 Pethig discusses the two main theories competing at present to explain the increase in conductivity produced in proteins by the adsorption of water and other substances. Both theories of course have strengths and weaknesses.

One is due to Professor D.D. Eley, and postulates that the conductivity increase arises due to injection of electrons into the conduction band of the protein through the electron-donating property of water, i.e. this is a theory based upon charge-transfer interactions.

The other theory is similar to that of King and Medley (1949b), and is based on the idea that the adsorption of polar substances such as water will increase the permittivity of the material and so lower any form of ionization energy, which will be inversely proportional to the local permittivity. The theory as given by Rosenberg (1962) represents a modification of the ideas of King and Medley (1949b). Rosenberg specifies that it is the activation energy for semiconduction which should be reduced by an increase in the permittivity of the material, and uses an equation of the form

$$\Delta E_w = \Delta E_d - ch \qquad (11.4.d.1)$$

where ΔE_d is the semiconduction activation energy of the hydrated protein, ΔE_d is the energy for the protein when dry, h is the amount of water adsorbed, expressed as a fraction of the maximum possible amount adsorbable at that temperature, and c is some constant independent of temperature.

As would be expected on the basis of (11.4.d.1), Rosenberg found that the conductivity of the protein he investigated, bovine haemoglobin, was approximately given by

$$\sigma_w = \sigma_d \exp\left[-(\Delta E_d - ch)/kT\right] \qquad (11.4.d.2)$$

although the effect saturated at high values of h.

Now King and Medley (1949b) found that the conductivity of hydrated horn keratin too could be described by

$$\sigma_w = A \exp(bh) \qquad A,b = \text{constants} \qquad (11.4.d.3)$$

and that the effect saturated at high values of h. Since equations (11.4.d.2) and (11.4.d.3) are of the same form, we may conclude that hydrated horn keratin also obeys Rosenberg's equation (11.4.d.1), at least for those values of h which are not too high. (Above such values a more accurate equation is needed, and one will be suggested later.) Of course we now need to know whether an equation of the form of (11.4.d.2) is also valid for the keratins of human skin, and fortunately Campbell et al. (1977) have examined this question by direct experimentation. They investigated the resistivity ($- 1/\sigma_w$) of human plantar stratum corneum as a function of water content, across a range of about 0.1 to 0.7 fractional water content. Their results, when plotted on a graph of logarithm of resistivity against fractional water content, certainly do not produce the straight line which adherence to (11.4.d.2) would require. However, (11.4.d.2) may nonetheless be an acceptable approximation if the water fraction is small, and the deviation from linear behaviour could then be explained by the "saturation effect" described by King and Medley, which we were expecting anyway.

The validity of equation (11.4.d.2) may also be investigated theoretically, and it will be profitable to do so since Pethig (1979, p.296) has pointed out that a strict adherence to (11.4.d.1) would force the other parts of Rosenberg's theory to make physically impossible predictions.

Let it be assumed then, following the spirit of the rest of Rosenberg's theory, that

$$\sigma_w = \sigma_d \exp\left(-\frac{\Delta E_d}{kT}\right) \exp\left[\frac{q^2}{kTR}\left(\frac{1}{\varepsilon_d} - \frac{1}{\varepsilon_d + h(\varepsilon_{sat} - \varepsilon_d)}\right)\right] \quad (11.4.d.4)$$

where q is the amount of charge escaping from a protein molecule assumed for simplicity to be a sphere of radius R, ε_d is the relative permittivity of the protein when completely dry, and ε_{sat} the relative permittivity of the protein when it has adsorbed its maximum amount of adsorbate for the temperature T and thus is "saturated". I have chosen the form of the term involving ε_{sat} merely for its simplicity.

From (11.4.d.4) we may then infer a more accurate replacement for Rosenberg's equation (11.4.d.1), namely

$$\Delta E_w = \Delta E_d - \frac{q^2}{kTR}\left[\frac{1}{\varepsilon_d} - \frac{1}{\varepsilon_d + h(\varepsilon_{sat} - \varepsilon_d)}\right] \qquad (11.4.d.5)$$

and neither this equation nor (11.4.d.4) leads to embarrassing physically impossible predictions. Indeed, such predictions vanish as soon as it is realised that (11.4.d.1) is just an approximation to something of the form (11.4.d.5). The assertion that one is an approximation for the other can be proved by Maclaurin expansion, since we have then

$$\frac{1}{\varepsilon_d + h(\varepsilon_{sat} - \varepsilon_d)} = \frac{1}{\varepsilon_d} - \frac{(\varepsilon_{sat} - \varepsilon_d)}{\varepsilon_d^2} \cdot h + \text{higher terms} \qquad (11.4.d.6)$$

so (11.4.d.5) can be rewritten as

$$\Delta E_w = \Delta E_d - \frac{q^2}{kTR}\,\frac{(\varepsilon_{sat} - \varepsilon_d)}{\varepsilon_d^2} \cdot h + \text{higher terms} \qquad (11.4.d.7)$$

and the higher terms can be ignored when

$$h \ll \frac{\varepsilon_d}{(\varepsilon_{sat} - \varepsilon_d)}, \quad (0 \leq h \leq 1) \qquad (11.4.d.8)$$

i.e. only for very low values of h, whereupon (11.4.c.7) reduces to something of the form of Rosenberg's equation (11.4.d.1), as expected.

Thus it is now possible to see exactly the conditions under which Rosenberg's equation is an acceptable approximation, as well as the conditions under which the less approximate equation (11.4.d.5) should be used. It is also clear that Pethig's rightful objection to Rosenberg's algebra need not shoot down Rosenberg's basic approach.

11.4.e The nature of the mobile charge carriers in hydrated corneum

As Baxter (1943) noted, it is difficult to decide whether the conductivity of non-metallic solids is ionic or electronic unless a Hall effect can be measured. (A simple introduction to the Hall effect is provided by Wright, 1979, pps. 48-50.) Pethig (1979) has reviewed the work completed to date on proteinaceous semiconductors and it appears that the necessary experimental investigations of partially hydrated keratin have not yet been made.

However, in agreement with that work on keratin which has been done (Baxter, 1943; King and Medley, 1949a, 1949b) and with the results obtained for collagen, cytochrome-c, haemoglobin, lecithin and melanin by Powell and Rosenberg (1970), Pethig points out (p.293) that: "a reasonable approach to take is that in the dry state most biopolymers can be considered to exhibit an essentially electronic conductivity involving the conduction of either electrons or holes in the appropriate energy bands, or via localized (trapping) states. With increasing water content, especially after the completion of one or two monolayers of sorbed water molecules, we may expect that protons and other ionic species are able to migrate around the surface of the hydrated proteins". This also agrees with the view of Cope (1970, p.19), who says that hydrated proteins are likely to be both ionic and electronic semiconductors.

To summarize, we may expect partially hydrated keratins to be mixed semiconductors in the sense that conduction will be both electronic (cf. Baxter, 1943) and ionic (cf. King and Medley, 1949a, 1949b). Collaborative work between the Slade Hospital and the School of Electronic Engineering Science, University College of North Wales, Bangor, is consequently being undertaken to establish the relative proportions of these

types of conduction in human stratum corneum as a function of hydration, and the results will eventually be discussed in detail elsewhere.

Concerning ionic mechanisms, it is likely that protonic conduction will occur through partially hydrated keratins via the icelike structure of their bound water (cf. Scheuplein and Morgan, 1967; Lampert and Mark, 1970, p.154). Moreover, since it is known that water can enter and move transcellularly through the stratum corneum (see e.g. Scheuplein, 1965, p.342 ff) it is reasonable to expect that other small polar molecules and (hydrated) ions can do so too, even if only slowly. We will return to this idea in subsection 12.2.b, since the absorption of water, other small polar molecules and hydrated ions will affect the electrical properties of skin in at least two ways.

Firstly, there will be a direct effect on the conductance of the corneum by increasing the number of semi-mobile charge carriers within it, and it is interesting that as was mentioned in subsection 9.2.c, Allenby et al. (1969) measured the activation energy of the electrical impedance at 1.5 Hz of human skin in vitro as 14.6 kcal/mole (0.633 eV), which is remarkably similar to that for the permeation of water molecules through skin, 15.4 kcal/mole (0.668 eV; cf. Scheuplein and Morgan, 1967, who quote 15 kcal/mole, 0.651 eV) and far higher than that for ionic conduction in free water (3.6 kcal/mole, 0.156 eV), or for the self-diffusion of free water (4.7 kcal/mole, 0.204 eV, according to Scheuplein and Morgan, 5.3 kcal/mole, 0.230 eV, according to Allenby et al.). *These results show that the conduction of charge in partially hydrated corneum involves a similar activation energy to that needed for the movement of water through the same tissue,* so perhaps under the conditions of measurement used by Allenby et al., the predominant charge carriers were (hydrated) ions moving through a lattice of bound water, just as water molecules themselves would have to do in order to diffuse across the corneum.

Secondly, there will be an indirect effect upon the conductance of the corneum because its semiconductive activation energy will decrease as its content of water and other polar substances increases. This concept of a decrease in semiconductive activation energy is made use of in subsection 11.9.h, and the corresponding increase in the conductance of the corneum is considered in subsection 12.2.d.

11.5 Shunted gradient models following Barnett and Tregear

11.5.a Introduction

We have seen that one may postulate the existence of a distribution of relaxation times in skin in order to interpret the fact that its complex impedance locus is an arc of a circle and not a semicircle. However, if this hypothesis is to be examined in anything more than a completely hit-or-miss way it is necessary at this point to begin to establish a framework for subsequent theories.

Suppose then that the relaxation time τ of each particular "relaxing unit" in skin (whatever such a relaxing unit turns out to be), is a function F of some quantity u,

$$\tau = F(u) \qquad (11.5.a.1)$$

where for example u may be an activation energy, or a spatial dimension. (In fact u may also be time, but this case presents special difficulties and it has been dealt with elsewhere: Salter, 1978c.)

If a range of u values exists, a range of τ values must also exist, producing a particular "distribution of relaxation times". Consequently we may write the complex impedance Z as

$$Z = R_{\infty} + \int_0^{\infty} \frac{y(\tau)\,d\tau}{1 + j\omega\tau} \qquad (11.5.a.2)$$

where $y(\tau)$ is known as the (unnormalized) distribution function, and describes the DRT.

It is important to note at this point that the formalism of distribution function theory assumes that relaxing units are coupled additively. This is implicit in equations of the type (11.5.a.2), and means that any equivalent circuit composed of pure resistances and pure reactances which is designed to model a particular non-semicircular complex impedance locus,

has to incorporate the complete range of relaxing units IN SERIES one with another and with the "infinite frequency" value of impedance, R_∞. For the same reason of course, when modelling particular non-semicircular complex admittance or complex permittivity loci, the relaxing units would be assumed to be connected together in PARALLEL.

From equation (11.5.a.2) it follows that we may write the resolved components of the complex impedance, the equivalent series resistance R_s and the equivalent series reactance X_s, as

$$R_s = R_\infty + \int_{\tau_2}^{\tau_1} \frac{y(\tau)\,d\tau}{1+(\omega\tau)^2} \qquad (11.5.a.3)$$

and

$$-X_s = \int_{\tau_1}^{\tau_2} \frac{y(\tau)\ \omega\tau\ d\tau}{1+(\omega\tau)^2} \qquad (11.5.a.4)$$

and, considering that at $\omega = 0$, $Z = R_o$ from the definition of R_o, it also follows from (11.5.a.2) that

$$(R_o - R_\infty) = \int_0^\infty y(\tau)\,d\tau \qquad (11.5.a.5)$$

However, for physical reasons we expect a non-zero minimum value of τ, τ_1, although experimentally this may be indistinguishable from zero. Also, the maximum value of τ, τ_2 will obey $\tau_2 \leq \infty$. Therefore since we have supposed that τ is a function of nothing but the single quantity u, we must also restrict ourselves to assuming a finite range of u, and write

$$(R_o - R_\infty) = \int_{\tau_1}^{\tau_2} y(\tau)\, d\tau$$

$$= \int_{u_{min}}^{u_{max}} y(\tau)\, \frac{d\tau}{du}\, du$$

$$= \int_{u_{min}}^{u_{max}} r(u)\, du \qquad (11.5.a.6)$$

where we interpret

$$r(u)\, du = y(\tau)\, d\tau \qquad (11.5.a.7)$$

as the contribution to the D.C. resistance R_o made by the relaxing units having a u value between u and (u + du). That is,

$$r(u)\, du = (\text{number of relaxing units having u between u and u + du}) \times (\text{Resistance contribution of each relaxing unit having u between u and u + du}) \qquad (11.5.a.8)$$

We are now in a position to be able to investigate the complex impedance loci produced by some particularly simple models of the physical condition of skin.

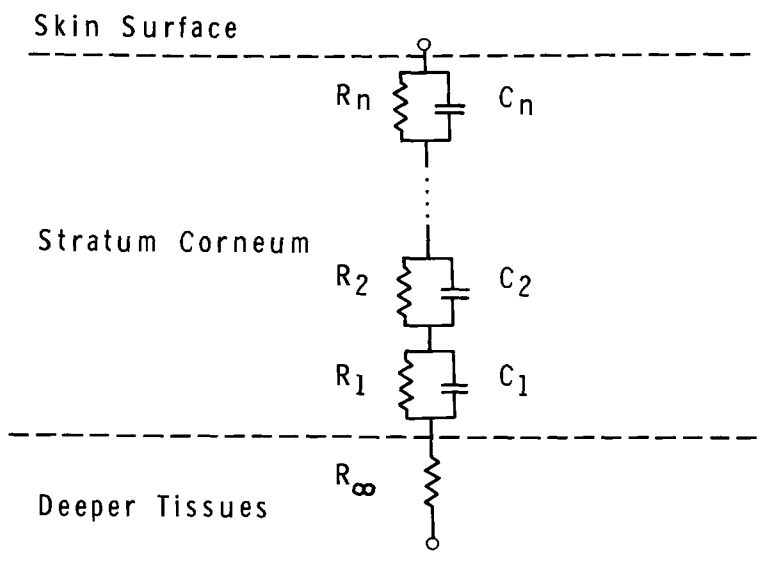

Skin Surface
R_n
C_n
Stratum Corneum
R_2
C_2
R_1
C_1
R_∞
Deeper Tissues

Fig. 11.5.b.I

11.5.b Chain networks with exponential resistance gradients

In 1938 Barnett pointed out that because there is a change in dryness of the skin with depth - the outer cell layers of the stratun corneum can be expected to be drier than the inner layers for example - then it is possible that there may be a corresponding variation of electrical properties with depth giving rise to an associated variation of time constant τ with depth. Thus he raised the possibility that the unknown variable "u" in the last subsection might be equated with depth.

Such hypotheses will be called "gradient models". They can be represented by the sort of equivalent circuit shown in Figure 11.5.b.I, where the time constant at the bottom of the stratum corneum is R_1C_1, and at the top, R_nC_n, which in general will have a different value. One may or may not assume that one particular such time constant can represent the value of τ for a whole cell layer in the corneum, but if one does, then n will be equal to the number ofcell layers in the corneum at the body site in question. Tissues below the corneum can be represented by a pure resistance, R_∞, since the electrical properties of these layers are practically independent of frequency (Gerstner and Gerbstädt, 1949, p.117; Yamamoto and Yamamoto, 1976a, p.152).

Barnett then restricted his hypothesis in two ways. Firstly, he postulated that it was resistivity which varied with depth (where the resistivity concerned might or might not be interpretable as intercellular resistivity), and secondly he specified that the particular form of this dependence upon distance was exponential. There are of course very good theoretical reasons for applying these particular restrictions as a first approximation rather than any others when modelling the biological and physical conditions pertaining to skin, and indeed recently there has appeared experimental evidence for these assumptions too (Yamamoto and Yamamoto, 1976a).

Barnett claimed that a model such as Fig. 11.5.b.I, with the resistors varying exponentially with depth and capacitors of constant value, would reproduce some of the features of skin impedance which he had observed, namely a phase angle which rose from zero at zero frequency to a "plateau" value which remained constant up to very high frequencies. This in fact is true. Barnett, however, despite promising to do so in a following paper, does not appear to have ever completed the working out of the theory behind his hypothesis. Also Tregear (1966a, pps. 66-69), who followed up the idea without explicit acknowledgement, did not complete the theory, but merely resorted to physically constructing particular electrical networks and measuring their properties.

Now, if like Tregear one only plots phase angle against frequency, then the Barnett type of network can indeed be so constructed as to reproduce the impedance behaviour of skin reasonably accurately. *If, however, one instead constructs the complex impedance locus on the complex impedance plane, one finds that it is skewed, and very plainly unacceptable as an approximation to the locus produced by the skin itself, which as we have seen (Section 9.5) is very accurately a minor arc of a circle.*

No-one appears to have realised this before however and so the work of Tregear is still widely quoted as the explanation of the problem of the origin and form of the DRT in skin. Indeed the concept is now being applied to other epithelia too (Clausen et al., 1979). It is therefore time for the inadequacies of the Barnett-Tregear model to be demonstrated very clearly, and thus to show the need for something better. We will begin by considering the theory which neither Barnett nor anyone else seems to have published, and then move on to examine computer-calculated complex impedance loci for particular Barnett-Tregear networks.

Let the local permittivity ε be independent of, but let the local resistivity ρ change exponentially with, position x in the skin according to

$$\rho(x) = \rho_1 \exp\left[\frac{\ln Q}{X} x\right] \quad o \leq x \leq X$$

$$= o \qquad x < o,\ x > X \qquad (11.5.b.1)$$

where

$$Q = \frac{\varepsilon\rho(X)}{\varepsilon\rho(o)} = \frac{\text{maximum } \tau}{\text{minimum } \tau} = \frac{\tau_2}{\tau_1} \qquad (11.5.b.2)$$

Then if

$$dx = \frac{X}{n}, \quad n \to \infty \qquad (11.5.b.3)$$

we may write for unit area

$$C(x,\ x + dx) = C(dx) = \varepsilon/dx \qquad (11.5.b.4)$$

and

$$Z(x,\ x + dx) = C(x,\ x + dx)\ R(x,\ x + dx) \qquad (11.5.b.5)$$

so

$$Z(x,\ x + dx) = \frac{\varepsilon}{dx} \int_x^{x+dx} \rho_1 \exp\left[\frac{\ln Q}{X} x\right] dx \qquad (11.5.b.6)$$

$$= \frac{\varepsilon}{dx}\ \rho_1 \frac{X}{\ln Q}\ \exp\left[\frac{\ln Q}{X} x\right] \Bigg|_x^{x+dx} \qquad (11.5.b.7)$$

$$= \frac{\varepsilon}{dx}\ \rho_1\ \frac{X}{\ln Q}\ \exp\ [\frac{\ln Q}{X}\ x]\ \left\{\ \exp\ [\frac{\ln Q}{X}\ dx]\ \ -1\right\} \qquad (11.5.b.8)$$

which, since dx << X, reduces to approximately

$$\frac{\varepsilon\rho_1}{dx}\ \ \frac{X}{\ln Q}\ \ \exp\ [\frac{\ln Q}{X}\ x]\ \left\{\ \frac{\ln Q}{X}\ dx\right\} \qquad (11.5.b.9)$$

so

$$\tau(x, x+dx) \ = \ \varepsilon\rho_1\ \exp\ [\frac{\ln Q}{X}\ x] \qquad (11.5.b.10)$$

Now the contribution to the D.C. resistance made by relaxing units having u between u and u+du is r(u)du from equation (11.5.a.8), which implies

$$r(u)\,du \ = \ \text{number}\ (x)\ \rho(x)\ dx \qquad (11.5.b.11)$$

if u is position ,x. Thus (11.5.a.7), which can be written

$$y(\tau) \ = \ \frac{du}{d\tau}\ \ \frac{r(u)\,du}{du} \qquad (11.5.b.12)$$

becomes

$$y(\tau) \ = \ \frac{1}{\tau}\ \ \frac{X}{\ln Q} \cdot \ \frac{n\ \frac{dx}{X}\ \rho_1\ \exp\ [\frac{\ln Q}{X}\ x]\ dx}{dx} \qquad (11.5.b.13)$$

making the most simple assumption that the (linear) spatial density of relaxing units is constant, so that for n relaxing units in a length X the number of relaxing units between x and x+dx is ndx/X.

Then applying (11.5.b.3),

$$y(\tau) \ = \ \frac{1}{\tau}\ \ \frac{X}{\ln Q}\ \rho_1\ \ \exp\ [\frac{\ln Q}{X}\ \ x] \qquad (11.5.b.14)$$

$$= \frac{1}{\tau} \frac{X}{\ln Q} \frac{\tau}{\varepsilon} \qquad (11.5.b.15)$$

$$= \frac{X}{\ln Q} \cdot \frac{1}{\varepsilon} \qquad (11.5.b.16)$$

and writing this in terms of

$$(R_o - R_\infty) = \int_{u_{min}}^{u_{max}} r(u)\, du \qquad (11.5.b.17)$$

$$= \int_o^X n \frac{dx}{X} \rho_1 \exp\left[\frac{\ln Q}{X} x\right] dx \qquad (11.5.b.18)$$

$$= \int_o^X \rho_1 \exp\left[\frac{\ln Q}{X} x\right] dx \qquad (11.5.b.19)$$

$$= \rho_1 \frac{X}{\ln Q} [Q - 1] \qquad (11.5.b.20)$$

$$= \frac{\gamma_1}{\varepsilon} \cdot \frac{X}{\ln Q} \cdot \frac{(\tau_2 - \tau_1)}{\gamma_1} \qquad (11.5.b.21)$$

produces

$$y(\tau) = \frac{(R_o - R_\infty)}{(\tau_2 - \tau_1)} \qquad \tau_1 \leq \tau \leq \tau_2$$

$$= 0 \qquad \tau < \tau_1,\ \tau > \tau_2 \qquad (11.5.b.22)$$

which is correctly normalized in that it satisfies (11.5.a.6).

Therefore substituting the $y(\tau)$ of (11.5.b.22) into (11.5.a.3) we have

$$R_s = R_\infty + \frac{(R_o+R_\infty)}{(\tau_2-\tau_1)} \int_{\tau_1}^{\tau_2} \frac{d\tau}{1 + (\omega\tau)^2} \qquad (11.5.b.23)$$

$$= R_\infty + \frac{(R_o+R_\infty)}{(\tau_2-\tau_1)} \int_{\tau_1}^{\tau_2} \frac{1}{1 + bx^2}\, dx, \quad b = \omega^2 \qquad (11.5.b.24)$$

and so from the standard integral

$$\int \frac{dx}{a + bx^2} = \frac{1}{\sqrt{ab}} \arctan \frac{x\sqrt{ab}}{a} \quad (ab > o) \qquad (11.5.b.25)$$

we have the final result that

$$\frac{R_s-R_\infty}{R_o-R_\infty} = \frac{\arctan(\omega\tau_2) - \arctan(\omega\tau_1)}{\omega(\tau_2 - \tau_1)} \qquad (11.5.b.26)$$

Similarly from (11.5.a.4) we have

$$-X_s = \frac{(R_o-R)}{(\tau_2-\tau_1)} \int_{\tau_1}^{\tau_2} \frac{\omega\tau\, d\tau}{1 + (\omega\tau)^2} \qquad (11.5.b.27)$$

$$= \frac{(R_o-R_\infty)}{(\tau_2-\tau_1)} \cdot \omega \int_{\tau_1}^{\tau_2} \frac{x}{1 + bx^2}\, dx \qquad (11.5.b.28)$$

and so from the standard integral

$$\int \frac{x\, dx}{a + bx^2} = \frac{1}{2b} \ln(a + bx^2) \qquad (11.5.b.29)$$

we have the final result that

$$\frac{-X_s}{R_o - R_\infty} = \frac{1}{2\omega(\tau_2-\tau_1)} \ln\left[\frac{1 + (\omega\tau_2)^2}{1 + (\omega\tau_1)^2}\right] \qquad (11.5.b.30)$$

Equations (11.5.b.26) and (11.5.b.30) define the resolved components of the complex impedance locus of a discrete lumped-element Barnett-Tregear network model for the "continuum" case $n \to \infty$ and $\tau_1 = CR_{min}$, $\tau_2 = CR$ max (Salter, 1981). The equations predict a skewed locus which is more Debye-like at low frequencies. Moreover, if minor arcs of circles are used to approximate the locus produced by these equations, the largest value of m which may be used is only about 0.23, obtained by fitting to the high-frequency side of the locus in the (physically impossible) extremum case $Q = \infty$ (cf. 11.5.b.2).

Therefore we may conclude that not only are Barnett-Tregear models incapable of producing a complex impedance locus which is a minor arc of a circle such as is found for the case of the skin, but they are also incapable of producing even a section of a complex impedance locus which can approximate a minor arc of a circle with an m value larger than 0.23. Such a value of m is however very often exceeded in clinical results.

Lest it be thought that these conclusions were being drawn merely from algebra which did not correspond sufficiently closely to the work of Barnett and (especially) Tregear, and which therefore did not in fact disprove the usefulness of their model, I repeated the work of Tregear by computer, which also served as a check on the form of the algebra above.

Consider then that in Fig. 11.5.b.I

$$C_1 = C_2 = C_3 = \ldots\ldots = C_n \qquad (11.5.b.31)$$

but that the corresponding resistors increase exponentially with increase in index number according to

$$R_k = R_1 \left[Q^{\left(\frac{k-1}{n-1}\right)}\right] \leq R_1, \qquad k = 1, 2, 3 \ldots n \qquad (11.5.b.32)$$

with $Q = R_n/R$ (11.5.b.32)

which is a discrete version of what we had before in (11.5.b.1) and (11.5.b.2).

Figures 11.5.b.II to 11.5.b.VII present the corresponding network complex impedance loci calculated by computer, with the least-squares-best-fitted minor arcs of circles also drawn in. The centres of these circles are enclosed in a small rectangle and a radius is drawn to the high-frequency intercept to define the value of m.

The model parameters were set such that

C_n = 0.2 microfarads

R_1 = 200 ohms

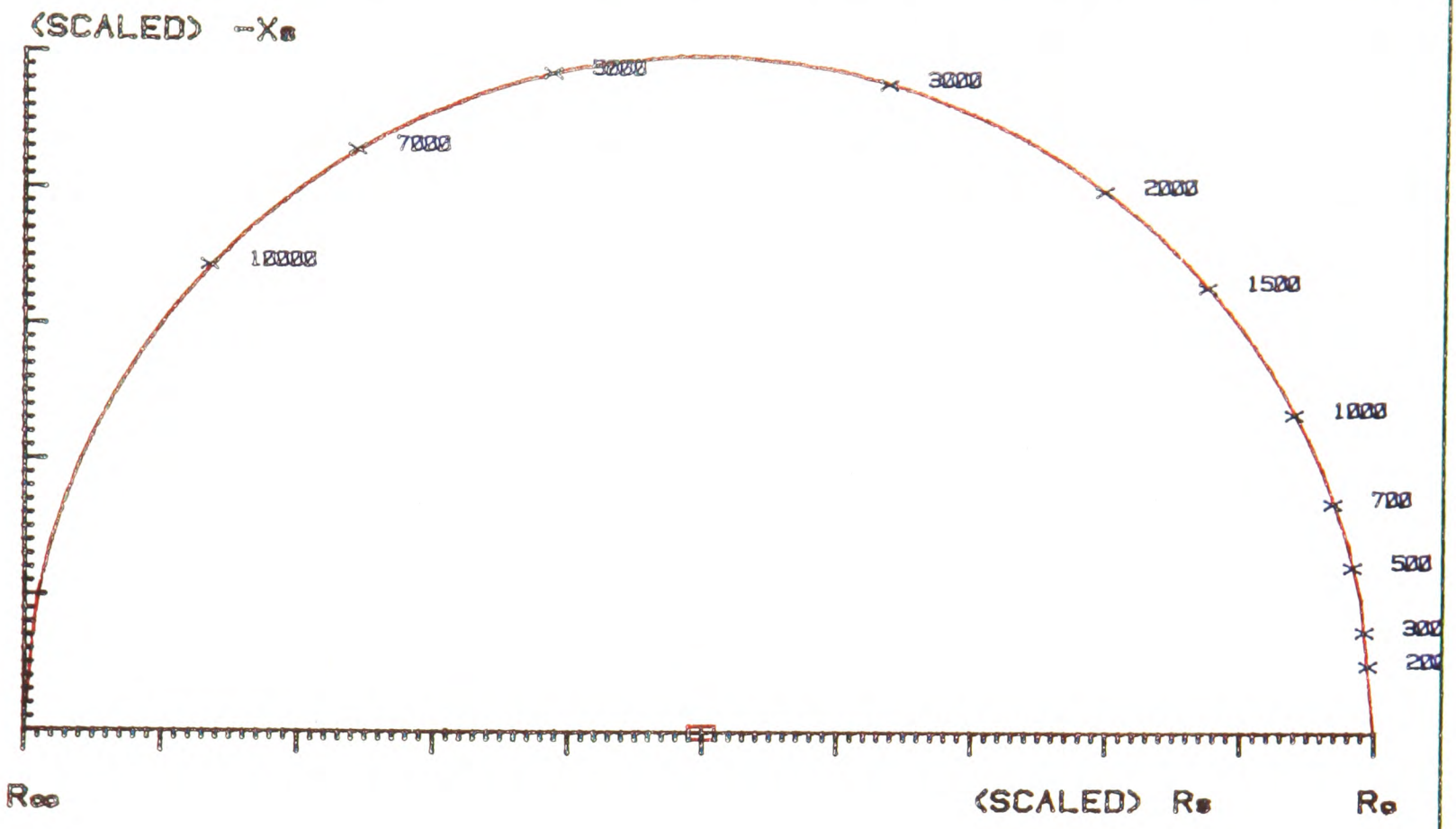
to correspond with the estimates of Barnett (1938) and Tregear (1966). It was considered reasonable, following the investigations of Holbrook and Odland (1974), to set the value of n equal to 20 as an average number of cell layers in the corneum (n = L(MAX) in the Figures). A Figure was then produced for each of the cases Q = 1, 50, 100, 500, 1,000 and 10,000. Given R_1, Q and n a particular value for the sum of the resistances in the chain followed by adding values obtained from (11.5.b.32), and this sum was called SUM R(L). The possibility of the corneum being shunted by skin appendages was allowed for by attaching in parallel with the network of Fig. 11.5.b.I a resistance R(SHUNT), the value of which was set at

S times SUM R(L). In the present series of simulations, S was set equal to 500, making R(SHUNT) enormous and consequently the effect of shunting quite irrelevant, so that the calculations were truly representative of the behaviour of a Barnett-Tregear network. The value of R_∞, which is small, was neglected.

The results of these calculations can be seen in Figures 11.5.b.II - VII, which show principally that the complex impedance locus is skewed for Q > 1, as was emphasized above. They also show that the fit to an arc of a circle becomes worse as Q increases, and that although the m value of the arc best-fitted by least squares over the whole of the complex impedance locus increases with increase in Q, even at Q = 10,000 the value of m is still less than 0.15. Moreover the larger is the value of Q, the less rapidly m increases with it. Of course by fitting to particular sections of the locus, m can be increased a little above the "whole locus" value, but there is still an absolute limit of about 0.23 predicted from the continuum model above, and this is quite inadequate to model the range of values observed clinically.

We may therefore conclude that the Barnett-Tregear model is useless in solving the problem of the origin and form of the DRT in human skin in vivo.

GRAPH OF POINTS ON THE COMPLEX IMPEDANCE LOCUS FITTED TO AN ARC BY LEAST SQUARES.



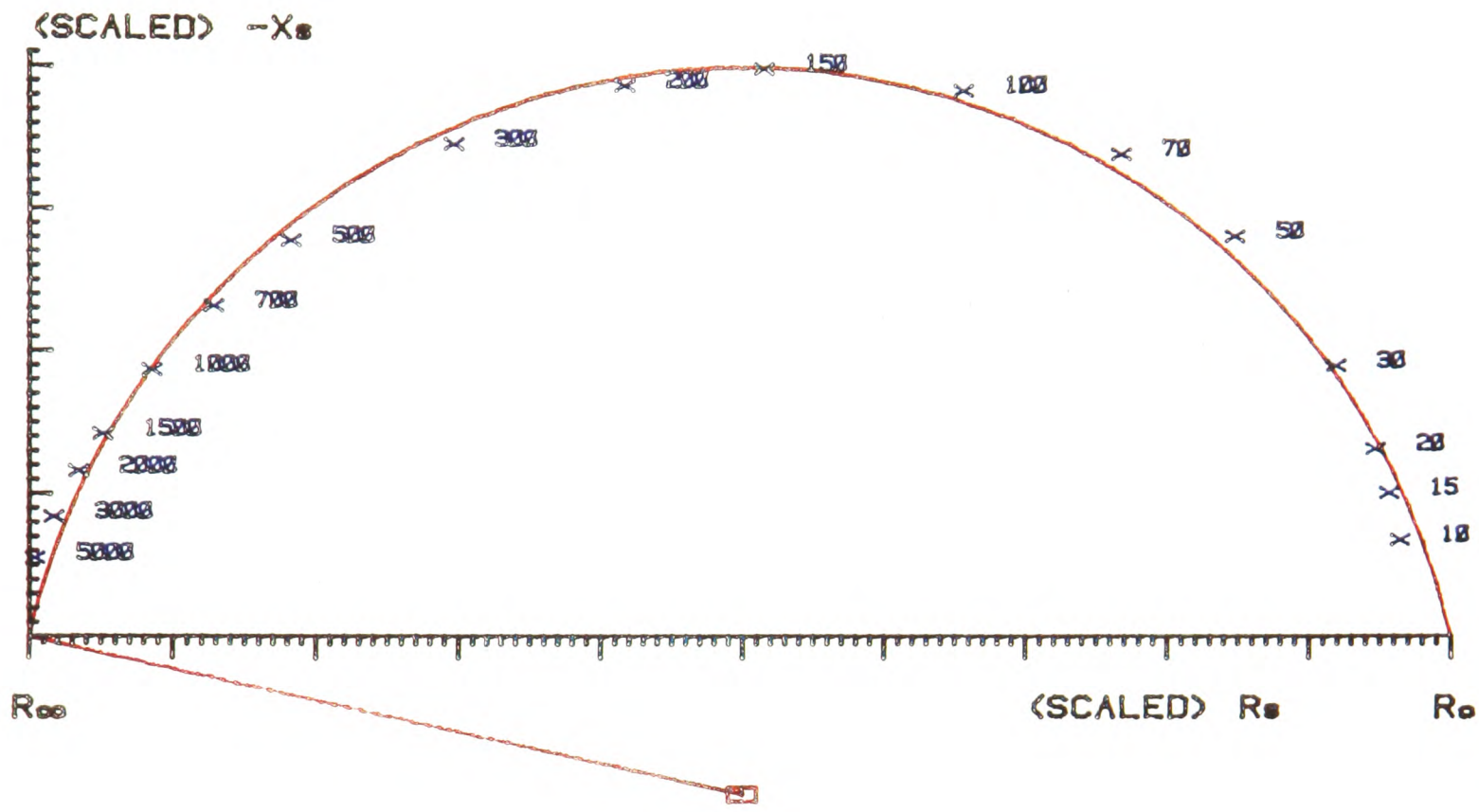
FOR THE SHUNTED GRADIENT MODEL
WITH CIRCUIT PARAMETERS

Q	=	1
S	=	500
R(SHUNT)	=	2.00000E+06
C	=	2.00000E-07
R1	=	200
L(MAX)	=	20
SUM R(L)	=	4000
R(D.C.)	=	3992.02

THE LEAST-SQUARES FIT RESULTS ARE.			+PSE	+/-SE	-PSE
R(ZERO)	=	3992.01		1.61781	
R(INFINITY)	=	.019937		1.61781	
F(PEAK) [USING M]	=	3986.8	120.008		116.502
F(PEAK) [USING M']	=	3986.81	87.377		85.5039
M FROM Z LOCUS ARC	=	-1.27005E-04		4.82505E-04	
M' FROM V/U PLOT	=	-6.10352E-05		2.60545E-03	
STUDENT'S T(M&M')	=	2.48967E-02		FOR 17 D.O.F.	
& WEIGHTED COEFF. DET. OF V/U PLOT	=	.999939			

Fig. 11.5.b.II

GRAPH OF POINTS ON THE COMPLEX IMPEDANCE LOCUS FITTED TO AN ARC BY LEAST SQUARES.



FOR THE SHUNTED GRADIENT MODEL
WITH CIRCUIT PARAMETERS

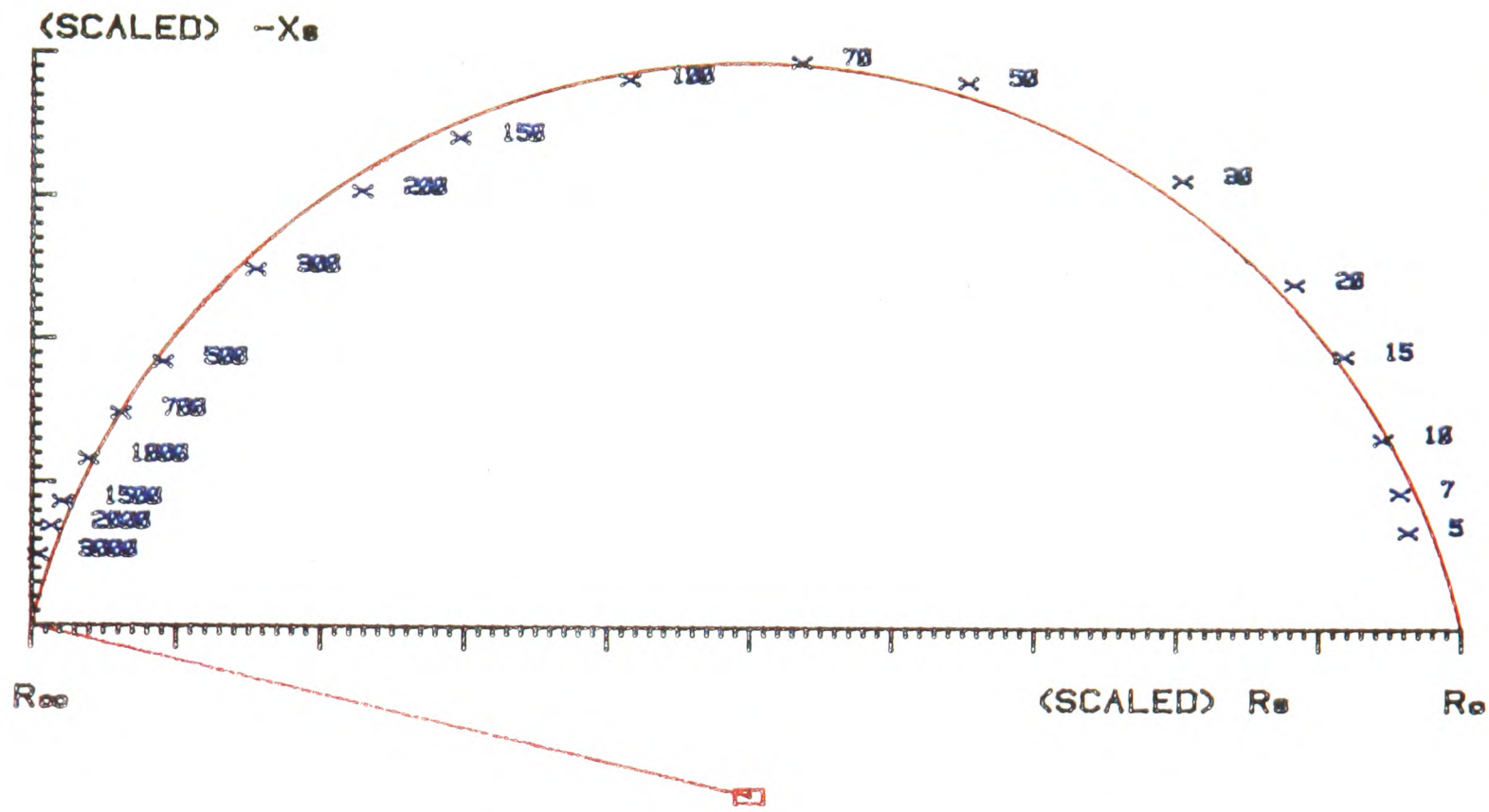
Q	=	50
S	=	500
R (SHUNT)	=	2.64324E+07
C	=	2.00000E-07
R1	=	200
L (MAX)	=	20
SUM R (L)	=	52864.9
R (D. C.)	=	52759.4

THE LEAST-SQUARES FIT RESULTS ARE.

			+PSE	+/-SE	-PSE
R (ZERO)	=	54273.2		404.451	
R (INFINITY)	=	211.255		404.451	
F (PEAK) [USING M]	=	157.941	15.8187		14.3785
F (PEAK) [USING M']	=	157.936	5.77905		5.57504
M FROM Z LOCUS ARC	=	-.140713		8.68922E-03	
M' FROM V/U PLOT	=	-.146237		6.03824E-03	
STUDENT'S T (M&M')	=	.522003		FOR 29 D.O.F.	
& WEIGHTED COEFF. DET. OF V/U PLOT	=	.99925			

Fig. 11.5.b.III

GRAPH OF POINTS ON THE COMPLEX IMPEDANCE LOCUS FITTED TO AN ARC BY LEAST SQUARES.



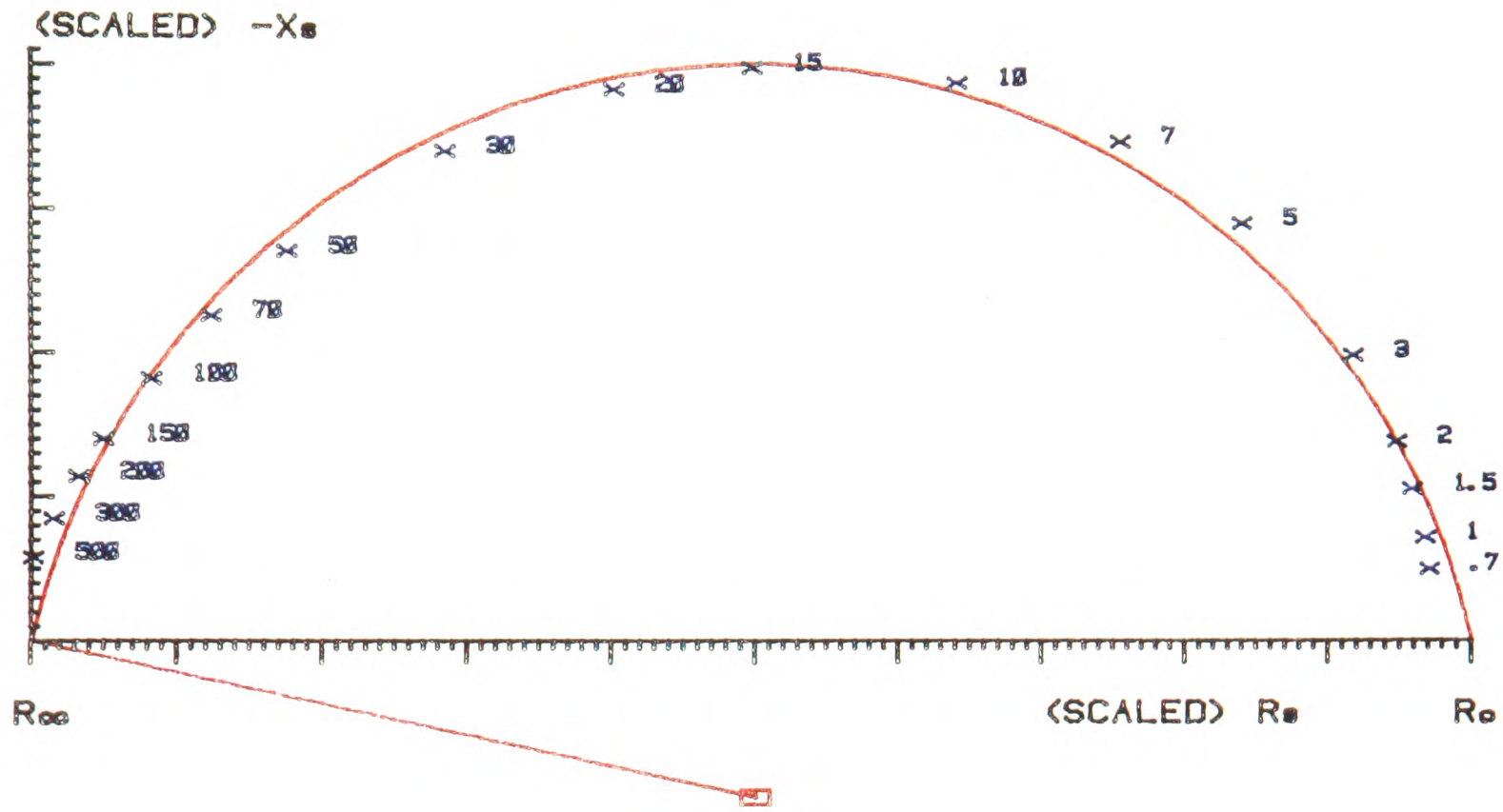
FOR THE SHUNTED GRADIENT MODEL
WITH CIRCUIT PARAMETERS

Q	=	100
S	=	500
R(SHUNT)	=	4.60952E+07
C	=	2.00000E-07
R1	=	200
L(MAX)	=	20
SUM R(L)	=	92190.3
R(D.C.)	=	92006.3

THE LEAST-SQUARES FIT RESULTS ARE.			+PSE	+/-SE	-PSE
R(ZERO)	=	94862.4		701.855	
R(INFINITY)	=	581.539		701.855	
F(PEAK) [USING M]	=	78.079	6.62177		6.10408
F(PEAK) [USING M']	=	78.0863	2.37289		2.3029
M FROM Z LOCUS ARC	=	-.148498		8.64455E-03	
M' FROM V/U PLOT	=	-.15411		5.75629E-03	
STUDENT'S T(M&M')	=	.540545		FOR 31 D.O.F.	
& WEIGHTED COEFF. DET. OF V/U PLOT	=	.99926			

Fig. 11.5.b.IV

GRAPH OF POINTS ON THE COMPLEX IMPEDANCE LOCUS FITTED TO AN ARC BY LEAST SQUARES.



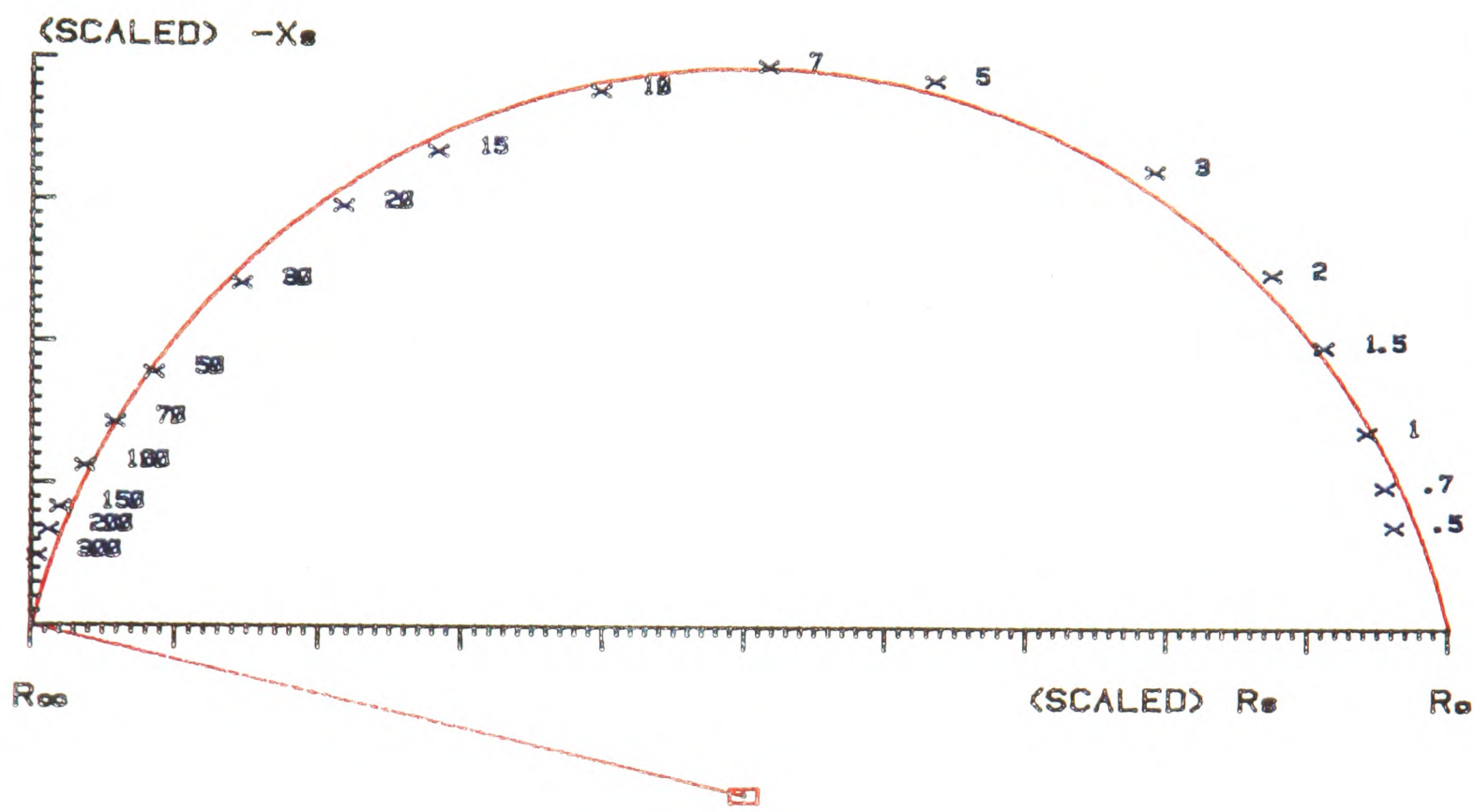
FOR THE SHUNTED GRADIENT MODEL
WITH CIRCUIT PARAMETERS

Q	=	500
S	=	500
R(SHUNT)	=	1.78968E+08
C	=	2.000000E-07
R1	=	200
L(MAX)	=	20
SUM R(L)	=	357935
R(D.C.)	=	357221

THE LEAST-SQUARES FIT RESULTS ARE:			+PSE	+/-SE	-PSE
R(ZERO)	=	366079		2915.78	
R(INFINITY)	=	5806.14		2915.78	
F(PEAK) [USING M]	=	15.0705	.970564		.911839
F(PEAK) [USING M']	=	15.0687	.298117		.292332
M FROM Z LOCUS ARC	=	-.138197		9.42155E-03	
M' FROM V/U PLOT	=	-.146508		8.07902E-03	
STUDENT'S T(M&M')	=	.741115		FOR 31 D.O.F.	
& WEIGHTED COEFF. DET. OF V/U PLOT	=	.999189			

Fig. 11.5.b.V

GRAPH OF POINTS ON THE COMPLEX IMPEDANCE LOCUS FITTED TO AN ARC BY LEAST SQUARES.



FOR THE SHUNTED GRADIENT MODEL
WITH CIRCUIT PARAMETERS

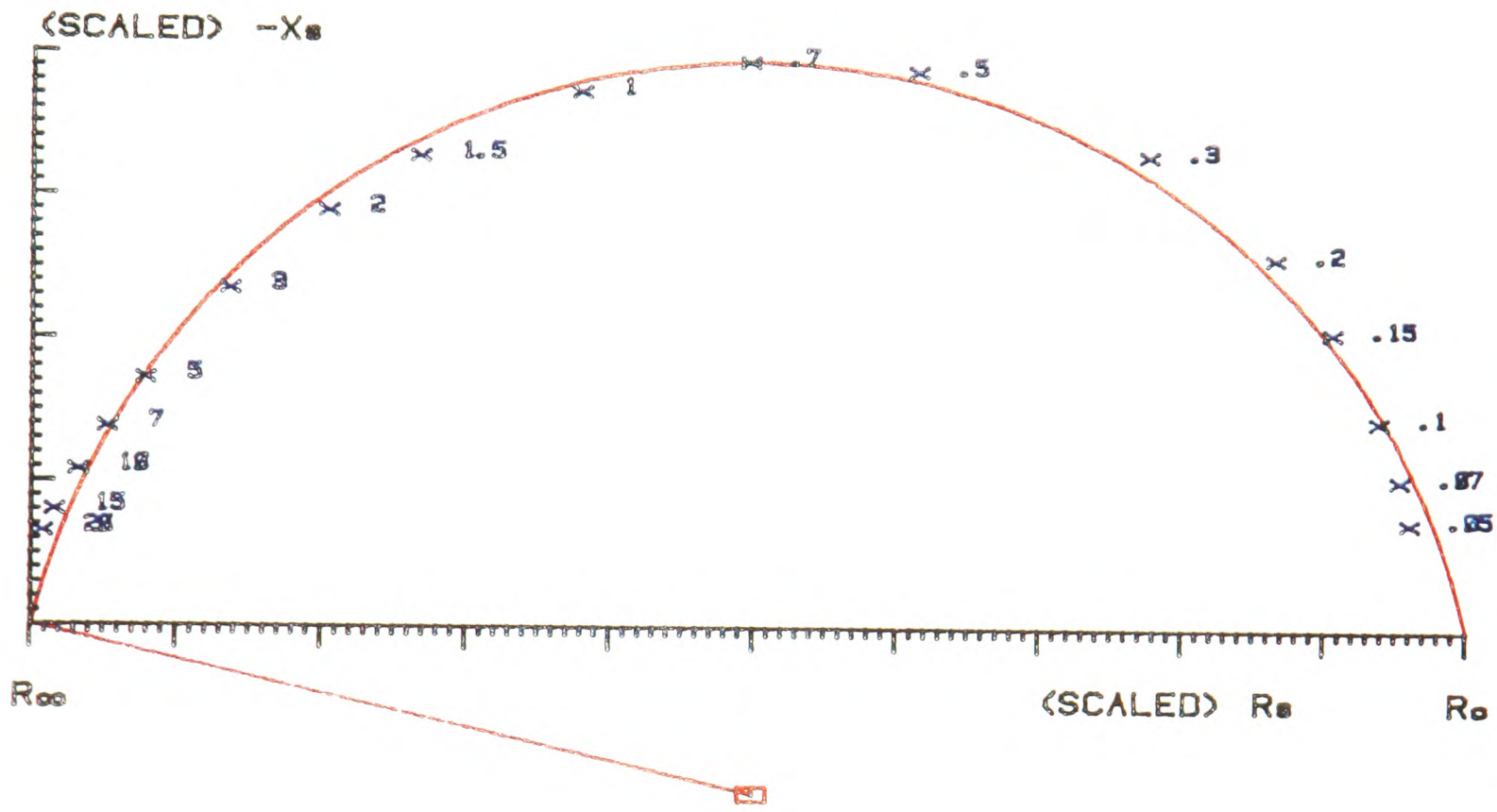
Q	=	1000
S	=	500
R(SHUNT)	=	3.27848E+08
C	=	2.00000E-07
R1	=	200
L(MAX)	=	20
SUM R(L)	=	655696
R(D.C.)	=	654388

THE LEAST-SQUARES FIT RESULTS ARE.

			+PSE	+/-SE	-PSE
R(ZERO)	=	675394		5058.38	
R(INFINITY)	=	7890.52		5058.38	
F(PEAK) [USING M]	=	7.38937	.233753		.226585
F(PEAK) [USING M']	=	7.3884	.110124		.108507
M FROM Z LOCUS ARC	=	-.149622		8.79784E-03	
M' FROM V/U PLOT	=	-.153623		6.06505E-03	
STUDENT'S T(M&M')	=	.374356		FOR 31 D.O.F.	
& WEIGHTED COEFF. DET. OF V/U PLOT	=	.999179			

Fig. 11.5.b.VI

GRAPH OF POINTS ON THE COMPLEX IMPEDANCE LOCUS FITTED TO AN ARC BY LEAST SQUARES.



FOR THE SHUNTED GRADIENT MODEL
WITH CIRCUIT PARAMETERS

Q	=	10000
S	=	500
R (SHUNT)	=	2.60298E+09
C	=	2.00000E-07
R1	=	200
L (MAX)	=	20
SUM R (L)	=	5.20595E+06
R (D. C.)	=	5.19558E+06

THE LEAST-SQUARES FIT RESULTS ARE.			+PSE	+/-SE	-PSE
R (ZERO)	=	5.36136E+06		42758.2	
R (INFINITY)	=	78839.7		42758.2	
F (PEAK) [USING M]	=	.69852	5.89097E-03		5.84173E-03
F (PEAK) [USING M']	=	.698386	2.69473E-03		2.68435E-03
M FROM Z LOCUS ARC	=	-.14593		9.43413E-03	
M' FROM V/U PLOT	=	-.150589		8.56136E-03	
STUDENT'S T (M&M')	=	.405443		FOR 29 D.O.F.	
& WEIGHTED COEFF. DET. OF V/U PLOT	=	.999106			

Fig. 11.5.b.VII

11.5.c Chain networks with exponential capacitance gradients

Having disproved the usefulness of the model used by Barnett and Tregear, although not that of their approach, the next thing to do seemed to be to investigate the behaviour of the network of Fig.11.5.b.I if the capacitors changed with depth and the resistors stayed constant, even though such a circumstance seemed highly unlikely in skin for both physical and biological reasons. However, quite arbitrarily an exponential dependence upon depth was chosen for the capacitors, and the results proved to be interesting.

Let the local resistivity ρ be independent of, but let the local permittivity ε change exponentially with, position x in the skin according to

$$\varepsilon(x) = \varepsilon_1 \exp\left[\frac{\ln Q}{X} x\right] \qquad 0 \leq x \leq X$$

$$= 0 \qquad x < 0,\ x > 0 \qquad (11.5.c.1)$$

where

$$Q = \frac{\rho\varepsilon(X)}{\rho\varepsilon(o)} = \frac{\text{maximum } \tau}{\text{minimum } \tau} = \frac{\tau_2}{\tau_1} \qquad (11.5.c.2)$$

then if

$$dx = \frac{X}{n}, \quad n \to \infty \qquad (11.5.c.3)$$

we may write for unit area

$$R(x,\ x+dx) = R(dx) = \rho\, dx \qquad (11.5.c.4)$$

and

$$\tau(x,\ x+dx) = R(x,\ x+dx)\ C(x,\ x+dx) \qquad (11.5.c.5)$$

so

$$\tau(x,\ x+dx) \quad = \quad \frac{\rho}{dx} \int_{x}^{x+dx} \varepsilon_1 \exp\left[\frac{\ln Q}{X} x\right] \ dx \qquad (11.5.c.6)$$

which for dx << X reduces to approximately

$$\tau(x, x+dx) \quad = \quad \rho\ \varepsilon_1 \ \exp\left[\frac{\ln Q}{X} x\right] \qquad (11.5.c.7)$$

Now the contribution to the D.C. resistance made by relaxing units having u between u and u + du is r(u)du from equation (11.5.a.8), which implies

$$r(u)\,du \quad = \quad \text{number } (x)\ p(x)\ dx \qquad (11.5.c.8)$$

if u is position ,x. Thus (11.5.a.7), which can be written

$$y(\tau) \quad = \quad \frac{du}{d\tau} \ \frac{r(u)\,du}{du} \qquad (11.5.c.9)$$

becomes

$$y(\tau) \quad = \quad \frac{1}{\tau} \frac{X}{\ln Q} \ \frac{n \frac{dx}{X} \rho\ dx}{dx} \qquad (11.5.c.10)$$

because $\rho(x) = \rho$. Again we have assumed a uniform linear density of relaxing units to obtain the ndx/X factor. Then applying (11.5.c.3),

$$y(\tau) \quad = \quad \frac{1}{\tau} \ \frac{X}{\ln Q} \rho \qquad (11.5.c.11)$$

and writing this in terms of

$$(R_o - R_\infty) \quad = \quad \int_{u_{min}}^{u_{max}} r(u)\ du \qquad (11.5.c.12)$$

$$= \int_{o}^{X} \frac{n\ dx}{X} \rho\ dx \quad = \quad \rho\ X \qquad (11.5.c.13)$$

produces

$$y(\tau) = \frac{(R_o - R_\infty)}{\ln Q} \frac{1}{\tau} \qquad \tau_1 \leq \tau \leq \tau_2$$

$$= 0 \qquad \tau < \tau_1,\ \tau > \tau_2 \qquad (11.5.c.14)$$

which is correctly normalized in that it satisfies (11.5.a.6).

Therefore substituting the $y(\tau)$ of (11.5.c.14) into (11.5.a.3) we have

$$R_s = R_\infty + \frac{(R_o - R_\infty)}{\ln Q} \int_{\tau_1}^{\tau_2} \frac{\frac{1}{\tau}\, d\tau}{1 + (\omega\tau)^2} \qquad (11.5.c.15)$$

and by means of the standard integral

$$\int \frac{dx}{x\,[1+x^2]} = \ln \frac{x}{\sqrt{1+x^2}} \qquad (11.5.c.15)$$

with $x = \omega\tau$, (11.5.c.15) leads (eventually) to the final result

$$\frac{R_s - R_\infty}{R_o - R_\infty} = \left[1 - \frac{1}{2 \ln Q} \ln \frac{[1+(\omega\tau_2)^2]}{[1+(\omega\tau_1)^2]} \right] \qquad (11.5.c.16)$$

which may be compared with the analogous equation of Fröhlich (1958, eqn.12.15), whose "log" is really "ln". (Incidentally, his Fig.15 should also be re-labelled $V_o/2kT$ instead of V_o/kT.)

Similarly from (11.5.a.4) we have

$$-X_s = \frac{(R_o - R_\infty)}{\ln Q} \int_{\tau_1}^{\tau_2} \frac{\frac{1}{\tau}\, \omega\tau d\tau}{1+(\omega\tau)^2} \qquad (11.5.c.17)$$

and using

$$\int \frac{a\, dx}{a^2+x^2} = \arctan\left(\frac{x}{a}\right) \qquad (11.5.c.18)$$

we find

$$\frac{-X_s}{R_o - R_\infty} = \frac{1}{\ln Q} \left[\arctan(\omega\tau_2) - \arctan(\omega\tau_1) \right] \qquad (11.5.c.19)$$

Equations (11.5.c.16) and (11.5.c.19) define the resolved components of the complex impedance locus of a "continuum" version of Fig. 11.5.b.I in which $n \to \infty$ and $\tau_1 = R\ C_{min}$, $\tau_2 = R\ C_{max}$. They predict a locus which is symmetrical but flattened, in fact a semi-ellipse because (11.5.c.14) is a log-uniform distribution (also known as a Fröhlich distribution after its greatest populariser. Its use has been reviewed by Gross (1953, p.67, section 10)).

The fact that the locus is a semi-ellipse means that it is possible to fit clinical data obtained on skin rather better using this model than the Barnett-Tregear models of the last subsection. Nevertheless, as we can see from the computer simulations shown in Figures 11.5.c.I - VIII, for $Q > 1$ the locus is still very evidently unlike a minor arc of a circle. These simulations were run with C1 =0.1 microfarads, a (constant) R of 10 kΩ, a negligible degree of shunting (S = 1,000), and increasing values of Q. The purpose of the series is to show that although m increases as Q increases, *by the time that m reaches clinically appropriate values of say 0.3 at about Q = 50, the complex impedance locus is very much distorted from a minor arc of a circle.*

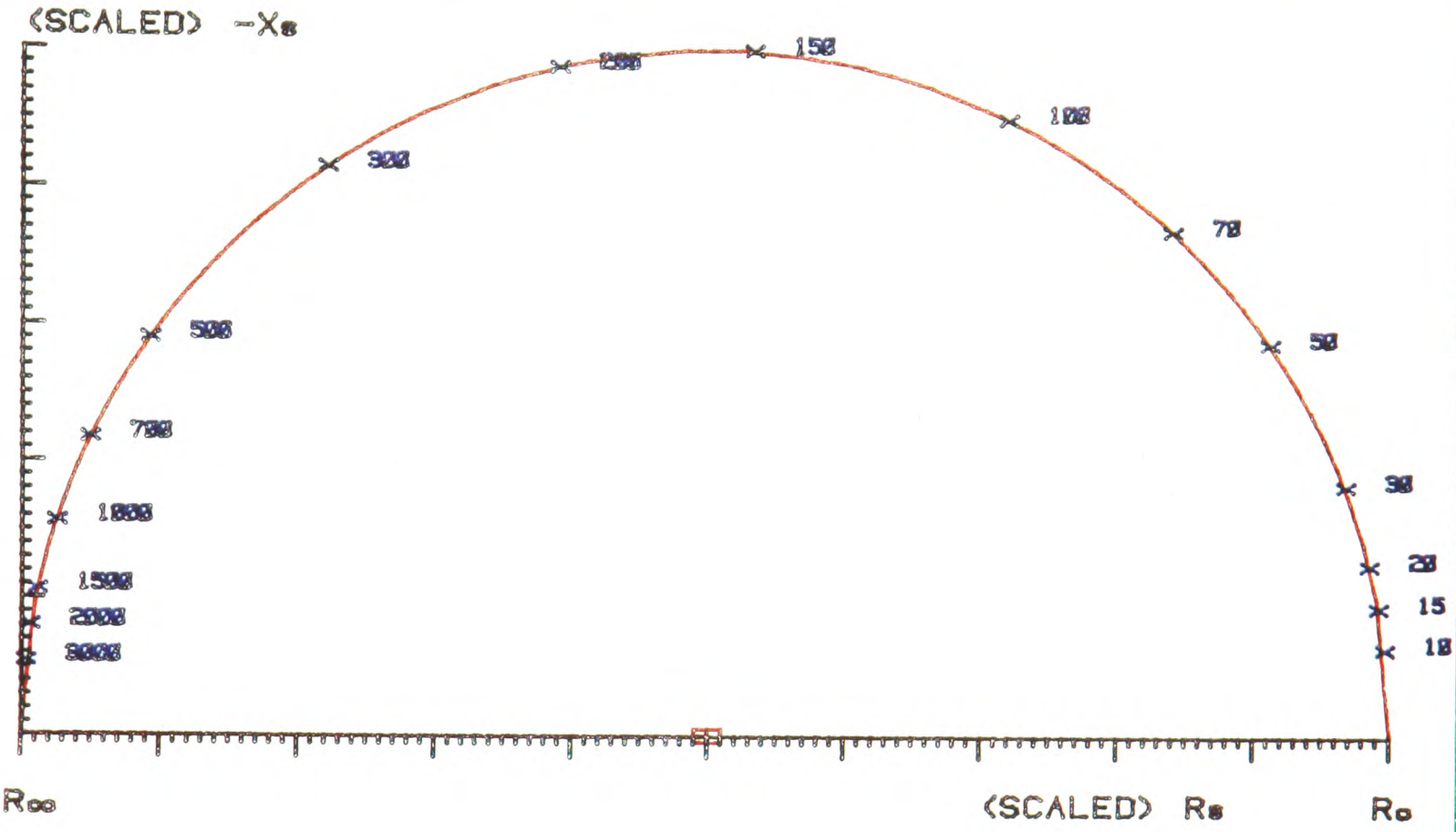
It should also be noted that there is no biological or physical reason to expect permittivity to change exponentially with depth through the corneum while resistivity stays constant, and indeed I can think of a number of reasons why these conditions are not at all likely.

It is therefore interesting that Yamamoto and Yamamoto (1976b) recently derived the same complex impedance locus we have been considering here from a Barnett-Tregear type of model in which the permittivity of skin remained

constant with depth while the resistivity varied, although in the totally arbitrary form of a rectangular hyperbola. (Incidentally, the "S" in their equation (20) should in fact be "-A".) Presumably they chose this bio-physically unsupported function for $\rho(x)$ simply in order to obtain a nicely symmetrical complex impedance locus, because in their (1976a) paper and in this one too they went to great lengths to prove that there is experimental evidence in favour of an EXPONENTIAL dependence of resistivity upon depth, and moreover that permittivity did NOT remain constant with depth, (cf. 1976b Fig.3), both these findings conflicting with the basic assumptions of their subsequent model.

Obviously, the chain network model most appropriate to their findings would have some of the features of the Barnett-Tregear version discussed in the last subsection, combined with some of the features of the version we examined here, in which the permittivity but not the resistivity is dependent upon depth. However, ~~since two blacks do not make a white,~~ even such a combined model is unlikely to be able to produce a circular arc locus unless the gradients of $\varepsilon(x)$ and $\rho(x)$ were very artfully chosen indeed, on no grounds other than to obtain the right answer.

GRAPH OF POINTS ON THE COMPLEX IMPEDANCE LOCUS FITTED TO AN ARC BY LEAST SQUARES.



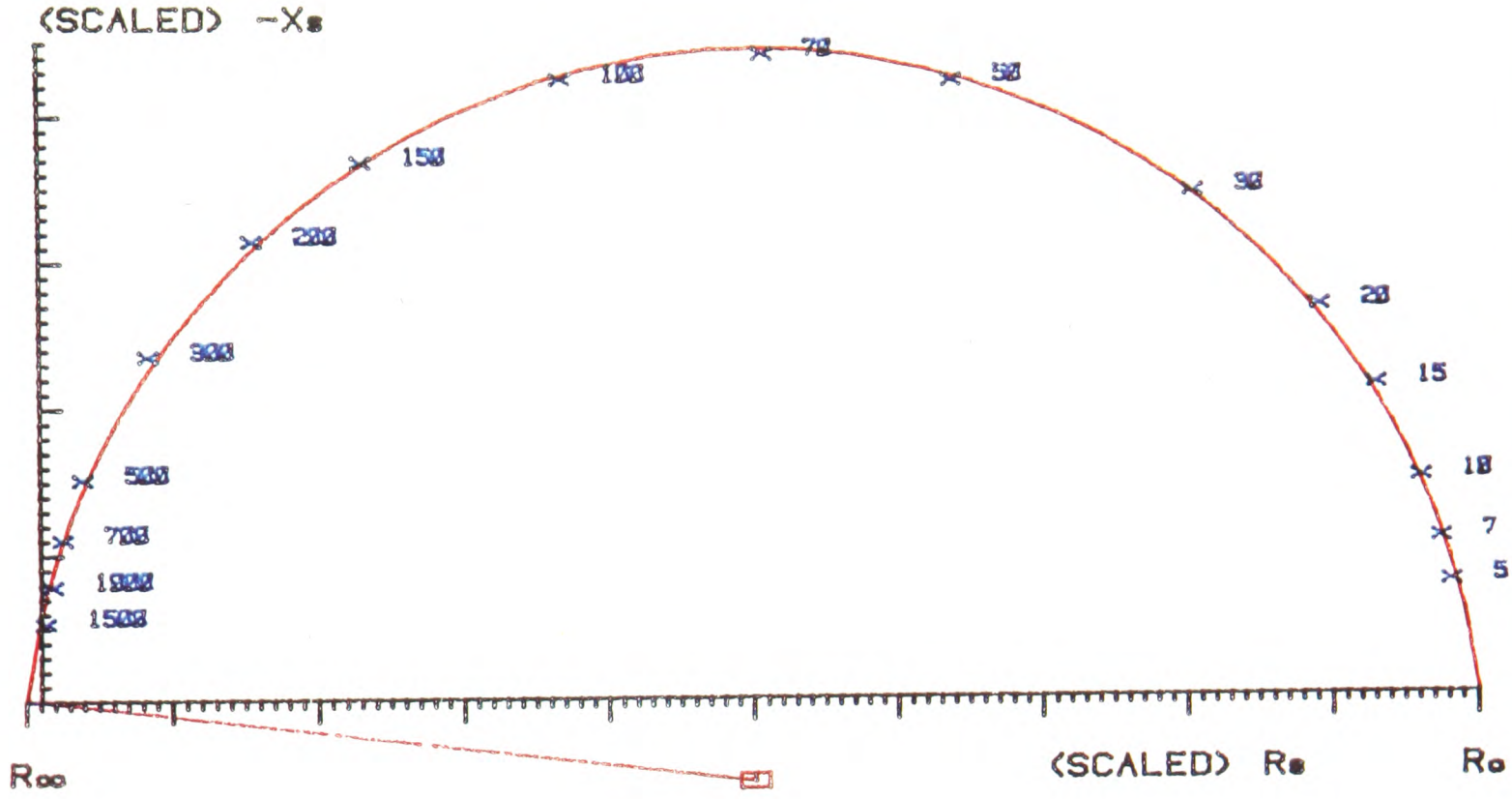
FOR THE SHUNTED GRADIENT MODEL
WITH CIRCUIT PARAMETERS

Q	=	1
S	=	1000
R(SHUNT)	=	2.000000E+08
C1	=	1.000000E-07
R	=	10000
L(MAX)	=	20
SUM R(L)	=	200000
R(D.C.)	=	199800

THE LEAST-SQUARES FIT RESULTS ARE.			+PSE	+/-SE	-PSE
R(ZERO)	=	199800		55.4109	
R(INFINITY)	=	0		55.4109	
F(PEAK) [USING M]	=	159.314	2.37033		2.33557
F(PEAK) [USING M']	=	159.314	1.09164		1.08423
M FROM Z LOCUS ARC	=	-1.26825E-04		3.18490E-04	
M' FROM V/U PLOT	=	2.52724E-05		1.34458E-03	
STUDENT'S T(M&M')	=	.110109		FOR 27 D.O.F.	
& WEIGHTED COEFF. DET. OF V/U PLOT	=	1.00003			

Fig. 11,5.c.I

GRAPH OF POINTS ON THE COMPLEX IMPEDANCE LOCUS FITTED TO AN ARC BY LEAST SQUARES.



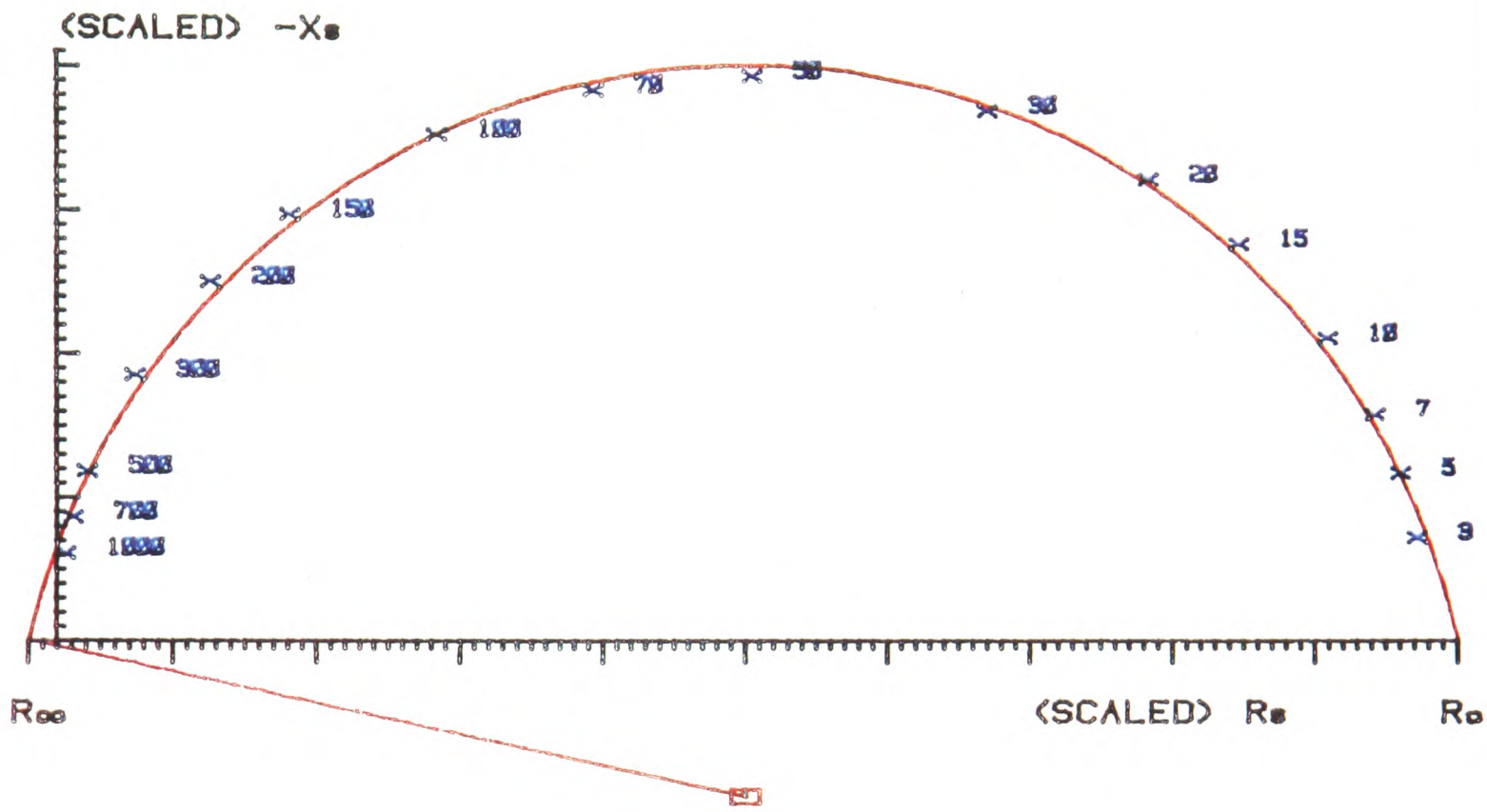
FOR THE SHUNTED GRADIENT MODEL
WITH CIRCUIT PARAMETERS

Q	=	5
S	=	1000
R(SHUNT)	=	2.00000E+08
C1	=	1.00000E-07
R	=	10000
L(MAX)	=	20
SUM R(L)	=	200000
R(D.C.)	=	199800

THE LEAST-SQUARES FIT RESULTS ARE.			+PSE	+/-SE	-PSE
R(ZERO)	=	202118		541.778	
R(INFINITY)	=	-2059.66		541.778	
F(PEAK) [USING M]	=	71.1575	11.4152		9.8371
F(PEAK) [USING M']	=	71.1378	.401718		.399475
M FROM Z LOCUS ARC	=	-7.47132E-02		3.04491E-03	
M' FROM V/U PLOT	=	-9.17082E-02		1.19111E-03	
STUDENT'S T(M&M')	=	5.19789		FOR 27 D.O.F.	
& WEIGHTED COEFF. DET. OF V/U PLOT	=	.999978			

Fig. 11.5.c.II

GRAPH OF POINTS ON THE COMPLEX IMPEDANCE LOCUS FITTED TO AN ARC BY LEAST SQUARES.



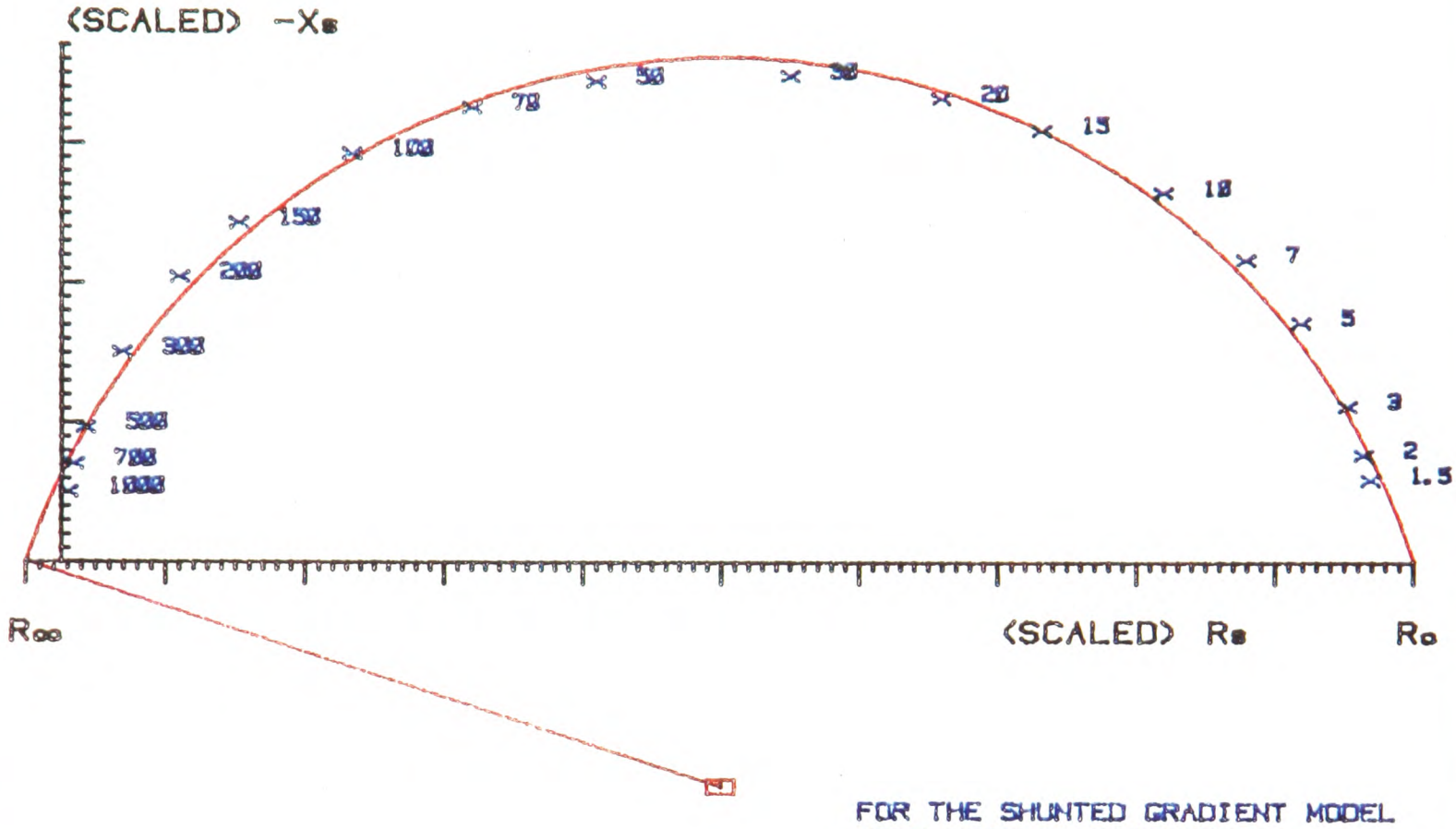
FOR THE SHUNTED GRADIENT MODEL
WITH CIRCUIT PARAMETERS

Q	=	10
S	=	1000
R(SHUNT)	=	2.00000E+08
C1	=	1.00000E-07
R	=	10000
L(MAX)	=	20
SUM R(L)	=	200000
R(D.C.)	=	199800

THE LEAST-SQUARES FIT RESULTS ARE.			+PSE	+/-SE	-PSE
R(ZERO)	=	204134		1045.8	
R(INFINITY)	=	-3991.57		1045.8	
F(PEAK) [USING M]	=	50.3549	9.8807	8.25993	
F(PEAK) [USING M']	=	50.2958	.716103	.706055	
M FROM Z LOCUS ARC	=	-.138832		5.85583E-03	
M' FROM V/U PLOT	=	-.166069		2.96533E-03	
STUDENT'S T(M&M')	=	4.14969		FOR 27 D.O.F.	
& WEIGHTED COEFF. DET. OF V/U PLOT	=	.999823			

Fig. 11.5.c.III

GRAPH OF POINTS ON THE COMPLEX IMPEDANCE LOCUS FITTED TO AN ARC BY LEAST SQUARES.



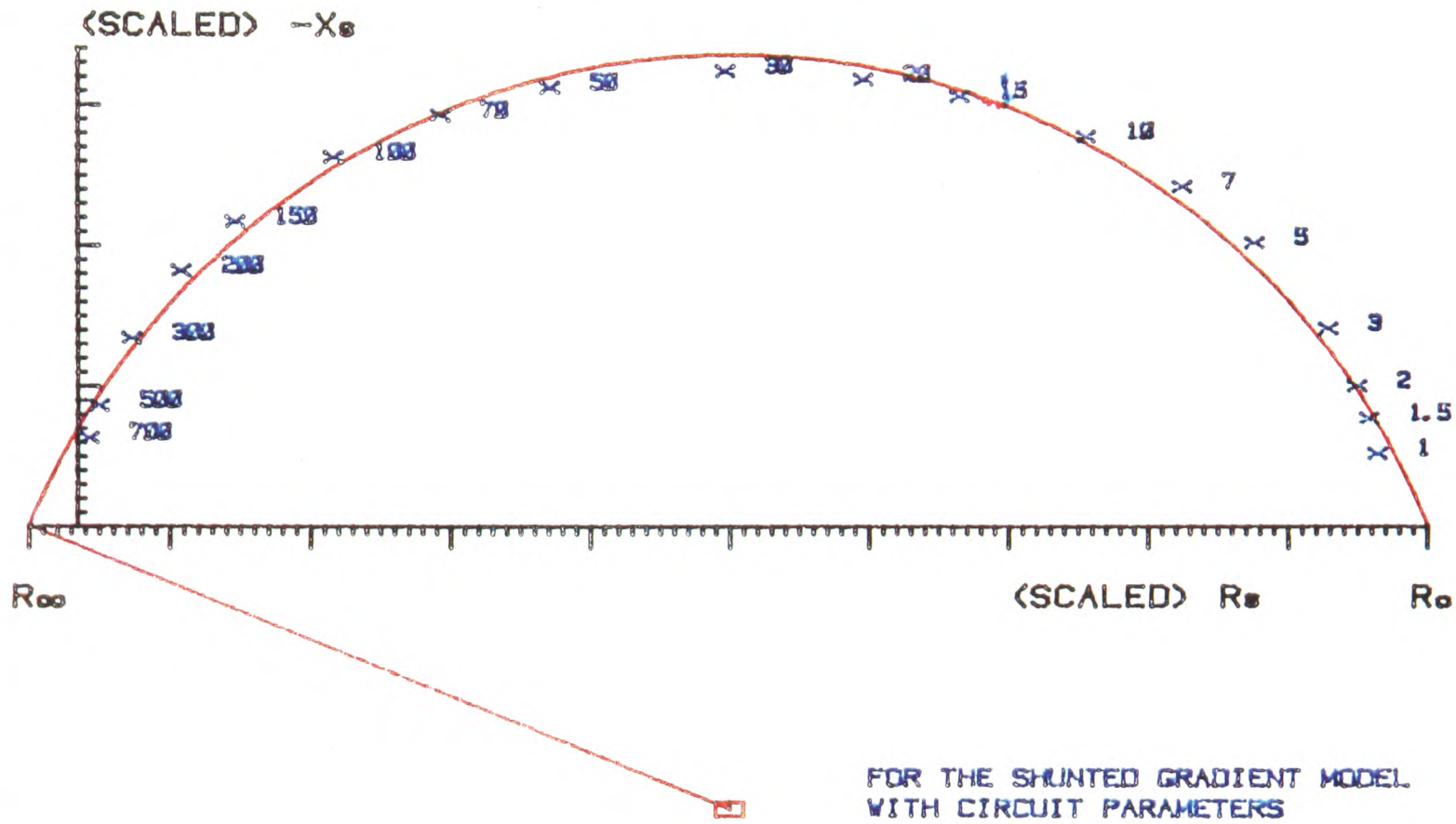
FOR THE SHUNTED GRADIENT MODEL
WITH CIRCUIT PARAMETERS

Q	=	20
S	=	1000
R(SHUNT)	=	2.00000E+08
C1	=	1.00000E-07
R	=	10000
L(MAX)	=	20
SUM R(L)	=	200000
R(D.C.)	=	199800

THE LEAST-SQUARES FIT RESULTS ARE.			+PSE	+/-SE	-PSE
R(ZERO)	=	205301		1624.25	
R(INFINITY)	=	-5347.35		1624.25	
F(PEAK) [USING M]	=	35.5584	7.59354		6.25729
F(PEAK) [USING M']	=	35.5811	.515076		.507736
M FROM Z LOCUS ARC	=	-.202298		9.01621E-03	
M' FROM V/U PLOT	=	-.243976		3.02286E-03	
STUDENT'S T(M&M')	=	4.38278		FOR 31 D.O.F.	
& WEIGHTED COEFF. DET. OF V/U PLOT	=	.999744			

Fig. 11.5.c.IV

GRAPH OF POINTS ON THE COMPLEX IMPEDANCE LOCUS FITTED TO AN ARC BY LEAST SQUARES.



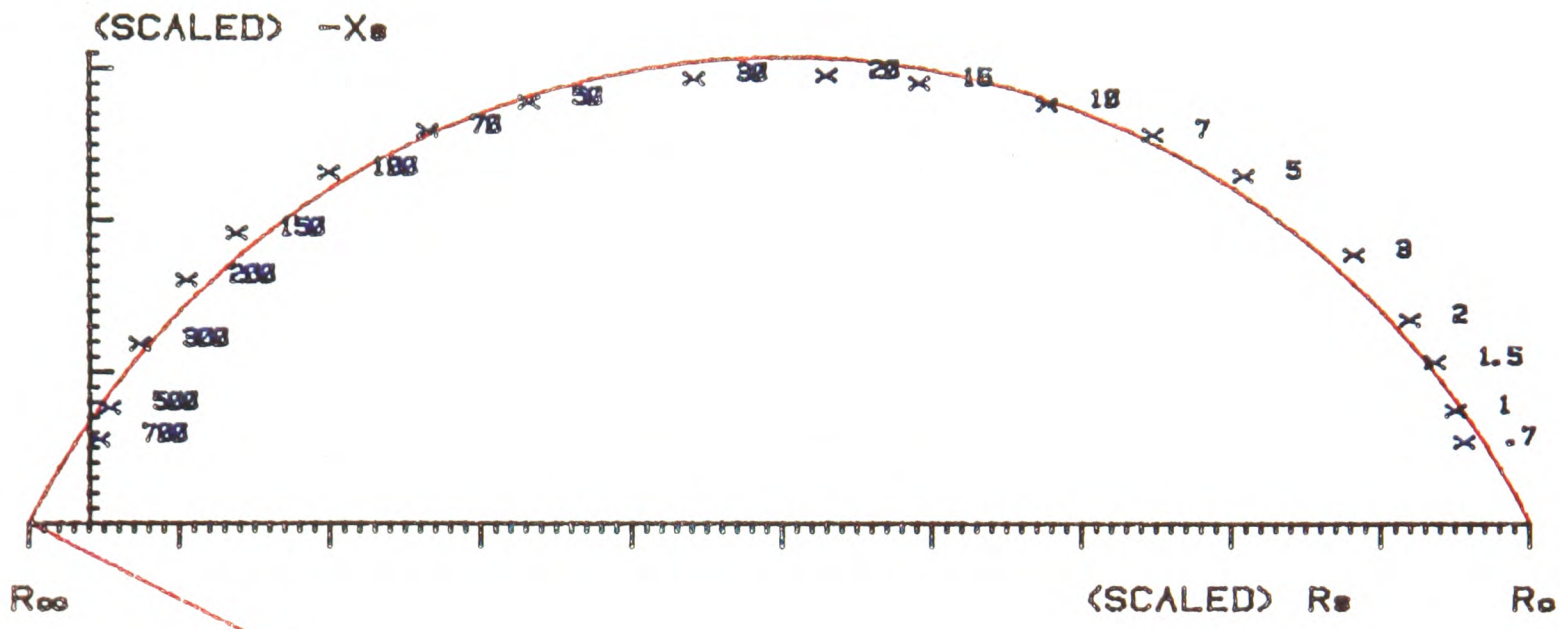
FOR THE SHUNTED GRADIENT MODEL
WITH CIRCUIT PARAMETERS

Q	=	30
S	=	1000
R(SHUNT)	=	2.00000E+08
C1	=	1.00000E-07
R	=	10000
L(MAX)	=	20
SUM R(L)	=	200000
R(D.C.)	=	199800

THE LEAST-SQUARES FIT RESULTS ARE.			+PSE	+/-SE	-PSE
R(ZERO)	=	206520		2179.91	
R(INFINITY)	=	-7213.84		2179.91	
F(PEAK) [USING M]	=	29.1879	6.03583		5.00096
F(PEAK) [USING M']	=	29.2149	.402889		.397411
M FROM Z LOCUS ARC	=	-.246486		1.17943E-02	
M' FROM V/U PLOT	=	-.288831		2.88064E-03	
STUDENT'S T(M&M')	=	3.47127		FOR 31 D.O.F.	
& WEIGHTED COEFF. DET. OF V/U PLOT	=	.999738			

Fig. 11.5.c.V

GRAPH OF POINTS ON THE COMPLEX IMPEDANCE LOCUS FITTED TO AN ARC BY LEAST SQUARES.



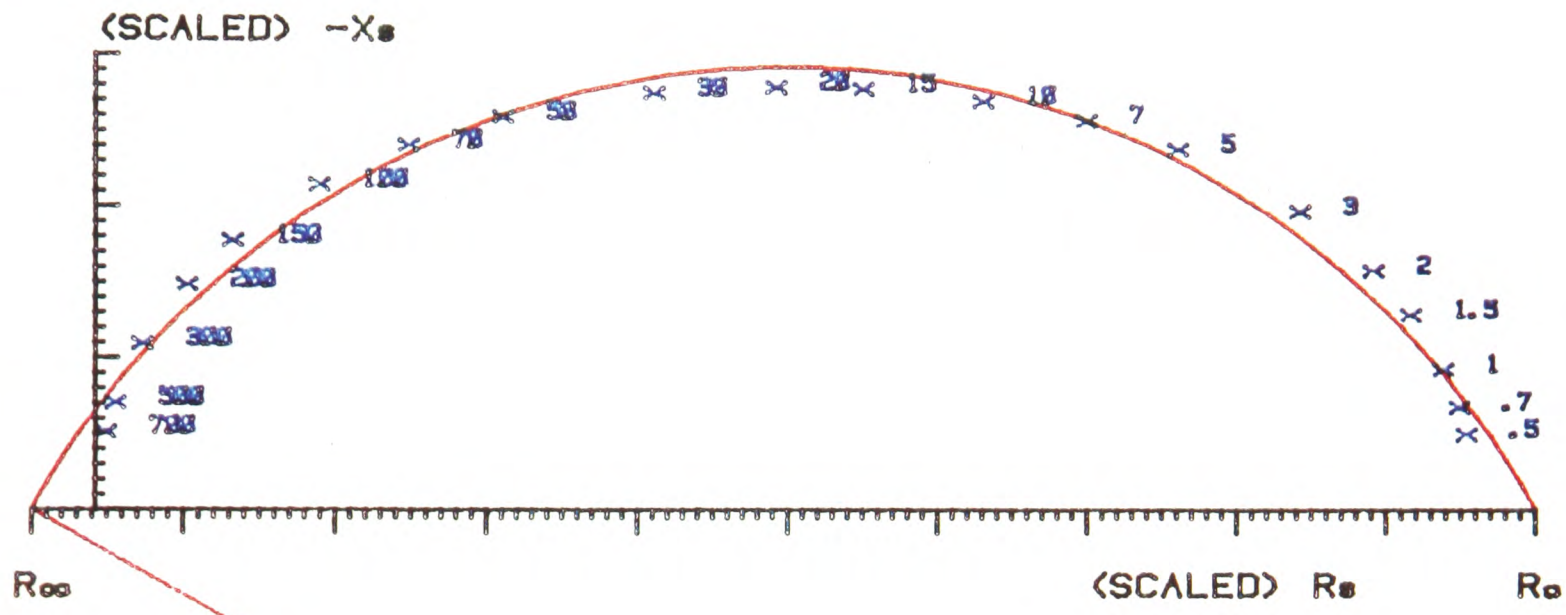
FOR THE SHUNTED GRADIENT MODEL
WITH CIRCUIT PARAMETERS

Q	=	50
S	=	1000
R(SHUNT)	=	2.00000E+08
C1	=	1.00000E-07
R	=	10000
L(MAX)	=	20
SUM R(L)	=	200000
R(D.C.)	=	199800

THE LEAST-SQUARES FIT RESULTS ARE.			+PSE	+/-SE	-PSE
R(ZERO)	=	208070		2936.78	
R(INFINITY)	=	-8575.61		2936.78	
F(PEAK) [USING M]	=	22.5338	4.37842		3.66608
F(PEAK) [USING M']	=	22.5928	.314396		.310081
M FROM Z LOCUS ARC	=	-.297005		1.52132E-02	
M' FROM V/U PLOT	=	-.340977		2.92017E-03	
STUDENT'S T(M&M')	=	2.8386		FOR 33 D.O.F.	
& WEIGHTED COEFF. DET. OF V/U PLOT	=	.999668			

Fig. 11.5.c.VI

GRAPH OF POINTS ON THE COMPLEX IMPEDANCE LOCUS FITTED TO AN ARC BY LEAST SQUARES.



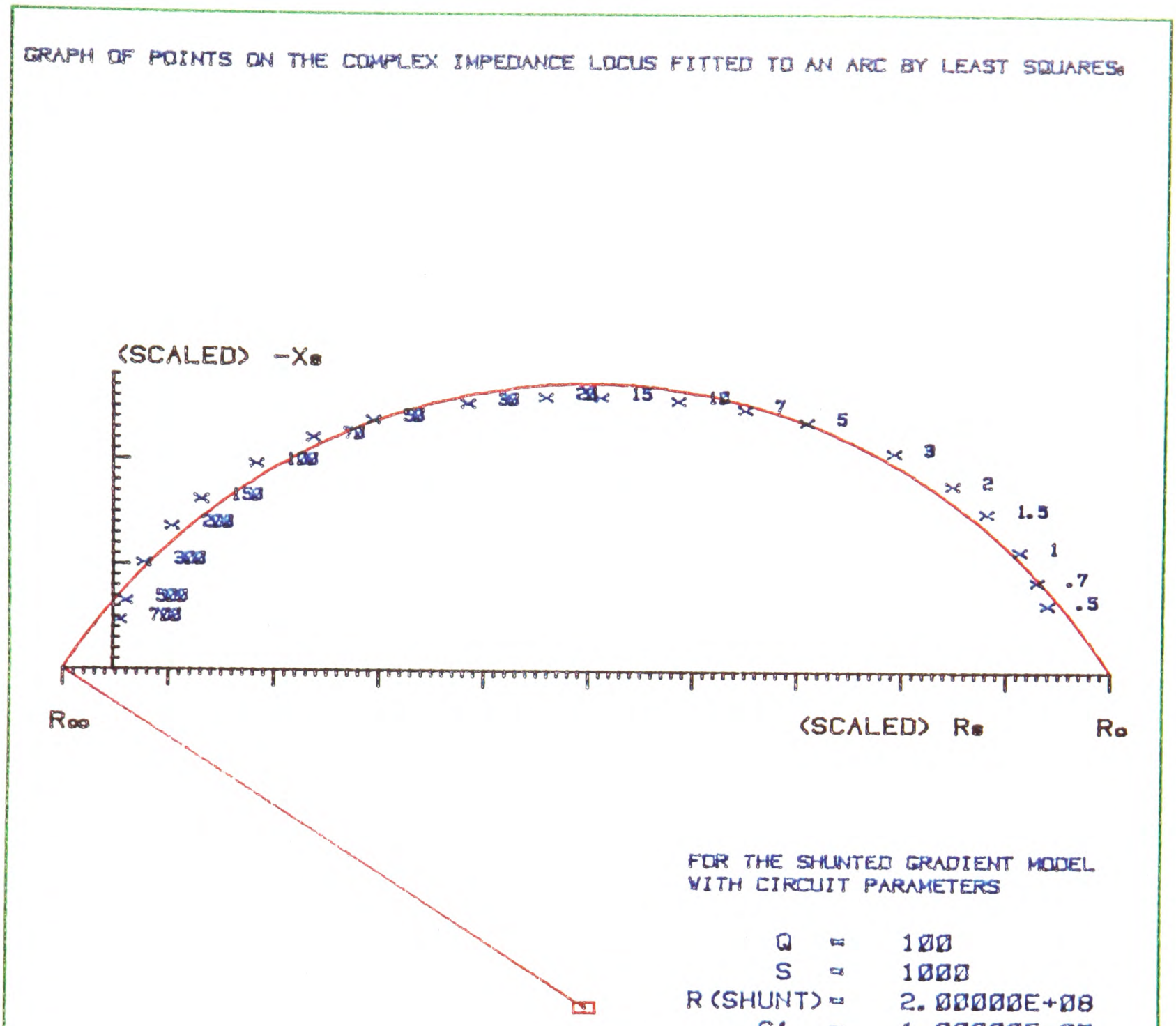
FOR THE SHUNTED GRADIENT MODEL
WITH CIRCUIT PARAMETERS

Q	=	70
S	=	1000
R (SHUNT)	=	2.00000E+08
C1	=	1.00000E-07
R	=	10000
L (MAX)	=	20
SUM R (L)	=	200000
R (D. C.)	=	199800

THE LEAST-SQUARES FIT RESULTS ARE.

			+PSE	+/-SE	-PSE
R (ZERO)	=	208745		3567.73	
R (INFINITY)	=	-9254.71		3567.73	
F (PEAK) [USING M]	=	19.0679	3.56895		3.00484
F (PEAK) [USING M']	=	19.1069	.258577		.253181
M FROM Z LOCUS ARC	=	-.328787		1.78312E-02	
M' FROM V/U PLOT	=	-.37292		2.82025E-03	
STUDENT'S T (M&M')	=	2.55543		FOR 35 D.O.F.	
& WEIGHTED COEFF. DET. OF V/U PLOT	=	.999638			

Fig. 11.5.c.VII



THE LEAST-SQUARES FIT RESULTS ARE.		+PSE	+/-SE	-PSE
R(ZERO)	= 210947		4553.59	
R(INFINITY)	= -10495.9		4553.59	
F(PEAK) [USING M]	= 15.792	2.78922		2.37053
F(PEAK) [USING M']	= 15.8093	.217733		.214777
M FROM Z LOCUS ARC	= -.363914		2.13821E-02	
M' FROM V/U PLOT	= -.408055		2.89390E-03	
STUDENT'S T(M&M')	= 2.04571		FOR 35 D.O.F.	
& WEIGHTED COEFF. DET. OF V/U PLOT	= .99957			

Fig. 11.5.c.VIII

11.5.d Shunted chain networks with exponential resistance gradients

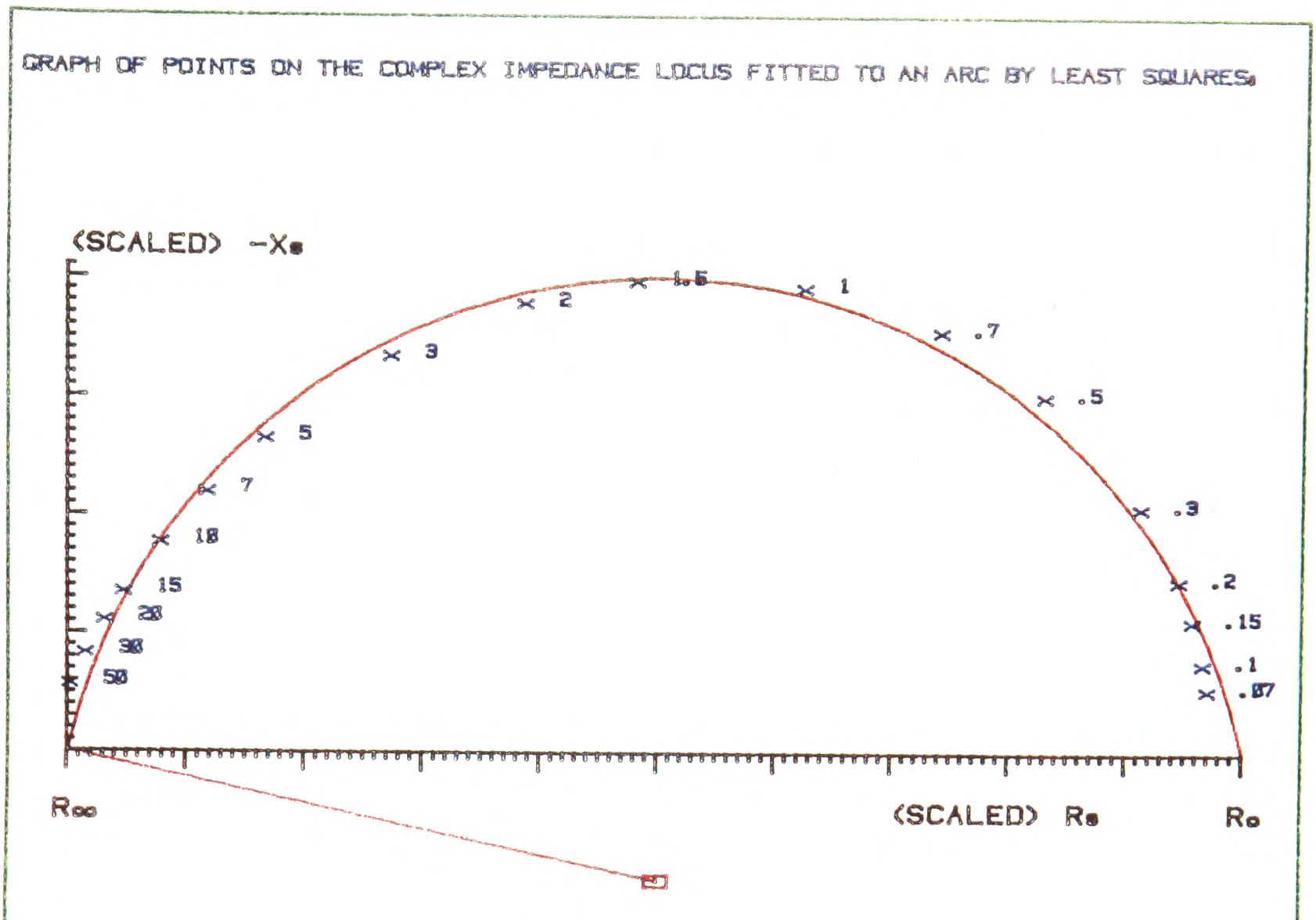
It occurred to me that it would be unfair to dismiss the chain network approach without investigating whether or not allowing for the shunting effect of skin appendages would so improve the fit of the loci to minor arcs of circles that the other deficiencies of this approach could be forgiven.

Consequently the computer simulations described in the previous two subsections were run again with new parameters.

This third series involved a Barnett-Tregear model with a resistivity gradient as before, but the purpose now was to hold Q constant and vary the degree of shunting from negligible values (S = 500) to very considerable values (S = 0.01). The series of Figures 11.5.d.I - VII shows that shunting the model much improves the goodness-of-fit, at least over a certain range of S values.

However, m is still very little dependent upon Q, as can be seen from the fourth series, Figures 11.5.d.VIII - XIII, in which Q is varied while S is maintained at a value (S = 0.05) representing a non-negligible degree of shunting. The Figures demonstrate that it is impossible to achieve clinically appropriate values of m by increasing Q even when shunting is also taking place. Finally, the fifth series, Figures 11.5.d.XIV - XVI, show that changing L(MAX), C or R_1 does not significantly affect the value of m either.

Thus we may conclude that including shunting in a Barnett-Tregear model *can* improve the goodness-of-fit to an arc of a circle, but *cannot* help with the problem of reaching the range of m values found in the skin.



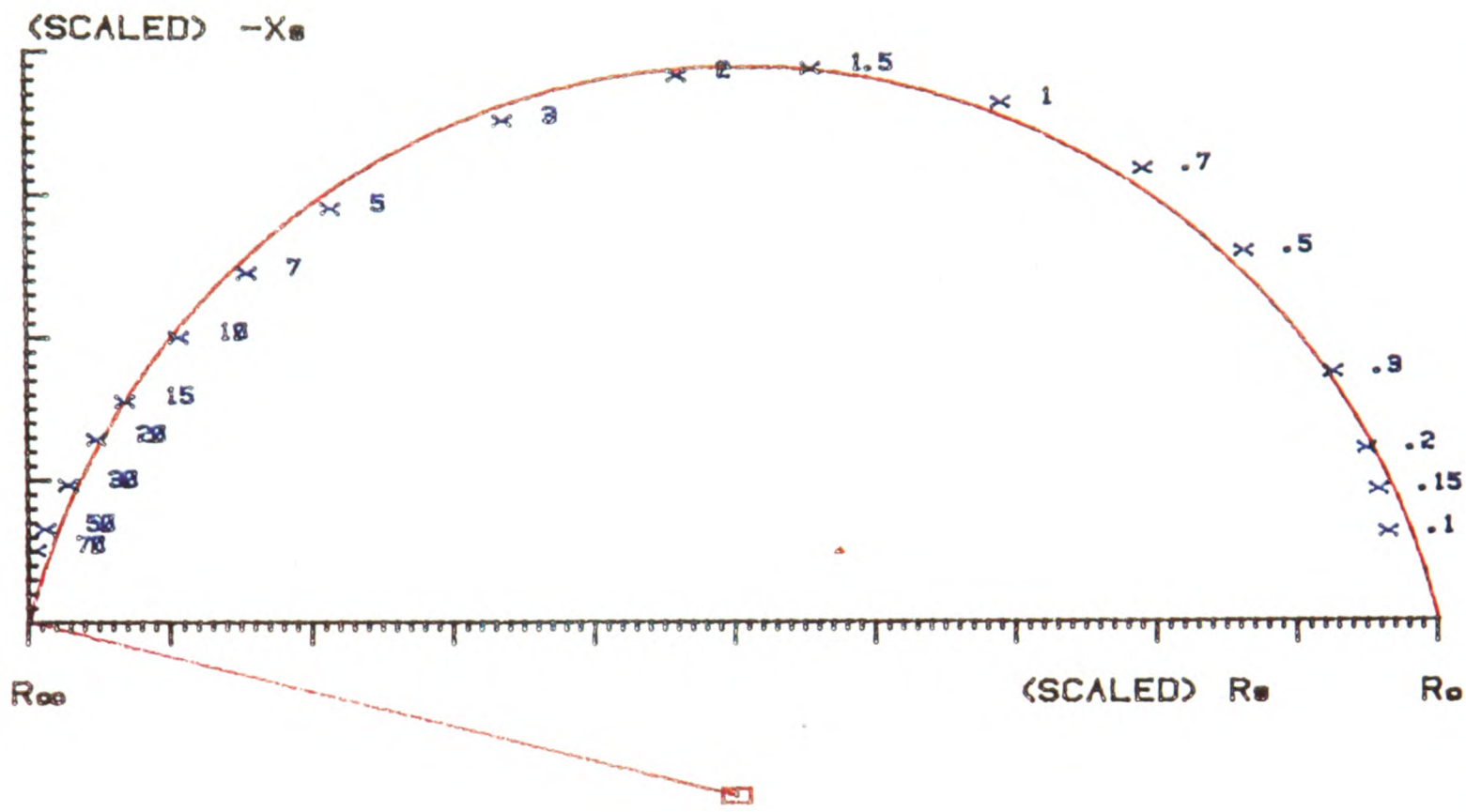
FOR THE SHUNTED GRADIENT MODEL
WITH CIRCUIT PARAMETERS

Q	=	5000
S	=	500
R (SHUNT)	=	1.38383E+09
C	=	2.00000E-07
R1	=	200
L (MAX)	=	20
SUM R (L)	=	2.76766E+06
R (D. C.)	=	2.76214E+06

THE LEAST-SQUARES FIT RESULTS ARE.			+PSE	+/-SE	-PSE
R (ZERO)	=	2.83256E+06		22397.6	
R (INFINITY)	=	47031		22397.6	
F (PEAK) [USING M]	=	1.42902	1.59657E-02		1.57893E-02
F (PEAK) [USING M']	=	1.4288	5.34439E-03		5.32460E-03
M FROM Z LOCUS ARC	=	-.13818		9.35198E-03	
M' FROM V/U PLOT	=	-.145058		5.90751E-03	
STUDENT'S T (M&M')	=	.623589		FOR 31 D.O.F.	
& WEIGHTED COEFF. DET. OF V/U PLOT	=	.999237			

Fig. 11.5.d.I

GRAPH OF POINTS ON THE COMPLEX IMPEDANCE LOCUS FITTED TO AN ARC BY LEAST SQUARES.



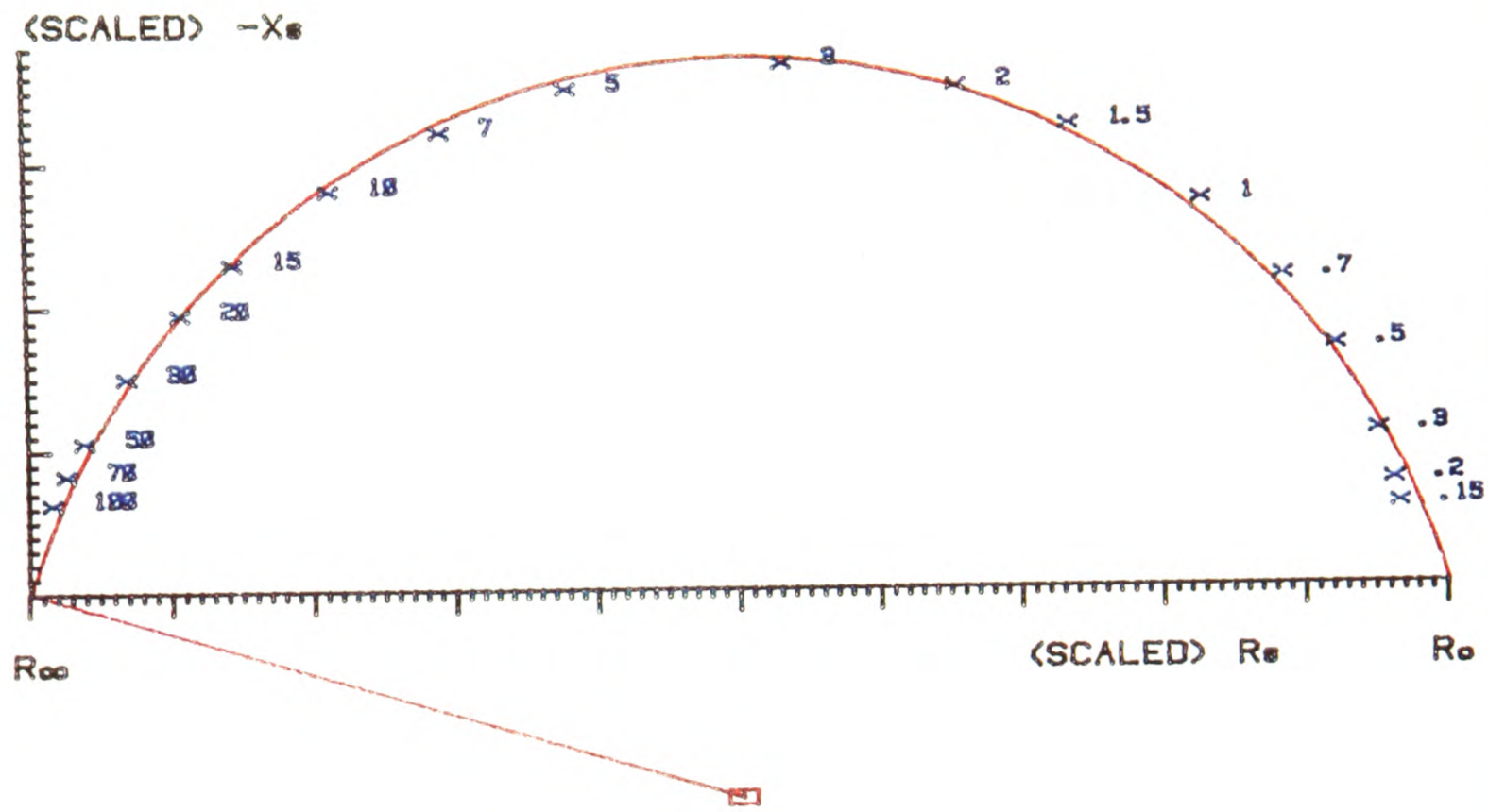
FOR THE SHUNTED GRADIENT MODEL
WITH CIRCUIT PARAMETERS

Q	=	5000
S	=	5
R(SHUNT)	=	1.38383E+07
C	=	2.00000E-07
R1	=	200
L(MAX)	=	20
SUM R(L)	=	2.78766E+06
R(D.C.)	=	2.30638E+06

THE LEAST-SQUARES FIT RESULTS ARE.			+PSE	+/-SE	-PSE
R(ZERO)	=	2.37542E+06		17695.6	
R(INFINITY)	=	27086.7		17695.6	
F(PEAK) [USING M]	=	1.76922	2.77147E-02		.027287
F(PEAK) [USING M']	=	1.76933	8.20875E-03		8.17108E-03
M FROM Z LOCUS ARC	=	-.155822		8.76570E-03	
M' FROM V/U PLOT	=	-.163877		5.84434E-03	
STUDENT'S T(M&M')	=	.772592		FOR 31 D.O.F.	
& WEIGHTED COEFF. DET. OF V/U PLOT	=	.999271			

Fig. 11.5.d.II

GRAPH OF POINTS ON THE COMPLEX IMPEDANCE LOCUS FITTED TO AN ARC BY LEAST SQUARES.



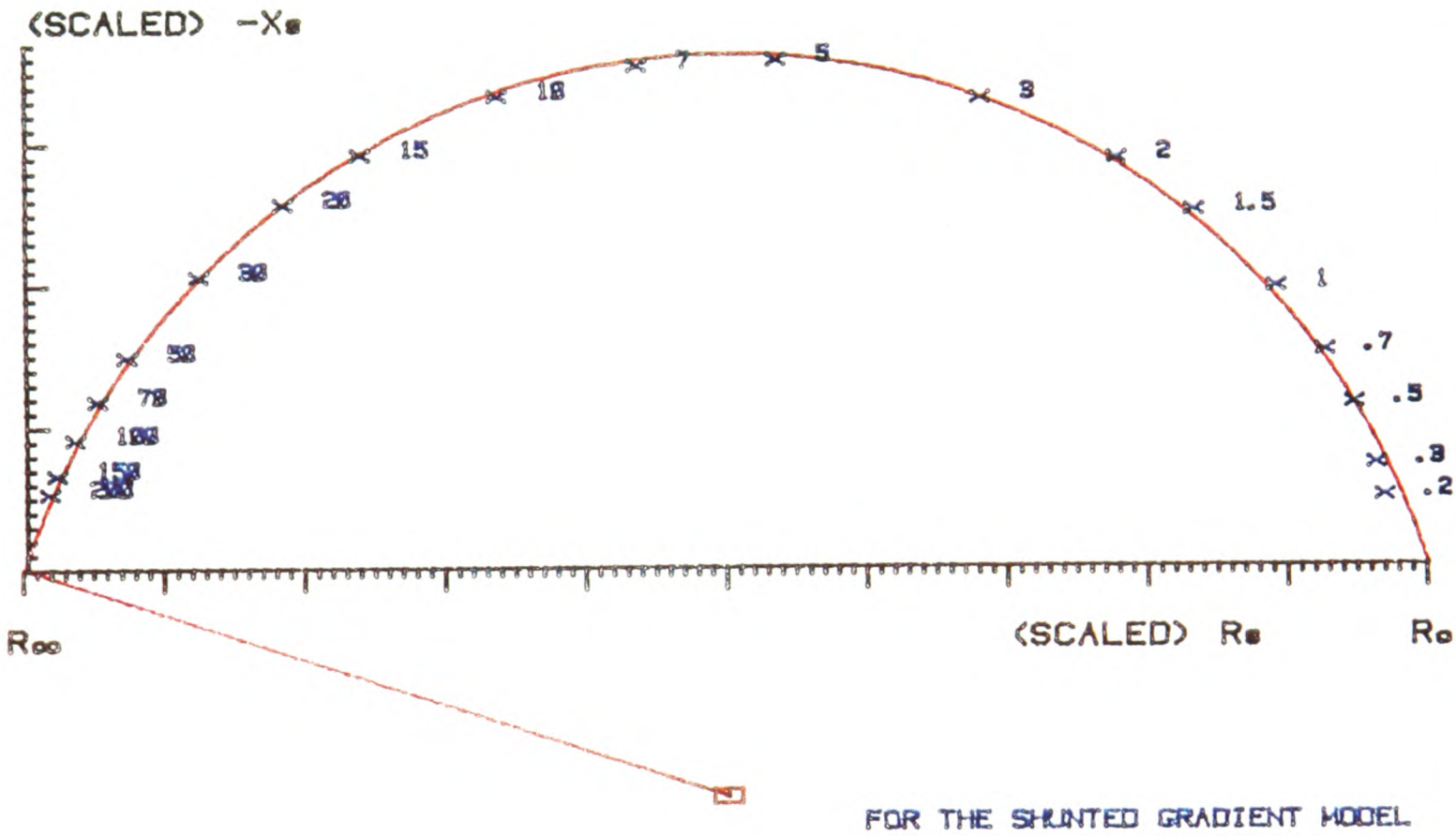
FOR THE SHUNTED GRADIENT MODEL
WITH CIRCUIT PARAMETERS

Q	=	5000
S	=	1
R(SHUNT)	=	2.78766E+06
C	=	2.00000E-07
R1	=	200
L(MAX)	=	20
SUM R(L)	=	2.78766E+06
R(D.C.)	=	1.38383E+06

THE LEAST-SQUARES FIT RESULTS ARE.			+PSE	+/-SE	-PSE
R(ZERO)	=	1.42359E+06		9016.46	
R(INFINITY)	=	5459.88		9016.46	
F(PEAK) [USING M]	=	3.34672	.148301	.142007	
F(PEAK) [USING M']	=	3.34784	1.51301E-02	1.50704E-02	
M FROM Z LOCUS ARC	=	-.18431		7.45292E-03	
M' FROM V/U PLOT	=	-.200656		2.81337E-03	
STUDENT'S T(M&M')	=	2.05199		FOR 31 D.O.F.	
& WEIGHTED COEFF. DET. OF V/U PLOT	=	.999802			

Fig. 11.5.d.III

GRAPH OF POINTS ON THE COMPLEX IMPEDANCE LOCUS FITTED TO AN ARC BY LEAST SQUARES.



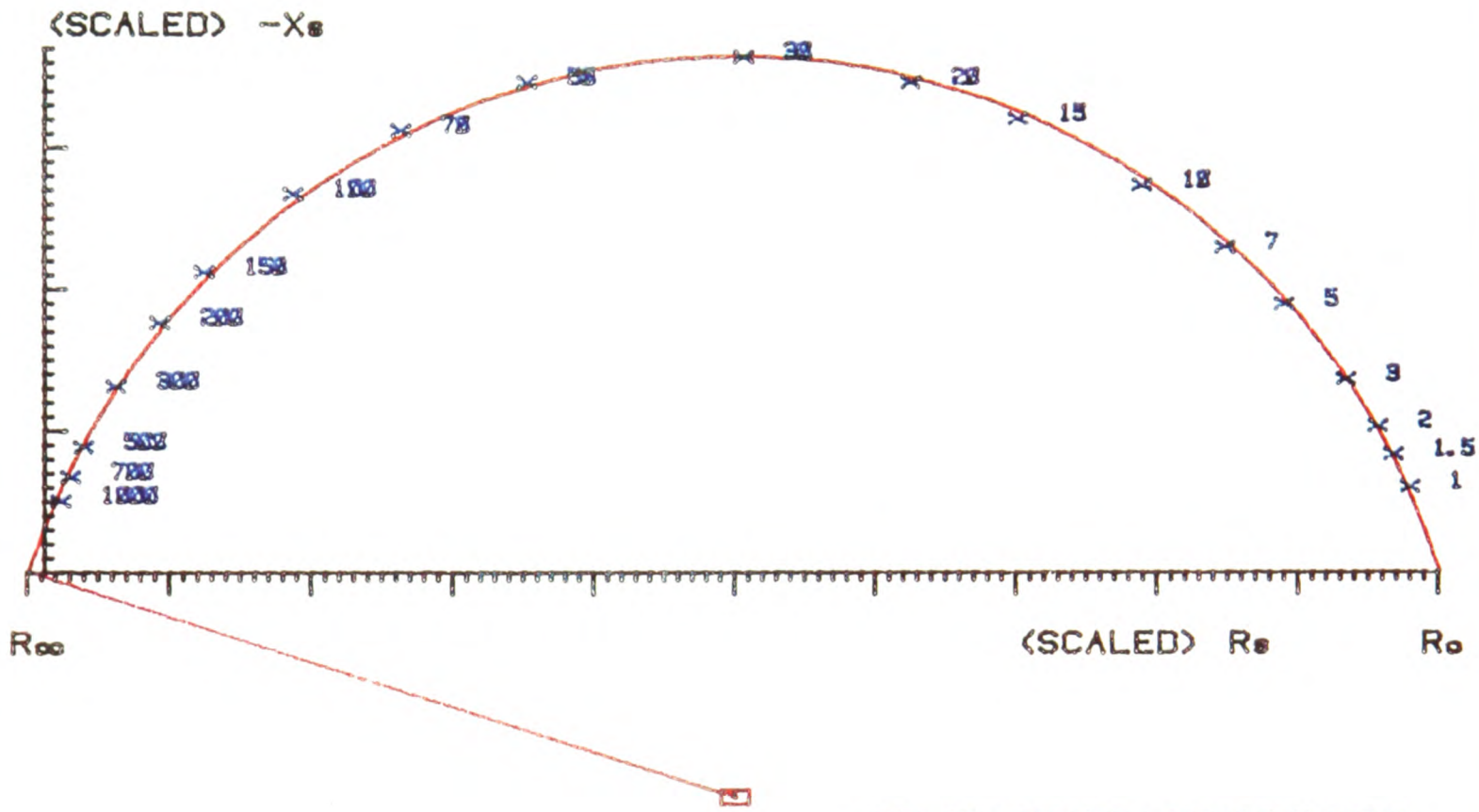
FOR THE SHUNTED GRADIENT MODEL
WITH CIRCUIT PARAMETERS

Q	=	5000
S	=	.5
R(SHUNT)	=	1.38383E+06
C	=	2.00000E-07
R1	=	200
L(MAX)	=	20
SUM R(L)	=	2.76766E+06
R(D.C.)	=	922554

THE LEAST-SQUARES FIT RESULTS ARE.			+PSE	+/-SE	-PSE
R(ZERO)	=	946650		3808.39	
R(INFINITY)	=	-3281.37		3808.30	
F(PEAK) [USING M]	=	5.65826	.312862	.298471	
F(PEAK) [USING M']	=	5.65487	1.33381E-02		1.33076E-02
M FROM Z LOCUS ARC	=	-.201293		4.81759E-03	
M' FROM V/U PLOT	=	-.214038		1.01536E-03	
STUDENT'S T(M&M')	=	2.58865		FOR 33 D.O.F.	
& WEIGHTED COEFF. DET. OF V/U PLOT	=	.990972			

Fig. 11.5.d.IV

GRAPH OF POINTS ON THE COMPLEX IMPEDANCE LOCUS FITTED TO AN ARC BY LEAST SQUARES.



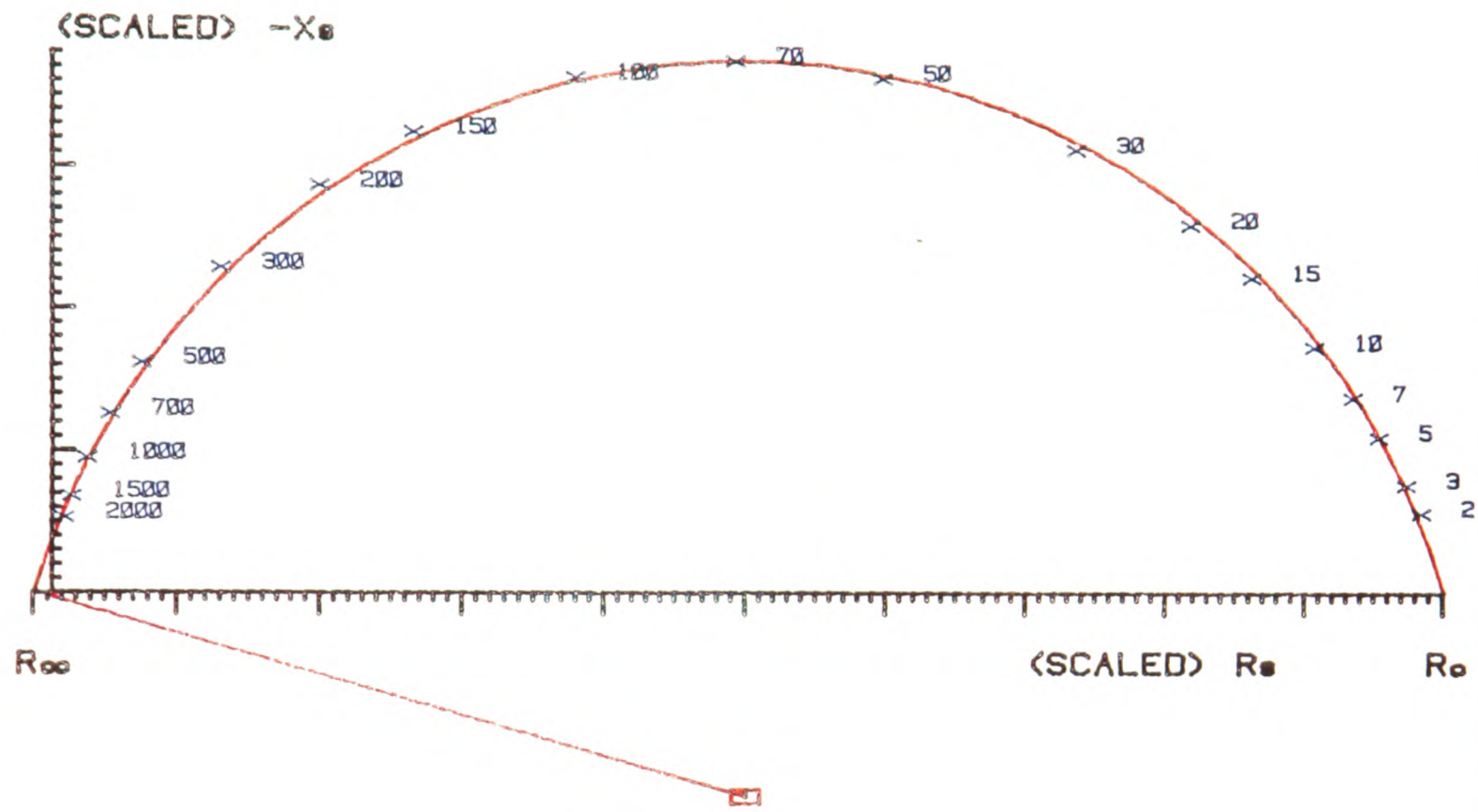
FOR THE SHUNTED GRADIENT MODEL
WITH CIRCUIT PARAMETERS

Q	=	5000
S	=	.1
R(SHUNT)	=	276766
C	=	2.00000E-07
R1	=	200
L(MAX)	=	20
SUM R(L)	=	2.76766E+06
R(D.C.)	=	251606

THE LEAST-SQUARES FIT RESULTS ARE:			+PSE	+/-SE	-PSE
R(ZERO)	=	253028		726.26	
R(INFINITY)	=	-3148.8		726.26	
F(PEAK) [USING M]	=	30.4884	1.17656		1.13285
F(PEAK) [USING M']	=	30.4908	.150337		.149601
M FROM Z LOCUS ARC	=	-.198248		3.32608E-03	
M' FROM V/U PLOT	=	-.200058		1.15319E-03	
STUDENT'S T(M&M')	=	.514077		FOR 33 D.O.F.	
& WEIGHTED COEFF. DET. OF V/U PLOT	=	.999985			

Fig. 11.5.d.V

GRAPH OF POINTS ON THE COMPLEX IMPEDANCE LOCUS FITTED TO AN ARC BY LEAST SQUARES.



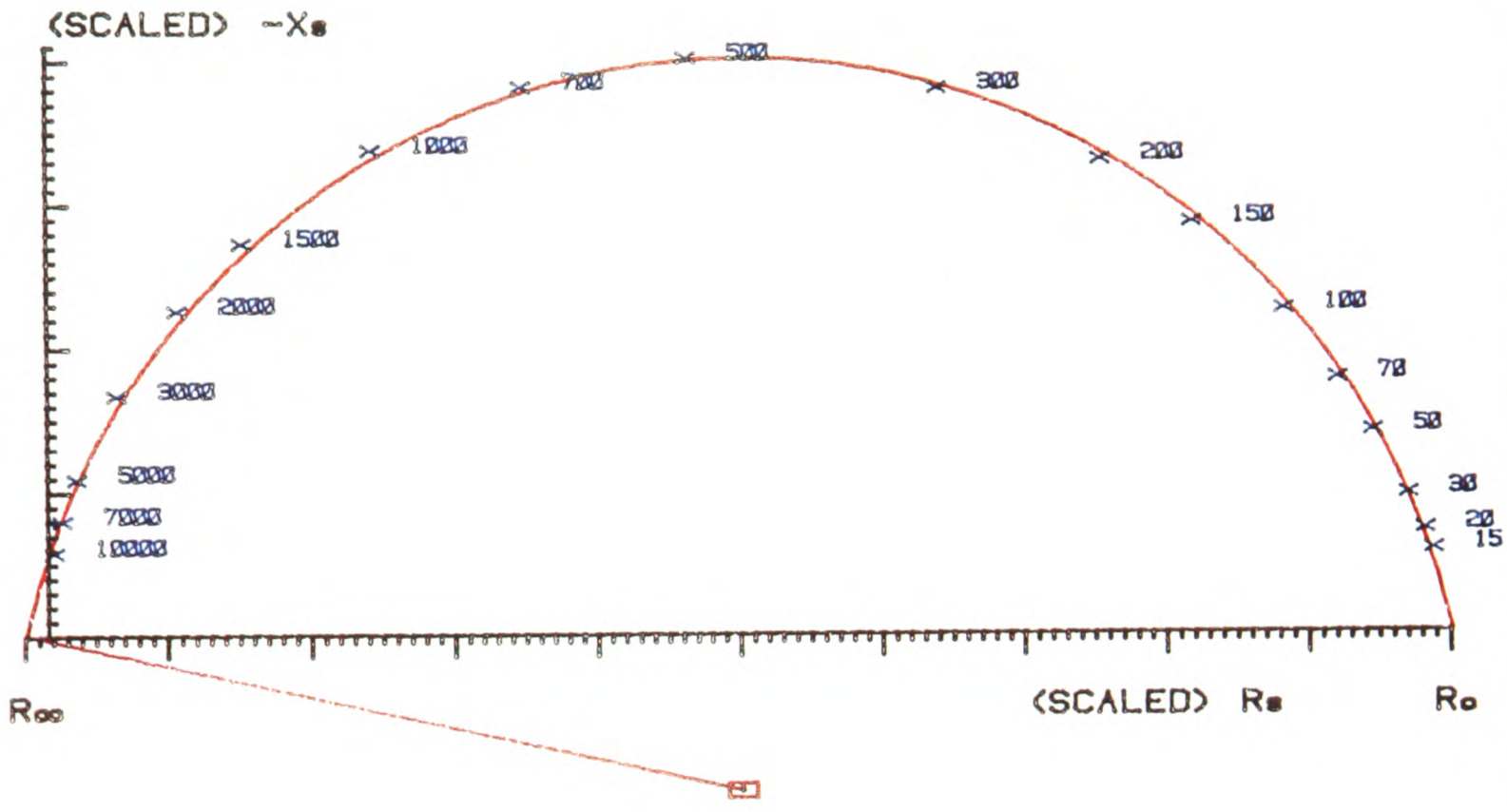
FOR THE SHUNTED GRADIENT MODEL
WITH CIRCUIT PARAMETERS

Q	=	5000
S	=	.05
R(SHUNT)	=	138383
C	=	2.00000E-07
R1	=	200
L(MAX)	=	20
SUM R(L)	=	2.76766E+06
R(D.C.)	=	131793

THE LEAST-SQUARES FIT RESULTS ARE:			+PSE	+/-SE	-PSE
R(ZERO)	=	131378		386.407	
R(INFINITY)	=	-1673.88		386.407	
F(PEAK) [USING M]	=	68.577	.739883		.731979
F(PEAK) [USING M']	=	68.5767	.79895		.789749
M FROM Z LOCUS ARC	=	-.180689		3.40257E-03	
M' FROM V/U PLOT	=	-.180885		2.22326E-03	
STUDENT'S T(M&M')	=	4.81952E-02		FOR 33 D.O.F.	
& WEIGHTED COEFF. DET. OF V/U PLOT	=	.999875			

Fig. 11.5.d.VI

GRAPH OF POINTS ON THE COMPLEX IMPEDANCE LOCUS FITTED TO AN ARC BY LEAST SQUARES.



FOR THE SHUNTED GRADIENT MODEL
WITH CIRCUIT PARAMETERS

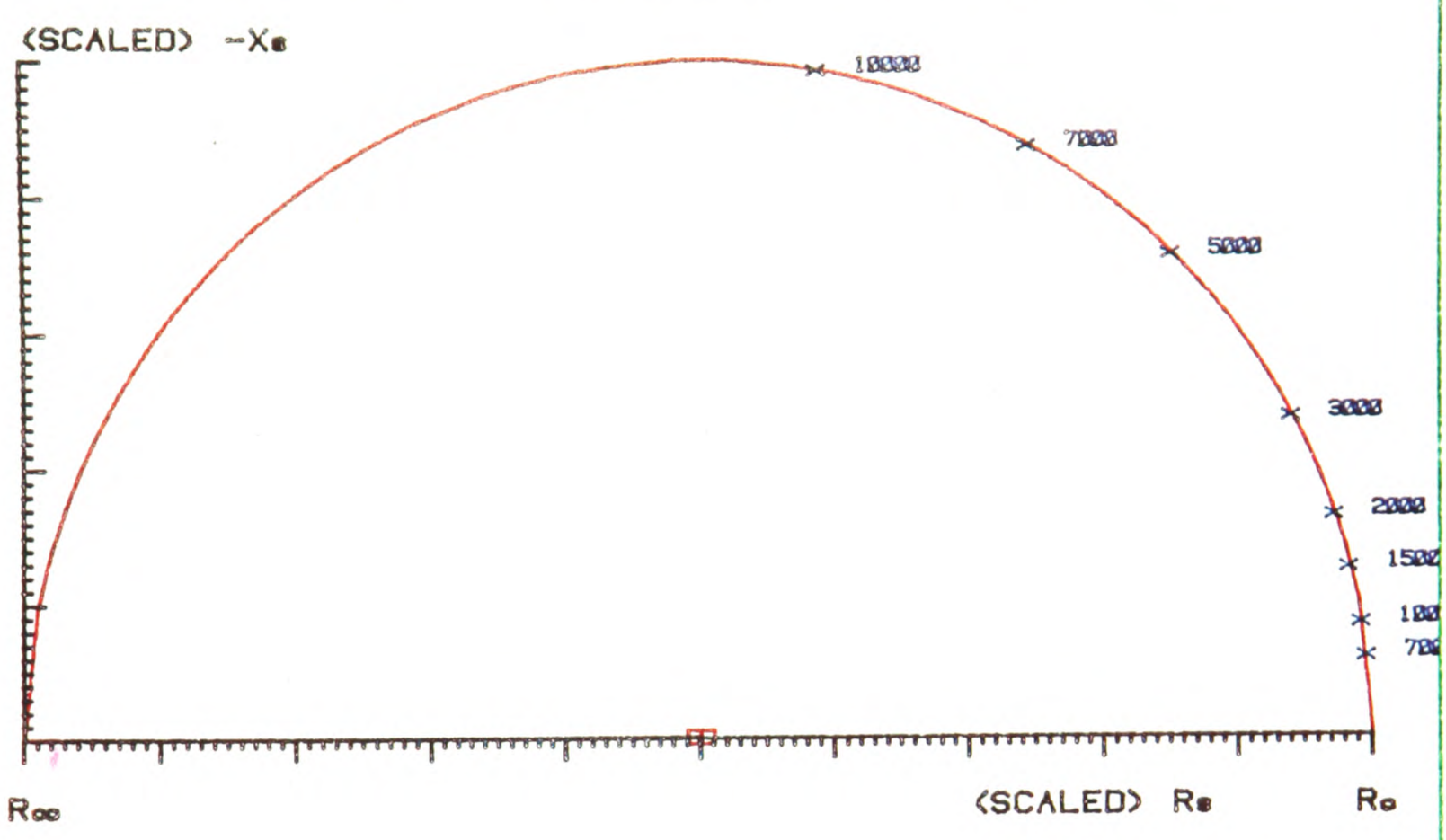
Q	=	5000
S	=	.01
R(SHUNT)	=	27676.6
C	=	2.00000E-07
R1	=	200
L(MAX)	=	20
SUM R(L)	=	2.76766E+06
R(D.C.)	=	27402.6

THE LEAST-SQUARES FIT RESULTS ARE:

			+PSE	+/-SE	-PSE
R(ZERO)	=	27108.2		77.9497	
R(INFINITY)	=	-441.7		77.9497	
F(PEAK) [USING M]	=	450.163	25.1242		23.7962
F(PEAK) [USING M']	=	450.142	6.31177		6.22455
M FROM Z LOCUS ARC	=	-.138507		3.30427E-03	
M' FROM V/U PLOT	=	-.139576		1.94416E-03	
STUDENT'S T(M&M')	=	.278715		FOR 31 D.O.F.	
& WEIGHTED COEFF. DET. OF V/U PLOT	=	1.00008			

Fig. 11.5.d.VII

GRAPH OF POINTS ON THE COMPLEX IMPEDANCE LOCUS FITTED TO AN ARC BY LEAST SQUARES.



FOR THE SHUNTED GRADIENT MODEL
WITH CIRCUIT PARAMETERS

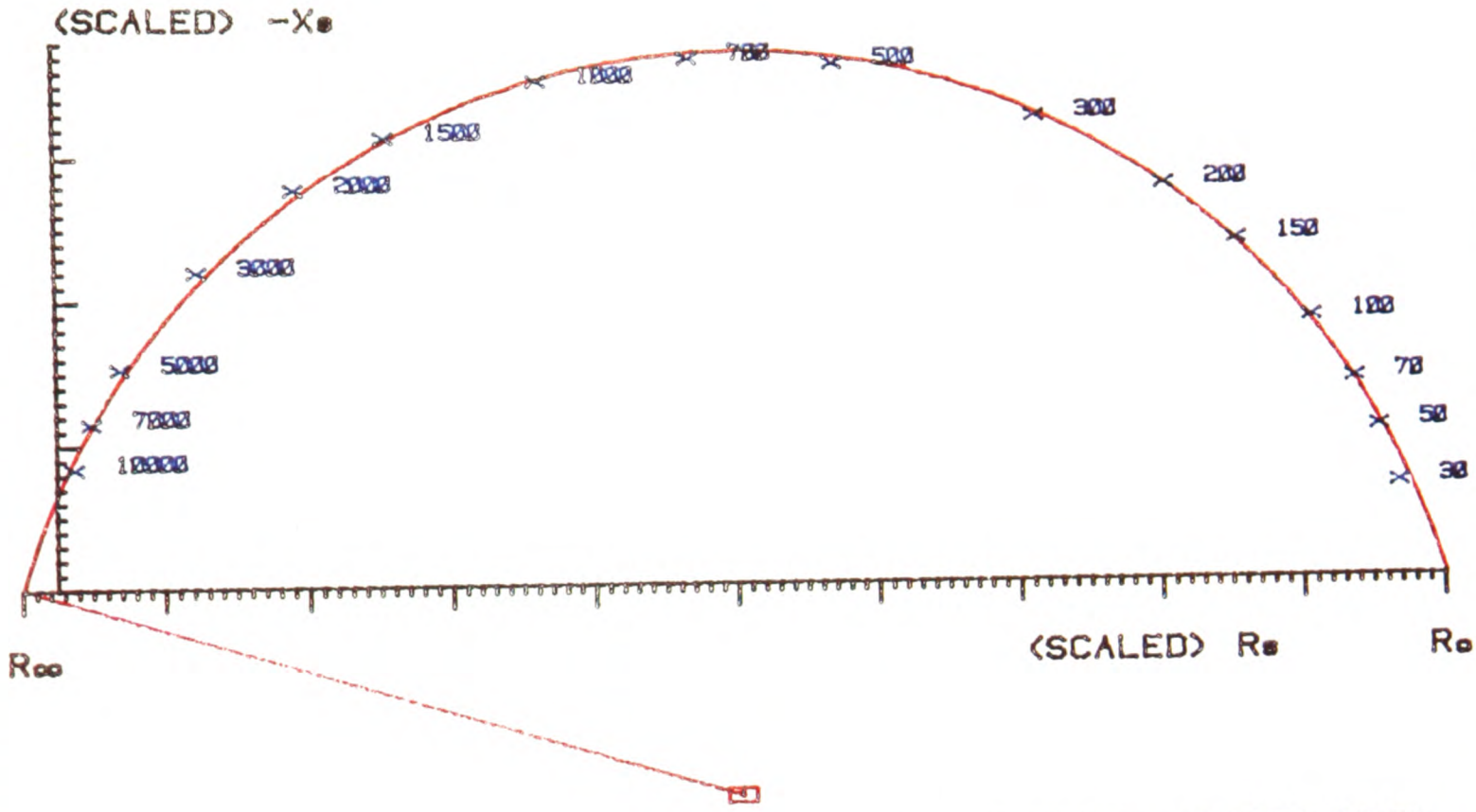
Q	=	1
S	=	.5
R(SHUNT)	=	2000
C	=	2.00000E-07
R1	=	200
L(MAX)	=	20
SUM R(L)	=	4000
R(D.C.)	=	1333.33

THE LEAST-SQUARES FIT RESULTS ARE:

			+PSE	+/-SE	-PSE
R(ZERO)	=	1333.34		1.94652	
R(INFINITY)	=	-8.28437E-02		1.94652	
F(PEAK) [USING M]	=	11937.8	476.102		457.844
F(PEAK) [USING M']	=	11937.6	424.018		409.479
M FROM Z LOCUS ARC	=	-1.26879E-04		.001716	
M' FROM V/U PLOT	=	-8.58307E-05		3.83571E-03	
STUDENT'S T(M&M')	=	9.76864E-03		FOR 11 D.O.F.	
& WEIGHTED COEFF. DET. OF V/U PLOT	=	.999912			

Fig. 11.5.d.VIII

GRAPH OF POINTS ON THE COMPLEX IMPEDANCE LOCUS FITTED TO AN ARC BY LEAST SQUARES.



FOR THE SHUNTED GRADIENT MODEL
WITH CIRCUIT PARAMETERS

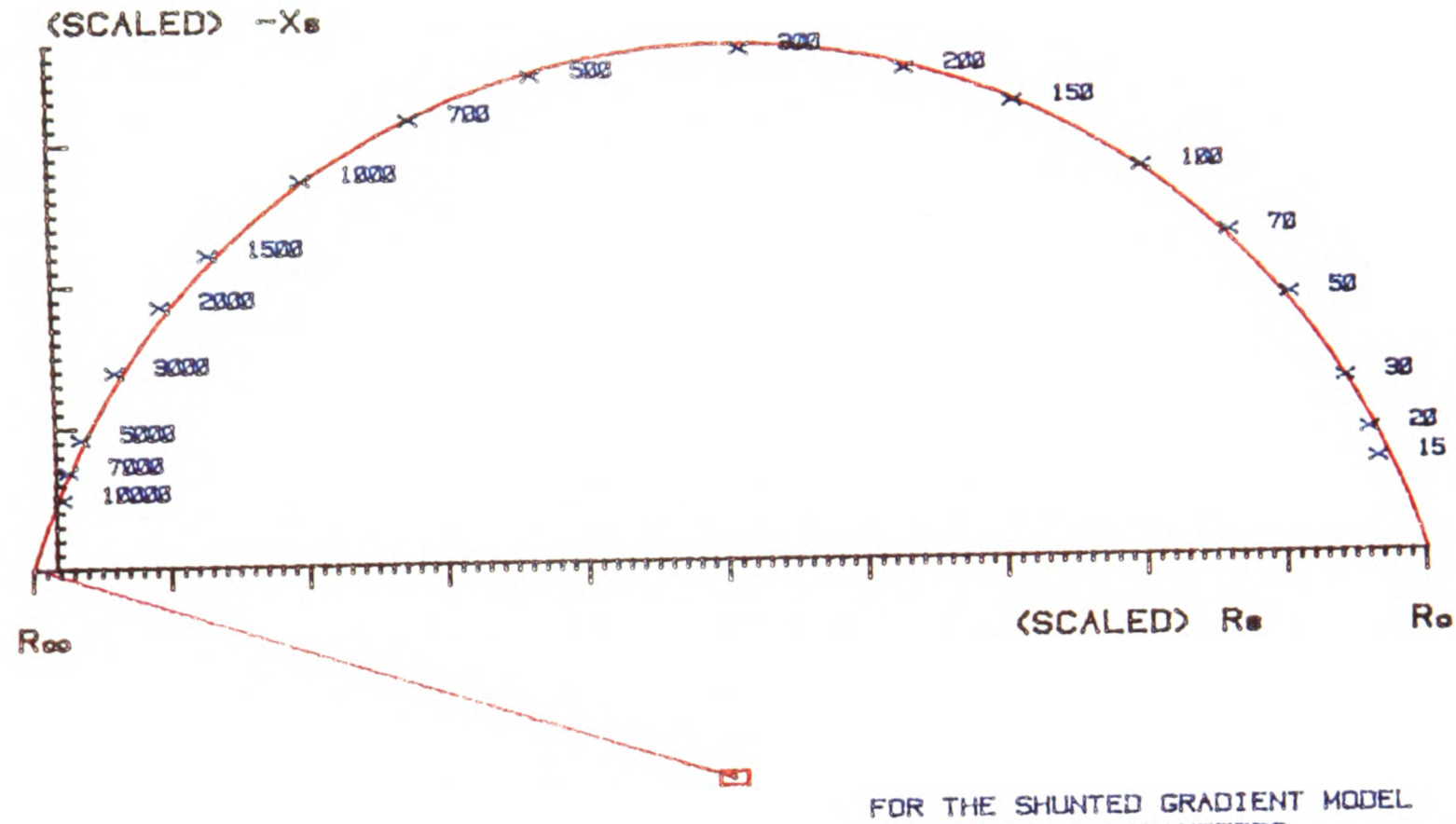
Q	=	50
S	=	.5
R(SHUNT)	=	26432.4
C	=	2.00000E-07
R1	=	200
L(MAX)	=	20
SUM R(L)	=	52864.9
R(D.C.)	=	17621.6

THE LEAST-SQUARES FIT RESULTS ARE.

			+PSE	+/-SE	-PSE
R(ZERO)	=	18039.6		75.6477	
R(INFINITY)	=	-468.808		75.6477	
F(PEAK) [USING M]	=	632.16	156.866		125.68
F(PEAK) [USING M']	=	631.797	12.0847		11.8578
M FROM Z LOCUS ARC	=	-.186267		4.79516E-03	
M' FROM V/U PLOT	=	-.200841		2.33150E-03	
STUDENT'S T(M&M')	=	2.73324		FOR 27 D.O.F.	
& WEIGHTED COEFF. DET. OF V/U PLOT	=	.999881			

Fig. 11.5.d.IX

GRAPH OF POINTS ON THE COMPLEX IMPEDANCE LOCUS FITTED TO AN ARC BY LEAST SQUARES.



FOR THE SHUNTED GRADIENT MODEL
WITH CIRCUIT PARAMETERS

Q	=	100
S	=	.5
R(SHUNT)	=	46095.2
C	=	2.00000E-07
R1	=	200
L(MAX)	=	20
SUM R(L)	=	92190.3
R(D.C.)	=	30730.1

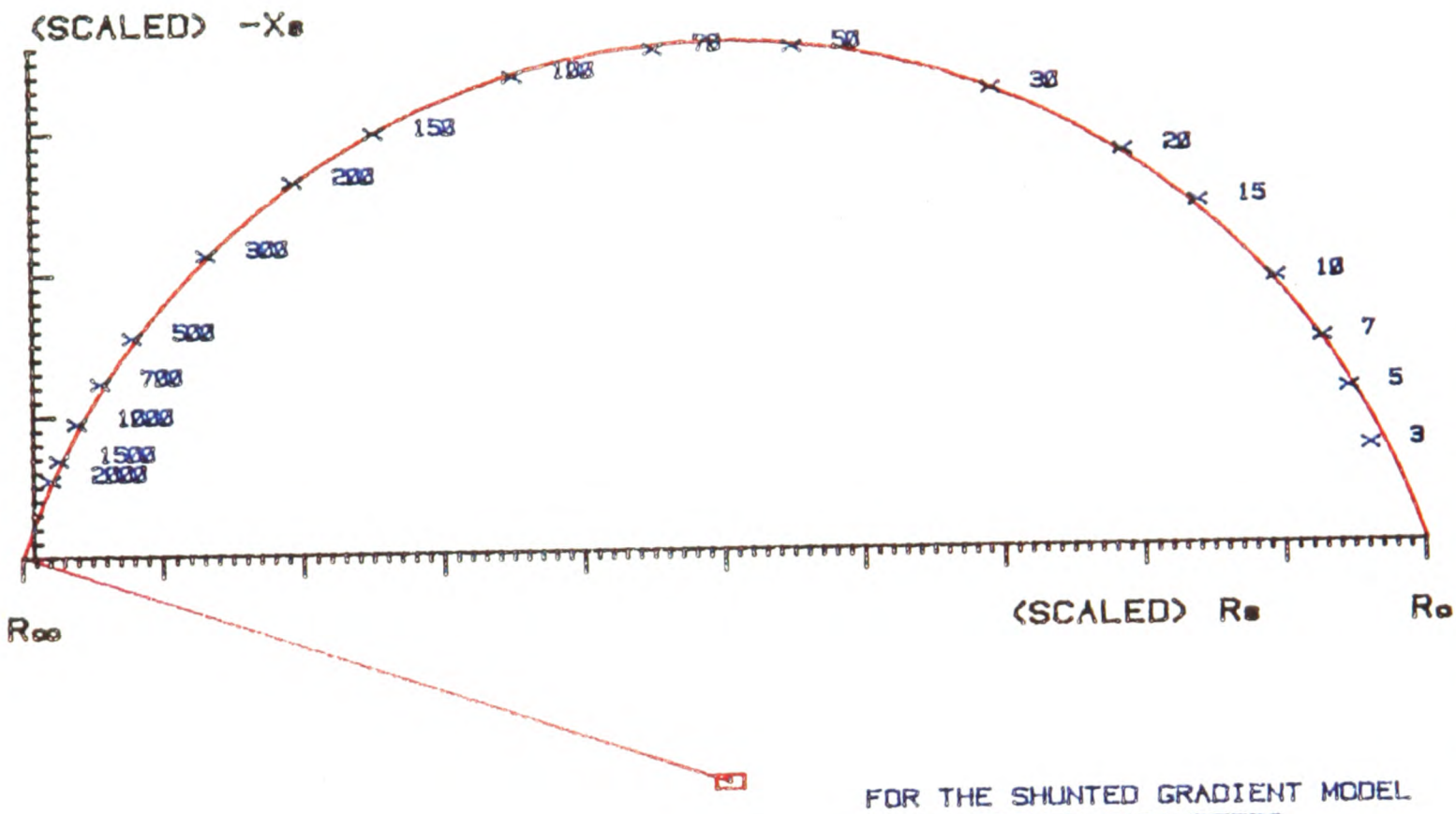
THE LEAST-SQUARES FIT RESULTS ARE.

			+PSE	+/-SE	-PSE
R(ZERO)	=	31499.8		110.837	
R(INFINITY)	=	-536.658		110.837	
F(PEAK) [USING M]	=	312.126	65.6392		54.2339
F(PEAK) [USING M']	=	312.302	3.19165		3.1593
M FROM Z LOCUS ARC	=	-.195184		4.05171E-03	
M' FROM V/U PLOT	=	-.210685		1.39982E-03	
STUDENT'S T(M&M')	=	3.61599		FOR 31 D.O.F.	

& WEIGHTED COEFF. DET. OF V/U PLOT = .99995

Fig. 11.5.d.X

GRAPH OF POINTS ON THE COMPLEX IMPEDANCE LOCUS FITTED TO AN ARC BY LEAST SQUARES.



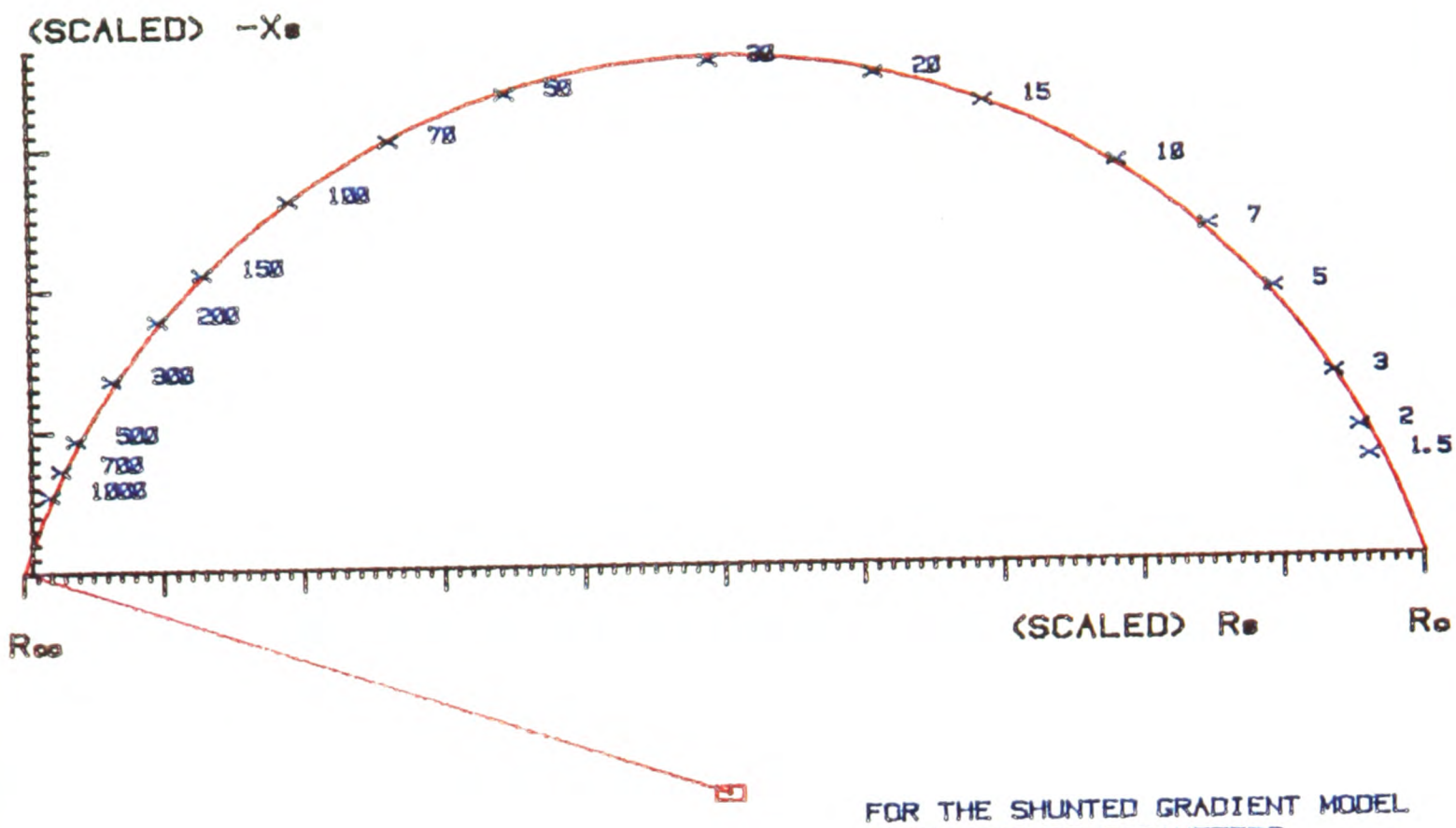
FOR THE SHUNTED GRADIENT MODEL
WITH CIRCUIT PARAMETERS

Q	=	500
S	=	.5
R(SHUNT)	=	178968
C	=	2.00000E-07
R1	=	200
L(MAX)	=	20
SUM R(L)	=	357935
R(D.C.)	=	119312

THE LEAST-SQUARES FIT RESULTS ARE.			+PSE	+/-SE	-PSE
R(ZERO)	=	122873		416.986	
R(INFINITY)	=	-1037.78		416.986	
F(PEAK) [USING M]	=	59.7214	6.92838		6.20817
F(PEAK) [USING M']	=	59.6943	.544762		.539841
M FROM Z LOCUS ARC	=	-.206136		3.94247E-03	
M' FROM V/U PLOT	=	-.215753		1.71686E-03	
STUDENT'S T(M&M')	=	2.23662		FOR 31 D.O.F.	
& WEIGHTED COEFF. DET. OF V/U PLOT	=	.999923			

Fig. 11.5.d.XI

GRAPH OF POINTS ON THE COMPLEX IMPEDANCE LOCUS FITTED TO AN ARC BY LEAST SQUARES.



FOR THE SHUNTED GRADIENT MODEL
WITH CIRCUIT PARAMETERS

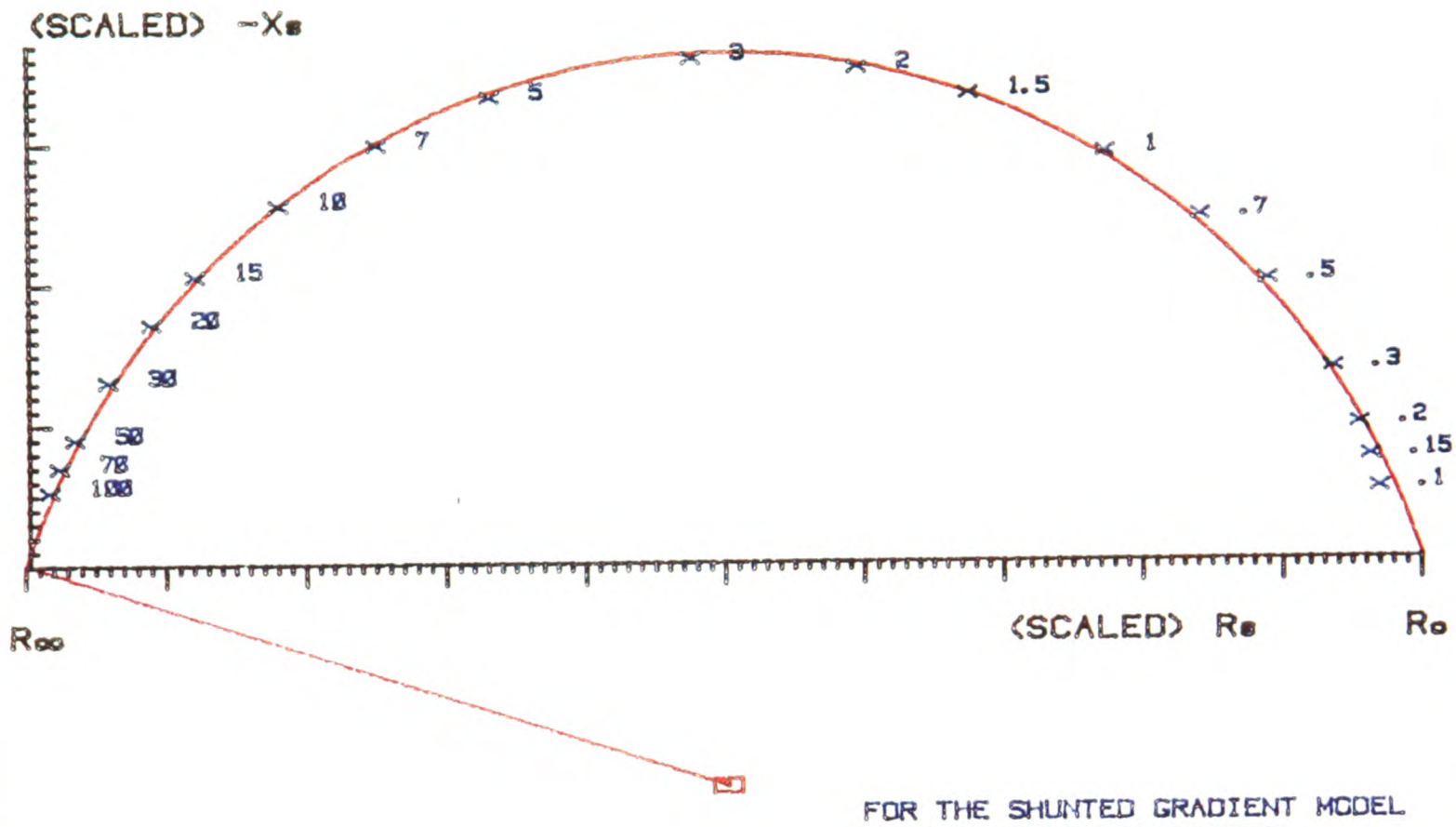
Q	=	1000
S	=	.5
R(SHUNT)	=	327848
C	=	2.00000E-07
R1	=	200
L(MAX)	=	20
SUM R(L)	=	655696
R(D.C.)	=	218566

THE LEAST-SQUARES FIT RESULTS ARE.

			+PSE	+/-SE	-PSE
R(ZERO)	=	224776		788.206	
R(INFINITY)	=	-1348.25		788.206	
F(PEAK) [USING M]	=	29.3335	2.97512		2.70116
F(PEAK) [USING M']	=	29.3448	.177937		.176865
M FROM Z LOCUS ARC	=	-.204404		4.08456E-03	
M' FROM V/U PLOT	=	-.215634		1.40183E-03	
STUDENT'S T(M&M')	=	2.6004		FOR 31 D.O.F.	
& WEIGHTED COEFF. DET. OF V/U PLOT	=	.999949			

Fig. 11.5.d.XII

GRAPH OF POINTS ON THE COMPLEX IMPEDANCE LOCUS FITTED TO AN ARC BY LEAST SQUARES.



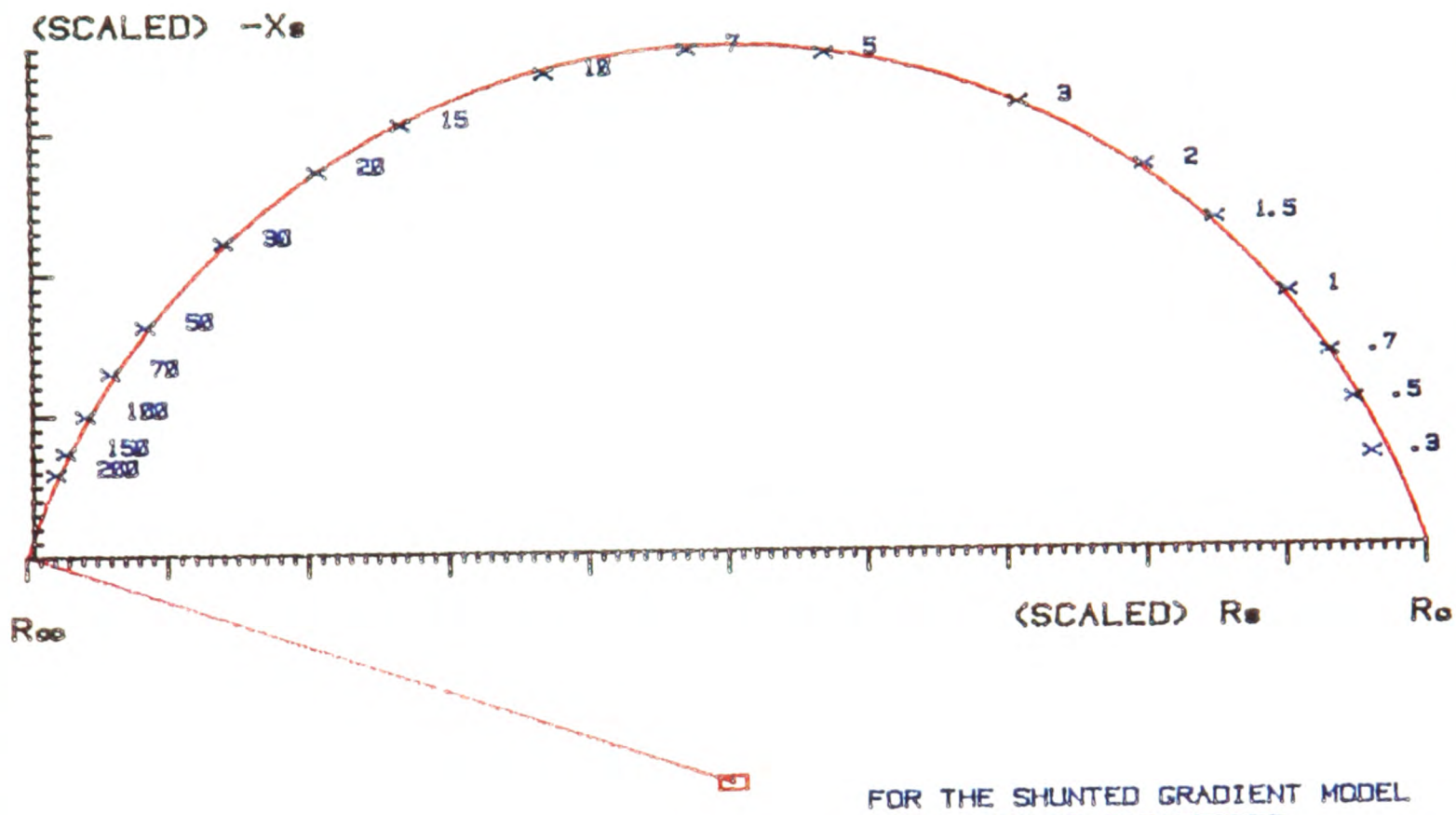
FOR THE SHUNTED GRADIENT MODEL
WITH CIRCUIT PARAMETERS

Q	=	10000
S	=	.5
R(SHUNT)	=	2.60298E+06
C	=	2.00000E-07
R1	=	200
L(MAX)	=	20
SUM R(L)	=	5.20595E+06
R(D.C.)	=	1.73532E+06

THE LEAST-SQUARES FIT RESULTS ARE.			+PSE	+/-SE	-PSE
R(ZERO)	=	1.77909E+06		7127.93	
R(INFINITY)	=	-5286.91		7127.93	
F(PEAK) [USING M]	=	2.78213	9.57303E-02		.092546
F(PEAK) [USING M']	=	2.78358	4.71115E-03		4.70352E-03
M FROM Z LOCUS ARC	=	-.199975		4.67685E-03	
M' FROM V/U PLOT	=	-.214014		1.21460E-03	
STUDENT'S T(M&M')	=	2.90544		FOR 33 D.O.F.	
& WEIGHTED COEFF. DET. OF V/U PLOT	=	.999959			

Fig. 11.5.d.XIII

GRAPH OF POINTS ON THE COMPLEX IMPEDANCE LOCUS FITTED TO AN ARC BY LEAST SQUARES.



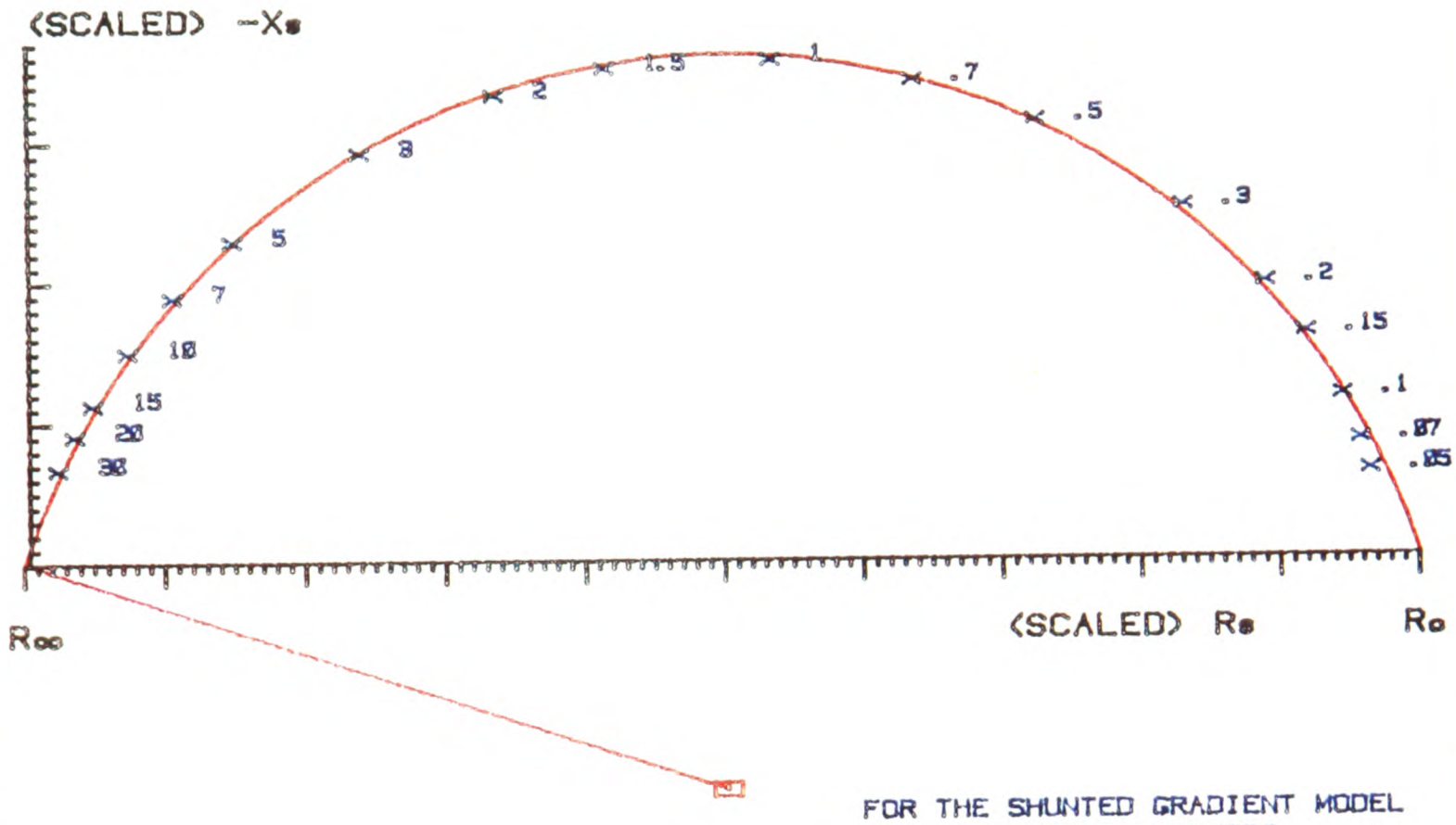
FOR THE SHUNTED GRADIENT MODEL
WITH CIRCUIT PARAMETERS

Q	=	5000
S	=	.5
R(SHUNT)	=	3.13325E+06
C	=	2.00000E-07
R1	=	200
L(MAX)	=	50
SUM R(L)	=	6.26649E+06
R(D.C.)	=	2.08883E+06

THE LEAST-SQUARES FIT RESULTS ARE.		+PSE	+/-SE	-PSE
R(ZERO)	=	2.14938E+06	7669.59	
R(INFINITY)	=	-10607.7	7669.59	
F(PEAK) [USING M]	=	6.40737	.34291	.325489
F(PEAK) [USING M']	=	6.40455	2.03133E-02	2.02503E-02
M FROM Z LOCUS ARC	=	-.206241	4.16068E-03	
M' FROM V/U PLOT	=	-.216139	1.27932E-03	
STUDENT'S T(M&M')	=	2.2739	FOR 31 D.O.F.	
& WEIGHTED COEFF. DET. OF V/U PLOT	=	.999957		

Fig. 11.5.d.XIV

GRAPH OF POINTS ON THE COMPLEX IMPEDANCE LOCUS FITTED TO AN ARC BY LEAST SQUARES.



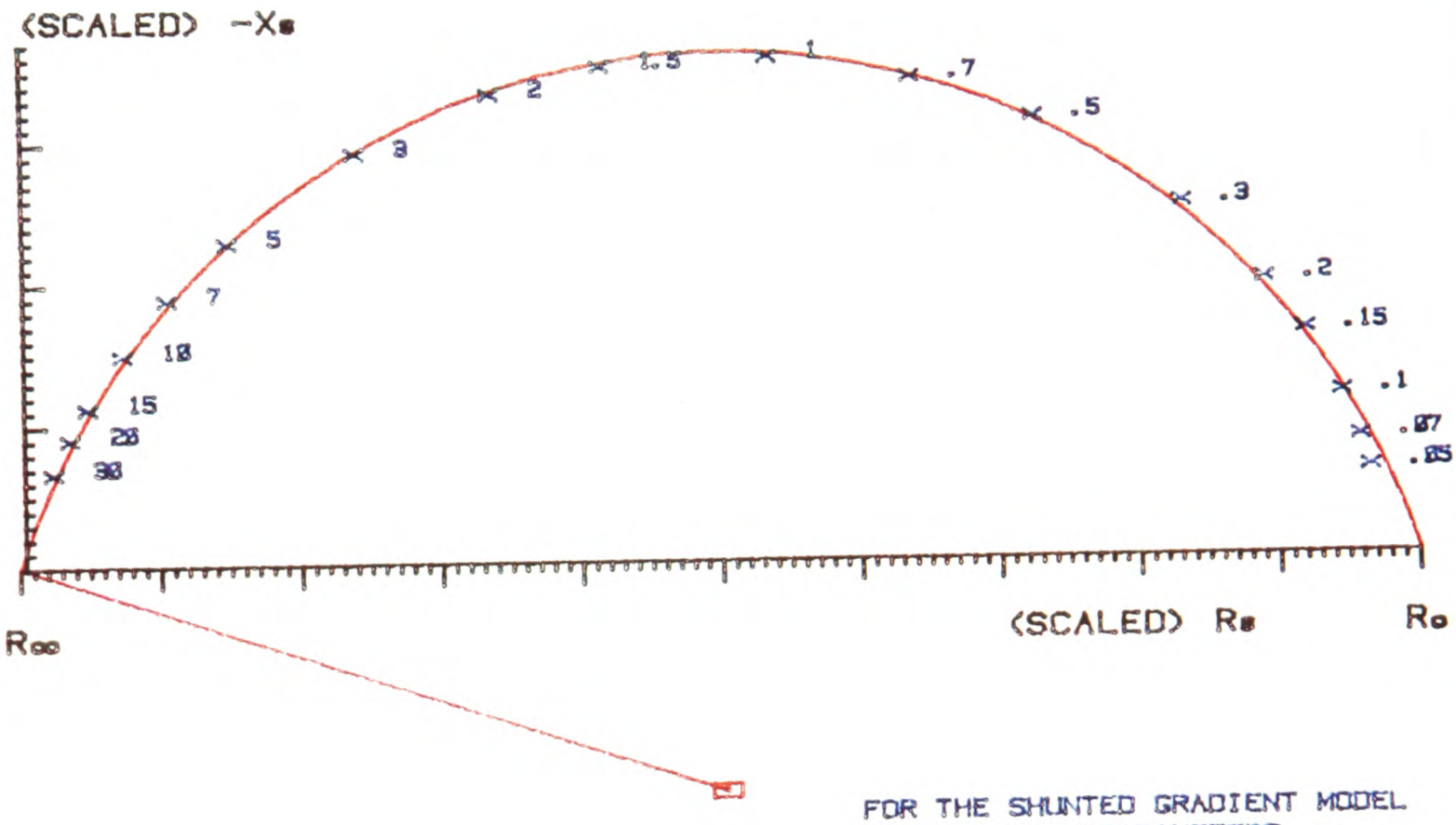
FOR THE SHUNTED GRADIENT MODEL
WITH CIRCUIT PARAMETERS

Q	=	5000
S	=	.5
R(SHUNT)	=	1.38383E+06
C	=	.000001
R1	=	200
L(MAX)	=	20
SUM R(L)	=	2.78766E+06
R(D.C.)	=	922554

THE LEAST-SQUARES FIT RESULTS ARE.			+PSE	+/-SE	-PSE
R(ZERO)	=	948088		3804.51	
R(INFINITY)	=	-4053.53		3804.51	
F(PEAK) [USING M]	=	1.12945	1.51336E-02		1.49338E-02
F(PEAK) [USING M']	=	1.12938	7.67231E-04		7.66754E-04
M FROM Z LOCUS ARC	=	-.203706	.004678		
M' FROM V/U PLOT	=	-.215527	1.17257E-03		
STUDENT'S T(M&M')	=	2.45113	FOR 31 D.O.F.		
& WEIGHTED COEFF. DET. OF V/U PLOT	=	.999964			

Fig. 11.5.d.XV

GRAPH OF POINTS ON THE COMPLEX IMPEDANCE LOCUS FITTED TO AN ARC BY LEAST SQUARES.



FOR THE SHUNTED GRADIENT MODEL
WITH CIRCUIT PARAMETERS

Q	=	5000
S	=	.5
R(SHUNT)	=	6.91915E+06
C	=	2.00000E-07
R1	=	1000
L(MAX)	=	20
SUM R(L)	=	1.38383E+07
R(D.C.)	=	4.81277E+06

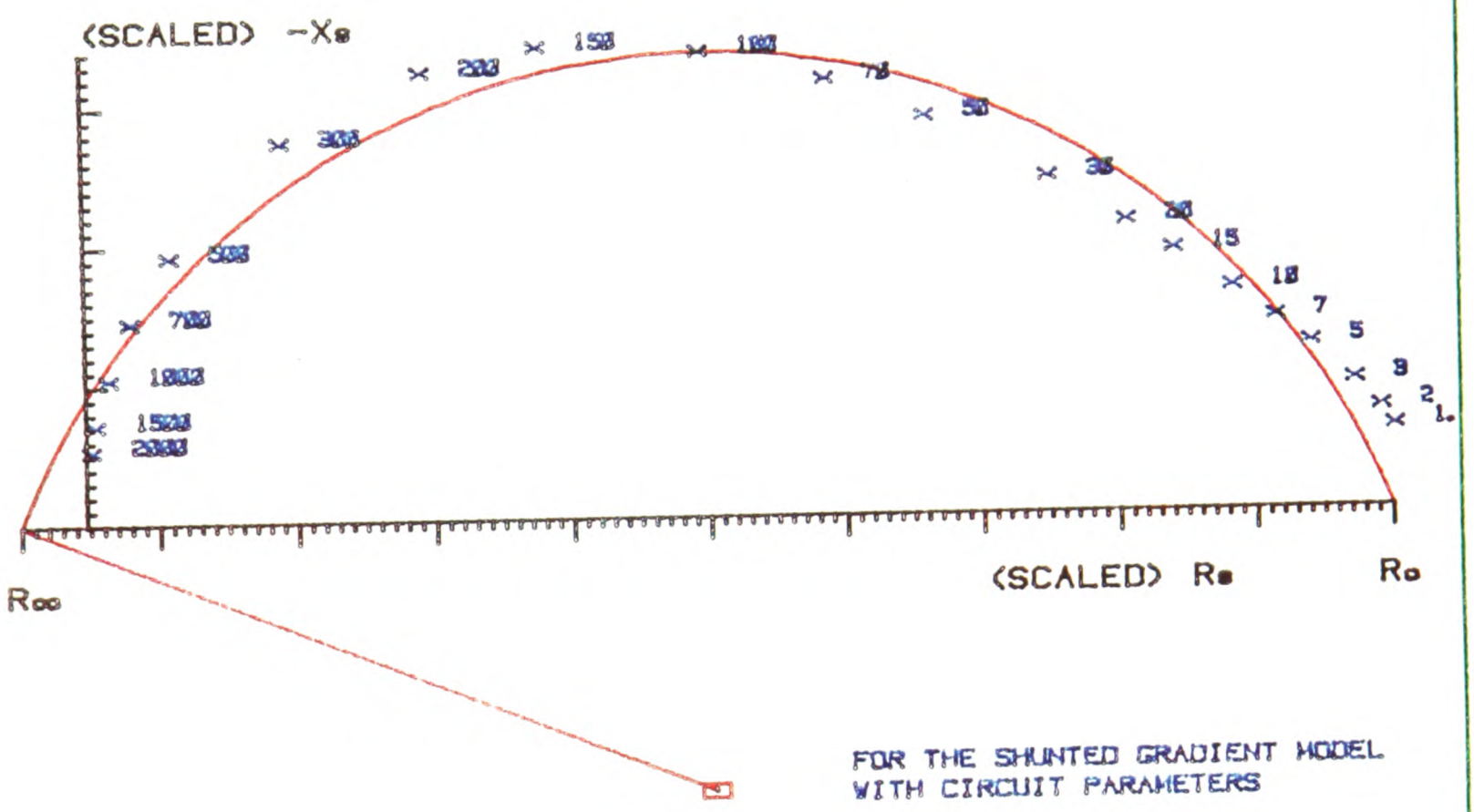
THE LEAST-SQUARES FIT RESULTS ARE.			+PSE	+/-SE	-PSE
R(ZERO)	=	4.74044E+06		18993.3	
R(INFINITY)	=	-20267.1		18993.3	
F(PEAK) [USING M]	=	1.12945	1.51341E-02		1.49341E-02
F(PEAK) [USING M']	=	1.12938	7.65800E-04		7.65085E-04
M FROM Z LOCUS ARC	=	-.203706		4.67081E-03	
M' FROM V/U PLOT	=	-.215527		1.17029E-03	
STUDENT'S T(M&M')	=	2.4550l		FOR 31 D.O.F.	
& WEIGHTED COEFF. DET. OF V/U PLOT		=	.999964		

Fig. 11.5.d.XVI

11.5.e Shunted chain networks with exponential capacitance gradients

I think that the simulation shown in Figure 11.5.e.I, run with S = 0.5, is enough to demonstrate that shunting the type of network reviewed in subsection 11.5.c makes such a thing even less suitable for modelling the complex impedance behaviour of human skin.

GRAPH OF POINTS ON THE COMPLEX IMPEDANCE LOCUS FITTED TO AN ARC BY LEAST SQUARES.



FOR THE SHUNTED GRADIENT MODEL
WITH CIRCUIT PARAMETERS

Q	=	100
S	=	.5
R(SHUNT)	=	100000
C1	=	1.00000E-07
R	=	10000
L(MAX)	=	20
SUM R(L)	=	200000
R(D.C.)	=	86666.7

THE LEAST-SQUARES FIT RESULTS ARE.			+PSE	+/-SE	-PSE
R(ZERO)	=	65221.4		1523.94	
R(INFINITY)	=	-3193.94		1523.94	
F(PEAK) [USING M]	=	98.1174	10.5904		9.53932
F(PEAK) [USING M']	=	98.148	7.01881		6.54131
M FROM Z LOCUS ARC	=	-.243054		.025823	
M' FROM V/U PLOT	=	-.2539		1.15139E-02	
STUDENT'S T(M&M')	=	.383587		FOR 35 D.O.F.	
& WEIGHTED COEFF. DET. OF V/U PLOT	=	.995732			

Fig. 11.5.e.I

11.5.f Conclusions

Subsections 11.5.b to 11.5.e have demonstrated that gradient models, or even shunted gradient models which do not appear to have been investigated before, are incapable of producing a good enough fit to a minor arc of a circle with a large enough value of m, unless perhaps the gradients of $\varepsilon(x)$ and $\rho(x)$ are chosen in just such a way as to force the right behaviour, even though gradients chosen in this way do not correspond to any biophysically plausible form - they would be entirely ad hoc.

On top of these considerations there are others which should finally dispose of any further hope of interpreting the problem of the origin and form of the DRT in human skin along these lines.

The first of these is that even very thin layers of the corneum still obey the Cole equation with the value of m little if at all different from that appropriate to the whole corneum from which the thin layer has been stripped, (Yamamoto and Yamamoto, 1976a, Appendix 2). On the basis of the gradient model approach, one would expect that m would probably be less for a thin stripped layer than for the whole corneum.

The second consideration is that of the effect of hydrating the corneum, which, as was seen in subsection 9.3.c, tends to increase the value of m. *Yet this is the reverse of what would be expected from gradient models,* since as the outer layers of the corneum become more hydrated their electrical properties will become more like those of the inner layers, the disparity in time constants will decrease, and the locus will become more Debye-like as Q diminishes.

In view of all this we may therefore conclude that gradient models are totally unacceptable as interpretations of the origin and form of the DRT in human skin in vivo, and it is pointless to consider them further, although no doubt the literature will continue to do so. A much better model is needed.

11.6 Alternatives to shunted gradient models

11.6.a Edith Clar's shunted Cole-Cole dielectric model

Apart from the gradient model proposed by Barnett and Tregear, the only other model presently available in the literature which seeks to interpret the origin and form of the DRT in skin is that due to Edith Clar.

Clar et al. (1973, 1975) decided to investigate the complex permittivity (ε^*) locus of skin, and having calculated it from their measurements of impedance modulus and phase angle, they proceeded to plot it, yet apparently without ever drawing the corresponding complex impedance locus which they had of course measured directly. This was, I think, an unfortunate omission.

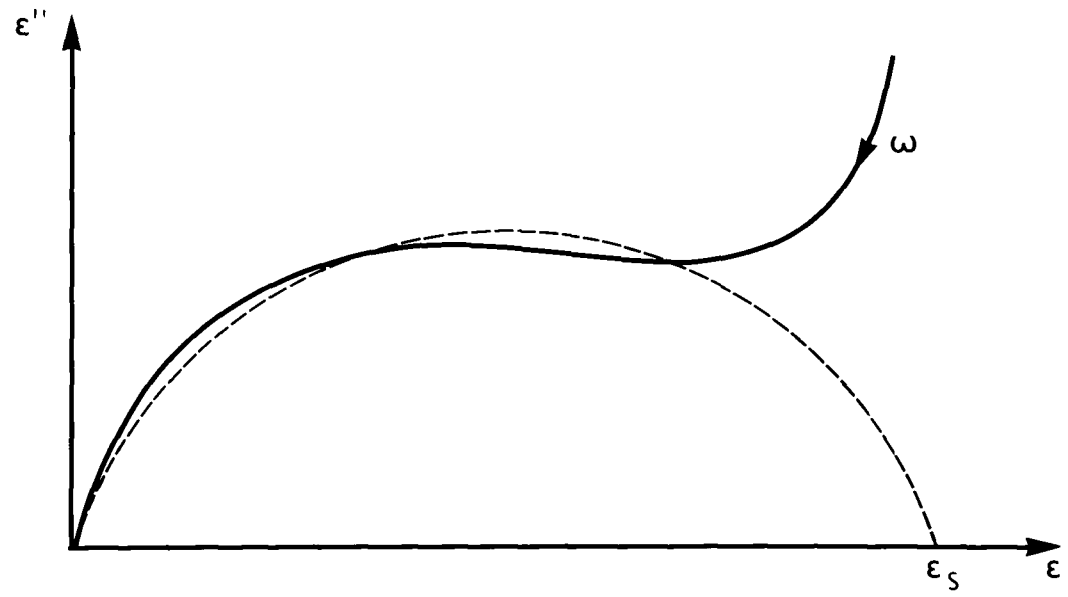


Fig. 11.6.a.I

It can be assumed that they must have derived a complex permittivity locus looking rather like the full line in Fig. 11.6.a.I, since this has been drawn to be of the form corresponding to the behaviour we know is

observed on the complex impedance plane, namely the relatively simple minor arc of a circle described by the Cole equation.

When Clar et al. saw a complex permittivity locus like that of Fig. 11.6.a.I, they were tempted to suggest that it resulted from a minor arc of a circle on the complex permittivity plane (such as has also been drawn in Fig. 11.6.a.I), distorted at low frequencies by conduction through some parallel pathway. In other words, they suggested that skin could be modelled by a Cole-Cole dielectric (Cole and Cole, 1941), which would produce a minor arc of a circle on the complex permittivity plane, shunted by a parallel conductance pathway, which would distort that minor arc in an appropriate way.

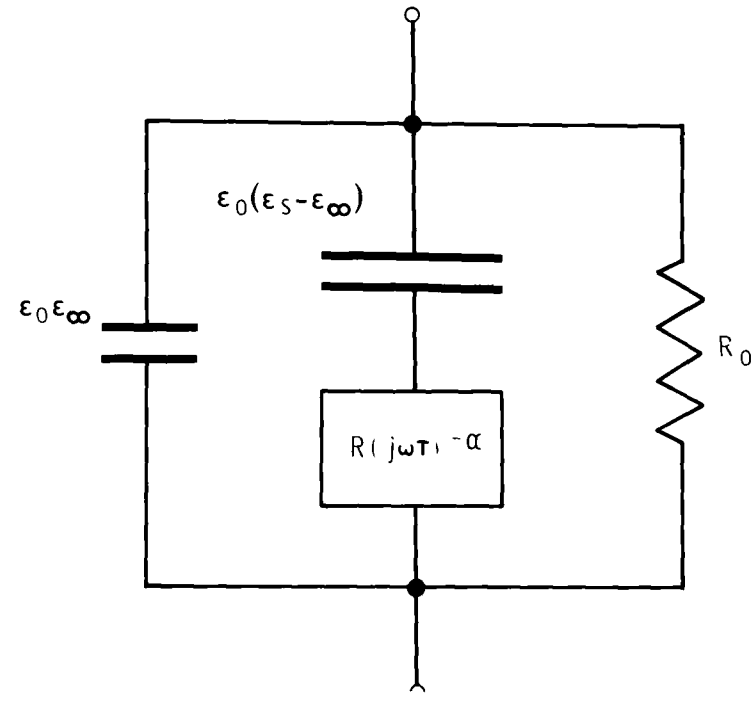


Fig. 11.6.a.II

The equivalent circuit corresponding to this suggestion is shown in Fig. 11.6.a.II, where R_o, the D.C. resistance of the circuit, is equal to the reciprocal of the assumed parallel conductance shunt, ε_o is the

permittivity of a vacuum (8.85×10^{-12} F m^{-1}), ε_∞ is the relative permittivity of skin at very high frequency and ε_s is the relative permittivity at very low frequency. (Instead of $\varepsilon_o(\varepsilon_s-\varepsilon_\infty)$ the "dielectric decrement", Clar et al. in fact wrote $\Delta\varepsilon$.) It is also convenient to define that for the polarization impedance in the circuit,

$$R = \frac{\tau}{\varepsilon_o(\varepsilon_s-\varepsilon_\infty)} \qquad (11.6.a.1)$$

since the complex permittivity of the Clar model of skin may then be written

$$\varepsilon^* = \varepsilon_o\varepsilon^*_r = \varepsilon_o\varepsilon_\infty + \frac{\varepsilon_o(\varepsilon_s-\varepsilon_\infty)}{1+(j\omega\tau)^{1-\alpha}} - j\frac{1}{\omega R_o} \qquad (11.6.a.2)$$

If the parameters of this equation are chosen with enough care, it can indeed produce a complex permittivity locus which looks quite like that corresponding to the Cole complex impedance equation, namely

$$\varepsilon^* = \frac{1}{j\omega}\left[\frac{1}{R_\infty} + \frac{(1/R_o) - (1/R_\infty)}{1 + \frac{R_\infty}{R_o}(j\omega\tau)^{1-m}}\right], \quad m = 1 - \alpha \qquad (11.6.a.3)$$

and Clar and colleagues were able, using a computer, to fit the parameters of an equation like (11.6.a.2) to their experimentally derived results to within an accuracy of 5% (Clar and Dugas du Villard, 1975). However, I am confident that their results would have fitted equation (11.6.a.3) to an even better accuracy, and certainly a fit to within 5% is not adequate to ensure that one is using the correct equation.

I therefore tested the Clar model against the Cole model (of Sections 4.2, 9.5 and 11.2) as follows. The first step was the more accurate procedure of plotting a Z locus directly from the data, and deriving R_o

from it by least squares (see Section 8.3 and subappendix B.1). Then a ε^* locus was plotted with the effect of the corresponding amount of parallel conductance subtracted off, i.e. a locus defined by the "processed" resolved components of permittivity

$$\varepsilon'_p = \frac{1}{\omega} \frac{X_s}{(R_s)^2 + (X_x)^2} \qquad (11.6.a.4)$$

and

$$\varepsilon''_p = \frac{1}{\omega} \left[\frac{R_s}{(R_s)^2 + (X_s)^2} - \frac{1}{R_o} \right] \qquad (11.6.a.5).$$

As we have seen already (Section 8.3, Figures 9.2.c.II and 9.3.c.I-III, and Section 9.5) this procedure reveals a complex permittivity locus which over the range of frequencies measured is a straight line to within experimental accuracy (Salter, 1981), and NOT a minor arc of a circle as the Clar model and equation (11.6.a.2) would predict. Such results consequently imply that ε_s is either infinite (meaning that we are not dealing with a dielectric at all, but a semiconductor), or too large to determine. In either case the complex impedance expected from the Clar model will reduce to the form of the Cole equation over the range of frequencies in question, the effect of ε_∞ apparently being negligible over this range, because the straight line can always be assumed to pass through the origin. Thus no advantage is gained by using the Clar model rather than the Cole model, unless the Clar model can actually be interpreted in plausible physical terms whereas the Cole model cannot be. In fact however the very reverse is the case; the Clar model cannot be interpreted according to reasonable physical mechanisms whereas the Cole model can be, as will be demonstrated in the subsections to follow.

One reason to say that the Clar model has no reasonable physical interpretation is that there is still no fundamental understanding of why a Cole-Cole dielectric behaves in the way it does (cf. subsections 11.2.a and 11.3.b). Thus to say that skin is a (shunted) Cole-Cole dielectric is merely an alternative way of describing the problem, not a solution to it.

Secondly, skin could behave rather like a shunted Cole-Cole dielectric if it were composed of a number of similar "mosaic elements" in parallel each consisting of a conductance in parallel with a series combination of a capacitance and a conductance. These latter conductances in series with the capacitances would have to have an approximately log-normal distribution of values, arising perhaps from an approximately normal distribution of activation energies for charge-carrier motion between two spatially-separated sites whose separation would have to be the same in each mosaic element. But although the skin appendages could provide an interpretation of the parallel conductanct shunts, there is no physiologically reasonable interpretation of suitable combinations of capacitors and resistors in series, even considering Maxwell-Wagner effects (cf. Pethig, 1979).

Finally, Clar's own interpretation of the model is based upon counter-ion relaxation phenomena which we will consider briefly in the next subsection. It is indeed possible in this way to explain the existence of large values of ε_s. It is also possible to explain qualitatively, via the concept of charge-carrier mobility, why the relaxation time $\tau_p = 1/2\pi f_p$ is large, and why it decreases as hydration increases, but such explanations would be common to many phenomenological models, including the ones to be reviewed later. And as to the heart of the Clar model, the Cole-Cole dielectric, counter-ion relaxation theory totally fails to explain the origin of the very distinctive Cole-Cole distribution of relaxation times,

as will be seen in the next subsection. It also fails to explain why the distribution parameter $\alpha = 1-m$ alters with hydration (cf. subsection 9.3.c).

We may therefore conclude that the Clar model offers only "insights" into the problem of the form of the DRT in skin which are not derived from any fundamental theory, and which are not borne out by processing the data more critically. Thus we should spend no further time on it.

11.6.b Counter-ion relaxation

Colloidal particles in aqueous electrolyte solutions are electrically charged by fixed or adsorbed ions and are surrounded by counter-ions, forming an electrical double layer around the particles. Theories of counter-ion relaxation have suggested that displacements of these counter-ions by an externally applied electric field may be responsible for the observation of very low frequency dielectric relaxation with very high dielectric decrements in such colloidal systems. These theories have very recently been reviewed by Pethig (1979, pps. 167-175).

Such concepts are relevant to the interpretation of relaxation phenomena in skin, since the distinctive relaxation properties of skin are due to the stratum corneum, formed of tightly-packed cells composed of proteins which are amphoteric (see subsection 12.2.e) and which thus tend to acquire a fixed charge of sign and magnitude depending upon the pH of their environment. For example, these proteins contain immobile or "fixed" carboxyl groups and amino groups which terminate polypeptide chains, and carboxyl groups (-COOH) tend to lose protons in environments less acidic than about pH 5.0, thus acquiring a net negative charge and becoming $-COO^-$, whereas in acidic solutions amino groups ($-NH_2$) tend to gain protons and thus acquire a net positive charge to become $-NH_3^+$. Such charged groups tend to attract to the protein molecule the type of counter-ion atmosphere we considered above. Therefore we may expect that the ions within the hydration sheath of the proteins of the corneum may produce the same sort of phenomena as are described by theories of counter-ion relaxation in suspensions of colloidal particles.

Clar et al. (1973, 1975) made use of a theory by Schwarz (1962). Unfortunately however Schwarz had had to invoke a distribution of relaxation times purely by fiat, i.e. without any physical justification, and

Clar simply changed Schwarz's ad hoc log-uniform DRT into an ad hoc Cole-Cole DRT, and then combined his work with some by Takashima (1967), who had extended the Schwarz analysis to the case of ellipsoidal particles.

Schwarz had shown that the frequency of maximum dielectric loss, f_p, was proportional to $1/a^2$ where "a" was the radius of the particle surrounded by the ionic atmosphere. On the basis of this and other work Pethig (1979, p.173) has for example estimated that f_p would be as low as 300 Hz for a particle of radius one micrometre. Seeking to explain the equally low value of f_p for skin led Clar et al (1973) to propose that counter-ion relaxation was taking place around particles equally large, or at least nearly so, namely whole cells in the corneum. However, as we have seen, involving this theory would not (at its present state of development) explain the form of the DRT in skin. Secondly, as Pethig has pointed out (1979, p.174), the work of Schwarz has subsequently been shown to predict f_p values which are much too low - perhaps by two orders of magnitude. Finally, since the cells of the corneum are very tightly packed indeed (see e.g. Hashimoto, 1971), they are hardly comparable to colloidal particles suspended in electrolyte solutions.

Consequently, I believe there is little point in continuing to think in terms of whole cells, but there may still be some point in thinking of protein molecules WITHIN cells if we wish to apply the concepts of counter-ion relaxation theory to the phenomena observed in skin. Similar considerations still of course apply on this smaller scale (cf. Cope, 1970, pps. 33, 34; Pethig, 1979, pps. 91-93).

11.6.c Taking stock

Having stated the problem of the origin and form of the DRT in skin in subsection 11.3.f, we proceeded in Section 11.5 to follow up the work of Barnett and Tregear. However, having thoroughly examined gradient models and shunted gradient models too, it was concluded in subsection 11.5.f that such models were unable to explain the form of the DRT in skin unless physiologically unreasonable assumptions were made. Furthermore, in Section 11.6 the interpretation due to Clar has also been called into question, and the present resources of the literature have thereby been exhausted.

Consequently it should by now have become clear that we need somehow to analyse in a properly rigorous way the transport of charge carriers through a very complicated and probably very heterogeneous system of hydrated proteins. This is of course a horribly difficult task, and one which has not so far as I know been attempted before in the biological literature.

However, if we now move to consider the literature of solid-state physics, it is possible to obtain a great deal of help in beginning to tackle the problem. This literature contains much more powerful theoretical approaches.

11.7 Models of charge transport in inhomogeneous materials

11.7.a Random network models

An introduction to most of the solved theoretical aspects of electrical conduction in inhomogeneous materials has recently been provided by Landauer (1978), so here we may immediately move on to consider particular ways of modelling such conduction.

The great need in theoretical physics for a practicable model of charge carrier migration in solids, particularly giant molecules, polymers and vitreous systems, soon led to the use of randomly-connected networks of randomly-valued resistances to simulate the direct-current conductivity of such materials. The application of these random resistance networks has been discussed by Straley (1977). However, they are only capable of modelling the zero-frequency conductivity of inhomogeneous solids, and since this was often not enough, Pollak (1974) extended the earlier work of Miller and Abrahams (1960) which suggested generalizing the technique to involve the use of random impedance networks.

From Pollak's paper and later related ones it can however be seen that actually using random impedance networks to simulate conduction in inhomogeneous materials involves the numerical manipulation of impedance matrices of very large order, since the larger the order, the better for the accuracy of the simulation. Ideally there should of course be as many loops in the network as there are charge carrier traps in the sample of material, although such an enormous number would require impossibly complicated calculations.

11.7.b The continuous-time random walk (CTRW) formalism

We have seen that the use of random networks is a very cumbersome way of modelling the conductivity of inhomogeneous materials. Consequently it was a welcome development when, following earlier workers, Scher and Lax (1973a, 1973b) presented a much more easily usable, yet still rigorous, general model of charge carrier movement via localized states in disordered material. This new model treats the movement of charge carriers as a random walk on a lattice, taking place in continuous (rather than discrete) time. A charge carrier executing such a "continuous time random walk" (CTRW) is assumed to move from each temporary site by a vectorial amount $\vec{s}$ during the time t between movements, the values of $\vec{s}$ and t obeying a certain distribution function $\psi(\vec{s}, t)$

The complex conductivity of the material entirely depends upon this distribution function, or rather upon Fourier transforms of two of its spatial moments. If we firstly define

$$\psi(j\omega) = \sum_{\vec{s}} \int_0^\infty \exp(-j\omega t)\ \psi(\vec{s}, t)\ dt \qquad (11.7.b.1)$$

then d_{rms}, the root-mean-square displacement due to each "hop" on the lattice, turns out to be given by

$$d_{rms}^2(\omega) = \sum_{\vec{s}} s^2 \left[\int_0^\infty \exp(-j\omega t)\ \psi(\vec{s}, t)\ dt \right] / \psi(j\omega) \qquad (11.7.b.2)$$

and thus to be frequency-dependent. However, some physical models involving the CTRW formalism will have the property that a small change in inter-site separation will make a very large difference to the time needed to hop between sites, and when this is so, the frequency-dependence of d_{rms} may be considered to be negligible (Scher and Lax, 1973a, p.4495). For such models, d_{rms} will effectively be a constant.

The elegance and convenience of the CTRW formalism is shown by the fact that only two more equations are needed to specify the complex conductivity of the material. The two previous equations define a complex frequency-dependent diffusion constant given by

$$D(j\omega) = \frac{1}{6} d^2_{rms}(\omega) \cdot j\omega \frac{\psi(j\omega)}{1 - \psi(j\omega)} \qquad (11.7.b.3)$$

and so we have that the complex conductivity is

$$\sigma^*(j\omega) = \frac{n q^2}{kT} D(j\omega) \qquad (11.7.b.4)$$

where n is the number of charge carriers per unit volune, q is their charge, k is Boltzmann's constant, and T is the absolute temperature.

Lastly, we can define the D.C. (zero frequency) conductivity of the system by

$$\sigma(o) = \frac{nq^2}{kT} D(o) = \frac{nq^2}{kT} \cdot \frac{1}{6} d^2_{rms}(o) \cdot \frac{1}{\bar{t}} \qquad (11.7.b.5)$$

where

$$\bar{t} = \int_o^\infty t\, \psi(t)\, dt \qquad (11.7.b.6)$$

and $\psi(t)$ is the inverse Laplace transform of $\psi(j\omega)$.

11.7.c Applying the CTRW formalism

The key to applying the CTRW formalism is to identify

$$\psi(j\omega) = \int_0^\infty \frac{G(\tau)\, d\tau}{1 + j\omega\tau} \qquad (11.7.c.1)$$

where $G(\tau)$ is the distribution of relaxation times present in the material. This equation can also be used in the forms

$$\psi(j\omega) = \int_{-\infty}^\infty \frac{F(s)\, ds}{1 + j\omega\tau} \quad (\text{for } s = \ln\frac{\tau}{\tau_o},\ \tau_o = \text{constant}) \qquad (11.7.c.2)$$

$$\text{or} \quad \psi(j\omega) = \int_0^\infty \frac{P(\lambda)\, d\lambda}{1 + j\omega\tau} \quad (\text{for } \lambda = \frac{1}{\tau}) \qquad (11.7.c.3)$$

$$\text{or} \quad \psi(j\omega) = \int_0^\infty \frac{\lambda P(\lambda)\, d\lambda}{j\omega + \lambda} \qquad (11.7.c.4)$$

which is the Stieltjes transform of $\lambda P(\lambda)$ as used for example by Pfister and Scher (1977, eqn.31),

$$\text{or} \quad \psi(j\omega) = \int_0^\infty \frac{D(\lambda)\, d\lambda}{j\omega + \lambda} \quad (\text{for } D(\lambda) = \lambda P(\lambda)) \qquad (11.7.c.5)$$

this being the form employed by Macdonald and Brachman (1956, eqn.57') in defining what they called the "network function".

The application of the CTRW formalism will be much clearer however if we now work through some illustrative examples.

Example 1 - Delta-function DRT

If there is only one time-constant, τ_o, in the system, for example because the material contains non-interacting traps all with the same trapping energy, then

$$G(\tau) = \delta(\tau-\tau_o) \quad \text{(cf. Macdonald and Brachman, 1956, p.412,no.6)} \qquad (11.7.c.6)$$

$$F(s) = \delta(s-s_o) \qquad (11.7.c.7)$$

and $$P(\lambda) = \delta(\lambda-\lambda_o) \quad \text{(cf. Pfister and Scher 1977, eqn.30c with i=1)} \qquad (11.7.c.8)$$

Inserting one of these three equations into the appropriate choice from equations (11.7.c.1) to (11.7.c.5) produces

$$\psi(j\omega) = \frac{1}{1 + j\omega\tau_o} \quad \text{(cf. Macdonald and Brachman, 1956, p.412, no.6)} \qquad (11.7.c.9)$$

so by inverse Laplace transformation

$$\psi(t) = \frac{1}{\tau_o} \exp\left(-\frac{t}{\tau_o}\right) = \lambda_o \exp(-\lambda_o t) \qquad (11.7.c.10)$$

and $$D(o) = \frac{1}{6} d^2_{rms}(o) \frac{1}{\tau_o} \qquad (11.7.c.11)$$

Thus from (11.7.c.9), (11.7.b.3) and (11.7.b.4) together with the limit (11.7.c.11), it can be seen that for this case the conductivity is constant, independent of frequency (cf. Scher and Lax 1973a, eqn.46).

Example 2 - Davidson-Cole DRT

Noting that (11.7.c.9) has the form of the normalized complex permittivity of a Debye dielectric may encourage us to use the equivalent expression due to Davidson and Cole (1951), namely

$$\psi(j\omega) = \frac{1}{(1 + j\omega\tau_o)^{1-\alpha}} \qquad (11.7.c.12)$$

so from (11.7.b.3) and (11.7.b.4)

$$\sigma(j\omega) = \frac{nq^2}{kT} \cdot \frac{1}{6} d^2_{rms}(\omega) \frac{j\omega}{(1 + j\omega\tau_o)^{1-\alpha} - 1} \qquad (11.7.c.13)$$

which at very high frequencies (i.e. $\omega >> \tau_o$) tends to

$$\sigma(j\omega)_{VHF} \simeq \frac{1}{\tau_o} (j\omega\tau_o)^{\alpha} \qquad (11.7.c.14)$$

Equation (11.7.c.12) is equivalent to

$$\Psi(t) = \frac{1}{\tau_o} \frac{1}{\Gamma(1-\alpha)} (\frac{t}{\tau_o})^{-\alpha} \exp(-t / \tau_o) \qquad (11.7.c.15)$$

so that at zero frequency we have from (11.7.b.6) and (11.7.b.5) that

$$\sigma(o) = \frac{nq^2}{kT} \cdot \frac{1}{6} d^2_{rms} \frac{1}{\tau_o} \qquad (11.7.c.16)$$

just as we found for example 1. Thus a Davidson-Cole DRT in the material produces a conductivity which rises from a non-zero D-C. value towards a power-law frequency dependence (in fact a "polarization admittance") at very high frequencies. This is very interesting because it is exactly the behaviour of the skin, but unfortunately there can be no justification for using a Davidson-Cole DRT with the CTRW formalism because there is still no physical interpretation of the physical origin of Davidson-Cole DRTs in materials.

We therefore need to know how to apply the CTRW formalism to a DRT which *does* have a physical interpretation. In general, given some

logarithmic expression of the DRT, F(s), existing between the limits $s_{min} \leq s \leq s_{max}$, we will then need to evaluate

$$\psi(j\omega) = \int_{s_{min}}^{s_{max}} \frac{F(s)\,ds}{1 + j\omega\tau} = \int_{s_{min}}^{s_{max}} \frac{F(s)\ ds}{1 + j\omega\tau_o \exp\ (s)} \quad (\text{since } s=\ln(\tau/\tau_o) \qquad (11.7.c.17)$$

$$= \psi'(\omega) - j\psi''(\omega) \qquad (11.7.c.18)$$

where

$$\psi'(\omega) = \int_{s_{min}}^{s_{max}} \frac{F(s)\,ds}{1 + [\omega\tau_o \exp\ (s)]^2} \qquad (11.7.c.19)$$

and

$$\psi''(\ ) = \int_{s_{min}}^{s_{max}} \frac{F(s)\ \ \omega\tau_o \exp(s)\ \ ds}{1 + [\omega\tau_o \exp\ (s)]^{\ 2}} \qquad (11.7.c.20)$$

Using (11.7.c.18), (11.7.b.3) and (11.7.b.4) we may then write the complex conductivity due to the CTRW as

$$\sigma^*_{CTRW}(j\omega) = \sigma'_{CTRW}(\omega) + j\,\sigma''_{CTRW}(\omega) \qquad (11.7.c.21)$$

where

$$\sigma'_{CTRW}(\omega) = \frac{nq^2}{kT} \cdot \frac{1}{6} d^2_{rms}(\omega) \cdot \frac{\omega\psi''}{(1 - \psi')^2 + (\psi'')^2} \qquad (11.7.c.22)$$

and

$$\sigma''_{CTRW}(\omega) = \frac{nq^2}{kT} \frac{1}{6} d^2_{rms}(\omega) \frac{\omega[\psi'(1-\psi') - (\psi'')^2]}{(1-\psi')^2 + (\psi'')^2} \qquad (11.7.c.23)$$

We will now proceed in Sections 11.8 and 11.9 to derive some suitable functions F(s), suitable because they do have a credible physical basis.

11.8 Some localized-state models of the Cole equation assuming conduction by electrons or holes

11.8.a Some work of Lewis

In Section 11.4 we saw that the conductive properties of the skin are usually determined by those of the stratum corneum, which is basically a matrix of proteins called keratins. Some of these are crystalline or micro-crystalline, and others are amorphous. We also saw that the keratins are semiconductors, and that at least some of the charge carriers in the protein matrix of the corneum are likely to be electrons or holes.

All this should indicate that theories dealing with electronic transport in amorphous semiconductors (see subsection 11.3.e) may well be very helpful in interpreting the phenomenology of charge transport through the stratum corneum too. As we noted before in subsection 11.3.e, Lewis (1977) has provided an extensive review of these theories and shown that if conduction takes place by means of electrons or holes, the most versatile interpretation of complex conductivities of the form

$$\sigma^*(j\omega) = \sigma_1 + \sigma_2 (j\omega\tau)^{\alpha} \qquad (11.8.a.1)$$

cf. (11.1.3)

is that they arise from the multi-phonon-activated hopping of charge carriers out of a bandtail of localized states, and into localized states of the same bandtail but in some other part of the material, the hop occurring via the band from which the bandtail extends.

At the heart of the theory is the assumption that in the bandgap there is a bandtail of localized states which may be described by a density-of-states function

$$g(\frac{\Delta E}{kT}) \quad = \quad C \exp[- \frac{\alpha}{2} \cdot \frac{\Delta E}{kT}] \qquad (11.8.a.2)$$

where ΔE is the multi-phonon activation energy for charge carrier release into a band, α is a constant usually having a value between zero and unity, and C is also a constant, provided for purposes of normalization. I will call (11.8.a.2) a "neo-exponential" bandtail. For electron conduction via the conduction band we expect

$$\Delta E \quad = \quad E_g - E \qquad (11.8.a.3)$$

where E is the energy associated with the localized state and E_g is the energy of the conduction band edge. Similarly for hole conduction in the valence band we expect

$$\Delta E \quad = \quad E - E_g \qquad (11.8.a.4)$$

Assuming, furthermore, following the evidence of Lewis (1977, p.202) that charges predominantly hop between states of equal activation energy, the probability that a pair of such states is only singly occupied and thus able to support the hopping process, is f(z)(1 - f(z)) where f is the Fermi function

$$f \quad = \quad (1 + \exp (z))^{-1} \qquad (11.8.a.5)$$

and $$z \quad = \quad (E - E_F) \ /kT \qquad (11.8.a.6)$$

E_F being the Fermi energy. If in the region of the localized states $(E - E_F) > 6kT$, this probability is well represented by a pure exponential.

Then the compound probability P of the operation of a particular hopping activation energy ΔE is approximately

$$P = g^2 (\Delta E) \exp [- (E - E_F) / kT] \qquad (11.8.a.7)$$

and this may be written entirely in terms of ΔE as

$$P(\Delta E) = C1 \exp [(1 - \alpha) . \Delta E / kT] \qquad (11.8.a.8)$$

with C1 as a new constant.

Lewis then proceeded to derive some very interesting results from this distribution of activation energies. Firstly he showed that it should lead us to expect a real component of complex conductivity of the form

$$\sigma'(\omega) = C3 . \omega^{\alpha} \qquad (11.8.a.9)$$

for arbitrary values of α over an arbitrarily large range of frequency. (C3 is another constant.) This versatility is quite startling and correspondingly important. Using the relation $\sigma^* = j\omega\varepsilon^*$, (11.8.a.9) was then shown to correspond to

$$\varepsilon''(\omega) = C3 . \omega^{\alpha-1} \qquad (11.8.a.10)$$

and one could then infer from earlier equations that if C4 was a further constant, then

$$\varepsilon'(\omega) = C4 . \omega^{\alpha-1} \qquad (11.8.a.11)$$

Such an inference is however only reasonable over a limited frequency range, since although (11.8.a.10) and (11.8.a.11) do indeed form a Hilbert transform pair, they do not form a Kramers-Kronig transform pair, since ε_o is not defined by them.

Finally, assuming that α depended on temperature T approximately according to

$$\alpha = a + bT \qquad (11.8.a.12)$$

with a and b as arbitrary constants, he was able to derive a temperature dependence for $\sigma'(\omega)$. This agreed well with the form required by very many experimental results, and since these had not previously been satisfactorily interpreted, a correspondingly greater value should be attached to this approach.

What especially impressed me however was the equation (11.8.a.9). This was because it was derived from a physical model apparently very suitable to the case of skin, and also because there seemed to be no restrictions upon its application over an arbitrarily wide frequency range with a constant (and arbitrary) value of α. Moreover I knew that insofar as (11.8.a.11) held, an equation for the imaginary component of conductivity having the same form as (11.8.a.9) could be derived, and this together with (11.8.a.9) itself would represent a polarization admittance which when added to some purely real shunt conductance σ_1 would exactly reproduce equation (11.8.a.1) and thus the Cole equation (see Section 11.1). However, I also knew that the pair (11.8.a.10) and (11.8.a.11) could not both hold over an arbitrarily large range of frequency, and so I set out to rework some aspects of Lewis's theory in order to better ascertain how applicable it might be to modelling the Cole equation in the case of human skin.

11.8.b The Matsumoto-Higasi distribution

When re-working a Lewis type of theory, it would seem to be desirable to incorporate in it the physical requirement that the bandtail cannot extend over an arbitrarily large range of ΔE. Therefore as a first approximation let us use instead of (11.8.a.2) the truncated density-of-states function

$$\overline{g(\frac{\Delta E}{kT})} = C \exp\left[-\frac{\alpha}{2} \cdot \frac{\Delta E}{kT}\right] \quad \Delta E_1 \leq \Delta E \leq \Delta E_2 < \infty$$

$$= 0 \qquad \Delta E < \Delta E_1,\ \Delta E > \Delta E_2 \quad (11.8.b.1)$$

which by similar reasoning to that employed in the last subsection leads us to expect a truncated distribution of activation energies

$$P(\Delta E) = C1 \exp\left[(1-\alpha)\frac{\Delta E}{kT}\right] \quad \Delta E_1 \leq \Delta E \leq \Delta E_2 < \infty$$

$$= 0 \qquad \Delta E < \Delta E_1,\ \Delta E > \Delta E_2 \quad (11.8.b.2)$$

Now if we define a relaxation time τ in the usual way

$$\tau = \tau_a \exp\left(\frac{\Delta E}{kT}\right) \quad (11.8.b.3)$$

with τ_a as some constant, then we may write (11.8.b.2) as

$$P(\Delta E) = C1 \left(\frac{\tau}{\tau_a}\right)^{1-\alpha} \qquad \tau_1 \leq \tau \leq \tau_2 < \infty$$

$$= 0 \qquad \tau < \tau_1,\ \tau > \tau_2 \quad (11.8.b.4)$$

and so defining a distribution of relaxation times $G(\tau)$ by

$$G(\tau) = P(\Delta E)\,\frac{d(\Delta E)}{d\tau} \qquad (11.8.b.5)$$

we have from (11.8.b.4) a DRT of the form

$$G(\tau) = A\,\tau^{-\alpha} \qquad \tau_1 \leq \tau \leq \tau_2 < \infty \qquad (11.8.b.6)$$

$$= 0 \qquad \tau < \tau_1,\ \tau > \tau_2 \qquad (11.8.b.6)$$

where A is a normalization constant which must be chosen such that

$$\int_0^\infty G(\tau)\,d\tau = 1 \qquad (11.8.b.7)$$

and so for example for $0 < \alpha < 1$,

$$A = \frac{(1-\alpha)}{[(\tau_2)^{1-\alpha} - (\tau_1)^{1-\alpha}]} \qquad (11.8.b.8)$$

The distribution of relaxation times (11.8.b.6) was first investigated by Matsumoto and Higasi (1962) although in its untruncated form $\tau_1 = 0$, $\tau_2 = \infty$ it was used by von Schweidler himself as long ago as 1907. However, the von Schweidler form is of course unnormalizable and thus unphysical. It should also be noted that the normalization of the Matsumoto-Higasi distribution function has, surprisingly, been incorrectly expressed in the review by Böttcher and Bordewijk (1978) but may be corrected by replacing p with (1-p) in their equation (9.127).

Now, in re-working aspects of the Lewis bandtail theory we are of course aiming to derive the complex permittivity and hence the complex conductivity associated with the physically more reasonable truncated bandtail (11.8.b.1). One way of doing this is to examine

$$\frac{\varepsilon^* - \varepsilon_\infty}{\varepsilon_s - \varepsilon_\infty} = \int_0^\infty \frac{G(\tau)\,d\tau}{1 + j\omega\tau} \qquad (11.8.b.9)$$

and so we took the trouble to derive the $G(\tau)$, equation (11.8.b.6), corresponding to the truncated bandtail (11.8.b.1). However, the next step, that of working out (11.8.b.9) is very much more difficult and indeed has not previously been solved. Consequently before meeting this problem head-on in subsection 11.8.d, let us consider an approximation.

11.8.c An approximation to illustrate shunted dielectric models in general

Let us temporarily assume that ΔE_1 is so small, for example because the top of the bandtail merges into the band, that τ_1 is approximately equal to τ_a, and that this may for practical purposes be assumed to equal zero, although the case $\tau_1 = 0$ is of course in reality physically impossible.

Then for $0 < \alpha < 1$ the Matsumoto-Higasi distribution (11.8.b.6) simplifies to

$$G(\tau) = (1 - \alpha)(\tau_2)^{\alpha-1} \tau^{-\alpha} \qquad 0 \leq \tau \leq \tau_2 < \infty$$

$$= 0 \qquad \tau < 0,\ \tau > \tau_2 \qquad (11.8.c.1)$$

which is reminiscent of the DRT used by Davidson and Cole (1951) for $0 \leq \alpha < 1$, namely

$$G(\tau) = \frac{\sin(\alpha\pi)}{\pi} (\tau_2 - \tau)^{\alpha-1} \tau^{-\alpha} \qquad 0 \leq \tau \leq \tau_2 < \infty$$

$$= 0 \qquad \tau < 0,\ \tau > \tau_2 \qquad (11.8.c.2)$$

From the form of equations (11.8.b.9) and (11.8.b.6) it can be seen that at high frequencies the overwhelming contribution to the complex permittivity comes from charge carriers subject to values of τ very much less than τ_2. Thus we may expect that at sufficiently high frequencies ($\omega\tau_2 >> 1$), the relevant τ values will be negligible in comparison with τ_2 and the Davidson-Cole DRT (11.8.c.2) will produce results indistinguishable from those of the distribution function

$$G(\tau) = \frac{\sin(\alpha\pi)}{\pi} (\tau_2)^{\alpha-1} \tau^{-\alpha} \qquad 0 \leq \tau \leq \tau_2 < \infty$$

$$= 0 \qquad \tau < 0, \ \tau > \tau_2 \qquad (11.8.c.3)$$

for $0 \leq \alpha \leq 1$. We also know (Davidson and Cole, 1951) that the Davidson-Cole DRT produces

$$\frac{\varepsilon^* - \varepsilon_\infty}{\varepsilon_s - \varepsilon_\infty} = (1 + j\omega\tau_2)^{\alpha-1} \qquad 0 \leq \alpha < 1 \qquad (11.8.c.4)$$

which at high frequencies ($\omega\tau_2 >> 1$) will produce results indistinguishable from

$$\frac{\varepsilon^* - \varepsilon_\infty}{\varepsilon_s - \varepsilon_\infty} = (j\omega\tau_2)^{\alpha-1} \qquad 0 \leq \alpha < 1 \qquad (11.8.c.5)$$

so we may expect that the distribution function (11.8.c.3) will also produce a complex permittivity of the form (11.8.c.5), and that the Matsumoto-Higasi distribution simplified by the assumption $\tau_1 = 0$, equation (11.8.c.1), will produce at sufficiently high frequencies results which are indistinguishable from those obeying

$$\frac{\varepsilon^* - \varepsilon_\infty}{\varepsilon_s - \varepsilon_\infty} = \frac{(1-\alpha)\pi}{\sin(\alpha\pi)} (j\omega\tau_2)^{\alpha-1} \qquad 0 < \alpha < 1 \qquad (11.8.c.6)$$

Then using the relation

$$j^{(\alpha-1)} = \sin\left(\frac{\alpha\pi}{2}\right) - j\cos\left(\frac{\alpha\pi}{2}\right) \qquad (11.8.c.7)$$

the complex expression (11.8.c.6) can be resolved into its real and imaginary components

$$\frac{\varepsilon' - \varepsilon_\infty}{\varepsilon_s - \varepsilon_\infty} = (1 - \alpha)\,\frac{\pi}{2}\,\sec\left(\frac{\alpha\pi}{2}\right)(\omega\tau_2)^{\alpha-1} \qquad (11.8.c.8)$$

and

$$\frac{\varepsilon''}{\varepsilon_s - \varepsilon_\infty} = (1 - \alpha)\,\frac{\pi}{2}\,\mathrm{cosec}\left(\frac{\alpha\pi}{2}\right)(\omega\tau_2)^{\alpha-1} \qquad (11.8.c.9)$$

which may be compared with Lewis's results (11.8.a.10) and (11.8.a.11) since our current set of assumptions is equivalent to abandoning the truncation of the bandtail. Consequently (11.8.c.6) may also be obtained by simple Steiltjes transformation of the von Schweidler distribution (cf. Macdonald and Brachman, 1956, Table I, no.4).

Now because these results we have obtained only hold for high frequencies ($\omega\tau_2 >> 1$), they would in fact be very little altered by expressing them in combination with the CTRW formalism. (At high frequencies the denominator of (11.6.b.3) tends to unity.) Thus we will not express them in combination with the CTRW formalism, but will instead employ these only approximate results merely as an example to illustrate the general principles of "shunted dielectric" models of skin. Such models assume it to be a dielectric (preferably a non-Debye dielectric) attributed usually to the corneum, in parallel with a purely real conductance attributable to the skin appendages and whatever other "holes through the corneum" may be assumed to exist (see e.g. Hashimoto, 1971). One such model was of course that of Clar, who as we considered in subsection 11.6.a suggested that skin could be represented as a shunted Cole-Cole dielectric. However, the model which will now be derived is more fundamental than the Clar model in that it relies upon a DRT based directly upon physical consideration of the material being tested, and not upon a completely empirical distribution. As it happens it is also better than the Clar model in that it produces a more accurate fit to the Cole equation.

Taking this approach, we may write the complex conductivity of the material as

$$\sigma^* = \sigma_o + j\omega\varepsilon^* = \sigma' + j\sigma'' \qquad (11.8.c.10)$$

where σ_o is the assumed conductance contribution of parallel shunts through the skin. Then since the effect of ε_∞ can probably be neglected in the frequency range of interest, we have from (11.8.c.6) that

$$\sigma^* = \sigma_o + \frac{(1-\alpha)\pi}{\sin(\alpha\pi)} \cdot \frac{\varepsilon_s}{\tau_2} (j\omega\tau_2)^\alpha \quad \omega_{min} \leq \omega \leq \infty$$

$$0 < \alpha < 1 \qquad (11.8.c.11)$$

Here ω_{min} is the minimum value of ω required to ensure that the product $\omega\tau_2$ is large enough to make (11.8.c.6) an acceptably accurate approximation. If, for example, we are willing to tolerate no more than a 5% error in either ε' or ε'', we require

$$\omega\tau_2 \leq 15 \quad \text{for} \quad 0.4 < \alpha < 0.99 \qquad (11.8.c.12)$$

Let us adopt this value as a standard. If we make use of a skin-dimensions correction factor D, equal to the area of skin covered by an electrode in one or our experiments, that is, one square centimetre, divided by the thickness of the corneum at a typical skin site, that is about 10 μm, then D equals ten metres and the complex impedance of the skin site can be expected to obey

$$Z = \frac{R_o}{1 + \frac{D.R_o.\ \varepsilon_s(1-\alpha)\pi}{\tau_2 \sin(\alpha\pi)} (j\omega\tau_2)^\alpha}, \quad \omega \geq 15/\tau_2 \qquad (11.8.c.13)$$

or alternatively

$$Z = \frac{R_o}{1 + (j\omega\tau_p)^{1-m}} \qquad (11.8.c.14)$$

using

$$m = 1 - \alpha \qquad (11.8.c.15)$$

and

$$\tau_p = \left[\frac{D.R_o.\varepsilon_s.(1-\alpha)\pi}{\sin(\alpha\pi)} . \tau_2^{\alpha-1} \right]^{\frac{1}{\alpha}} \qquad (11.8.c.16)$$

as long as

$$\omega \geq 15/\tau_2 = 15. \left[\frac{\tau_p^{\alpha} . \sin(\alpha\pi)}{D.R_o.\varepsilon_s.(1-\alpha)\pi} \right]^{\frac{1}{1-\alpha}} \qquad (11.8.c.17)$$

so using the semi-empirical trial values (in S.I. units where appropriate)

$$\alpha = 0.6$$

$$\tau_p = 1 \times 10^{-3} s$$

$$D = 10 \text{ m}$$

$$R_o = 1 \times 10^{5} \text{ ohms}$$

and $$\varepsilon_s \simeq 60 \times 8.85 \times 10^{-12} \text{ Fm}^{-1} \qquad (11.8.c.18)$$

we find that the behaviour of the model is likely to begin to stray detectably from that of the Cole equation (11.8.c.14) for frequencies

$$\omega \leq 3.6274 \times 10^{4}$$

i.e. $$f \leq 5.77 \text{ kHz} \qquad (11.8.c.19)$$

These values are only intended to serve as a guideline, since of course they depend upon the values chosen in (11.8.c.18). Nevertheless, we saw earlier (in subsection 11.6.a) that departures from the Cole equation were to be expected at "low" frequency using the Clar shunted dielectric model, and it seems that our present more fundamental shunted dielectric model is likely to have similar difficulties. However, we have made a large number of simplifying assumptions in deriving the model, and since these may well be contributing to the problem, it is now time to derive the behaviour of the truncated bandtail model without such approximations.

11.8.d A shunted CTRW-truncated-bandtail model

If we are to derive the behaviour expected from a model involving charge carriers executing a continuous-time random walk via localized states of a truncated Lewis-type bandtail, it is necessary to solve an equation equivalent to

$$\psi(j\omega) = \int_0^\infty \frac{G(\tau)\,d\tau}{1 + j\omega\tau} \qquad \text{(11.8.d.1) and (11.6.c.1)}$$
compare also (11.8.b.9)

in which $G(\tau)$ is the Matsumoto-Higasi distribution (11.8.b.6). In this instance the right-hand-side of (11.8.d.1) has not previously been worked out for the general case $0 < \alpha < 1$. Macdonald (1963) promised that he was going to publish a general solution, but I have not been able to find it. It seems in fact that people have either had to resort to numerical integration, as for example did Vaughan, Lovell and Smyth (1962), or else they have been restricted to solving particular fractional cases of α, as were Matsumoto and Higasi themselves (1962). Consequently the analytic solution for the general case $0 < \alpha < 1$ which will now be given here may well be found to be useful in other contexts as well as the present one.

Now equations (11.8.d.1) and (11.6.c.18) imply that

$$\psi'(\omega) = \int_0^\infty \frac{G(\tau)\,d\tau}{1 + \omega^2\tau^2} \qquad \text{(11.8.d.2)}$$

and

$$\psi''(\omega) = \int_0^\infty \frac{G(\tau)\ \omega\tau\ d\tau}{1 + \omega^2\tau^2} \qquad \text{(11.8.d.3)}$$

Considering firstly the real component (11.7.d.2), when the distribution function has the Matsumoto-Higasi form we have

$$\psi'(\omega) = A \int_{\tau_1}^{\tau_2} \frac{\tau^{-\alpha} d\tau}{1 + \omega^2\tau^2} \qquad (11.8.d.4)$$

$$= A\omega^{\alpha} \int_{\omega\tau_1}^{\omega\tau_2} \frac{(\omega\tau)^{-\alpha} \frac{d\tau}{d(\omega\tau)} d(\omega\tau)}{1 + (\omega\tau)^2} \qquad (11.8.d.5)$$

and since

$$d\tau/d(\omega\tau) = 1/\omega \qquad (11.8.d.6)$$

$$\psi'(\omega) = A\ \omega^{\alpha-1} \left[\int_{o}^{x_2} \frac{x^{-\alpha} dx}{1 + x^2} - \int_{o}^{x_1} \frac{x^{-\alpha} dx}{1 + x^2} \right], \quad x = (\omega\tau) \qquad (11.8.d.7)$$

Now the integral

$$\int_{o}^{X} \frac{x^{-\alpha} dx}{1 + x^2} \qquad (11.8.d.8)$$

can be solved in the general case $0 < \alpha < 1$ by series expansion followed by term-by-term integration, but we must ensure that the series expansion used is valid for all values of x within the range of integration, i.e. $0 \leq x \leq X$. In the present case, this means that we have to split the integral into two parts when $X > 1$. Thus firstly consider

(a) $X \geq 1$

We may write

$$\int_0^X \frac{x^{-\alpha}dx}{1+x^2} = \int_0^1 \frac{x^{-\alpha}dx}{1+x^2} + \int_1^X \frac{x^{-\alpha}\,dx}{1+x^2} \qquad (11.8.d.9)$$

then using suitable series expansions and integrating term-by-term

$$\int_0^X \frac{x^{-\alpha}dx}{1+x^2} = \sum_{n=1}^{n=\infty} \frac{(-1)^{(n+1)}\, x^{(2n-1-\alpha)}}{(2n-1-\alpha)} \Bigg|_0^1$$

$$+ \sum_{n=0}^{n=\infty} \frac{(-1)^{(n+1)}\, x^{-(2n+1+\alpha)}}{(2n+1+\alpha)} \Bigg|_1^X \qquad (11.8.d.10)$$

which reduces to

$$\int_0^X \frac{x^{-\alpha}dx}{1+x^2} = \sum_{n=0}^{n=\infty} \frac{(-1)^{(n+1)}\, X^{-(2n+1+\alpha)}}{(2n+1+\alpha)}$$

$$- \sum_{n=0}^{n=\infty} \frac{(-1)^{n+1}\, 2(2n+1)}{(2n+1)^2 - \alpha^2} \quad ,$$

$$X \geq 1, \ \alpha \neq -1, -3, -5, \ldots \qquad (11.8.d.11)$$

the two infinite series being kept separate for computational convenience.

Secondly,

(b) $X \leq 1$

In this case a single series expansion will be valid over the whole range of integration and so we have

$$\int_o^X \frac{x^{-\alpha} dx}{1 + x^2} = \sum_{n=1}^{n=\infty} \frac{(-1)^{(n+1)} x^{(2n-1-\alpha)}}{(2n - 1 - \alpha)} \Bigg|_o^X$$

$$= \sum_{n=1}^{n=\infty} \frac{(-1)^{n+1} X^{(2n-1-\alpha)}}{(2n - 1 - \alpha)}$$

$$X \leq 1, \ \alpha \neq 1, 3, 5, \ldots \qquad (11.8.d.12)$$

Thus finally the value of equation (11.8.d.17) can be calculated from

$$\psi'(\omega) = A\omega^{\alpha-1} \left[\begin{pmatrix} k_1 \\ \text{or} \\ k_2 \end{pmatrix} - \begin{pmatrix} k_3 \\ \text{or} \\ k_4 \end{pmatrix} \right] \qquad (11.8.d.13)$$

where k_1 = the value of (11.8.d.12) with $X = \omega\tau_2$ if $\omega\tau_2 \leq 1$

k_2 = " " " (11.8.d.11) " " $= \omega\tau_2$ if $\omega\tau_2 \geq 1$

k_3 = " " " (11.8.d.12) " " $= \omega\tau_1$ if $\omega\tau_1 \leq 1$

k_4 = " " " (11.8.d.11) " " $= \omega\tau_1$ if $\omega\tau_1 \geq 1$

and A is obtained from (11.8.b.8).

Considering secondly the imaginary component (11.8.d.3), following a similar approach and making use of the integrals

$$\int_0^X \frac{x^{(1-\alpha)}\,dx}{1+x^2} = \sum_{n=0}^{n=\infty} \frac{(-1)^{(n+1)}\, X^{-(2n+\alpha)}}{(2n+\alpha)}$$

$$- \sum_{n=0}^{n=\infty} \frac{(-1)^{(n+1)}\, 2(2n+1)}{(2n+1)^2 - (\alpha-1)^2}$$

$$X \geq 1, \quad \alpha \neq 0, -2, -4, \ldots \qquad (11.8.d.14)$$

and

$$\int_0^X \frac{x^{(1-\alpha)}\,dx}{1+x^2} = \sum_{n=1}^{n=\infty} \frac{(-1)^{(n+1)}\, X^{(2n-\alpha)}}{(2n-\alpha)}$$

$$X \leq 1, \quad \alpha \neq 0, 2, 4, \ldots \qquad (11.8.d.15)$$

leads us to the result that

$$\psi''(\omega) = A\omega^{\alpha-1} \left[\begin{pmatrix} k_5 \\ \text{or} \\ k_6 \end{pmatrix} - \begin{pmatrix} k_7 \\ \text{or} \\ k_8 \end{pmatrix} \right] \qquad (11.8.d.16)$$

where k_5 = the value of (11.8.d.15) with $X = \omega\tau_2$ if $\omega\tau_2 \leq 1$

k_6 = " " " (11.8.d.14) " " $= \omega\tau_2$ if $\omega\tau_2 \geq 1$

k_7 = " " " (11.8.d.15) " " $= \omega\tau_1$ if $\omega\tau_1 \leq 1$

k_8 = " " " (11.8.d.14) " " $= \omega\tau_1$ if $\omega\tau_1 \geq 1$

and A is obtained from (11.8.b.8).

This completes the solution of (11.8.d.1). Equations (11.8.d.13) and (11.8.d.16) were tested by converting them into a computer program, and there was found to be full agreement with the results of Matsumoto and Higasi (1962) and Vaughan, Lovell and Smyth (1962).

We may now use (11.8.d.13) and (11.8.d.16) to complete the shunted CTRW-truncated bandtail model. By substituting them into (11.7.c.22) and (11.7.c.23), and adding to (11.7.c.22) a purely real conductance τ_{shunts} to represent the shunting effect of the skin appendages, we obtain particular values of

$$\sigma'(\omega) = \sigma_{shunts} + \sigma'_{CTRW}(\omega) \qquad (11.8.d.17)$$

and $$\sigma''(\omega) = \sigma''_{CTRW}(\omega) \qquad (11.8.d.18)$$

Then we may calculate the complex impedance of skin site expected on the basis of this model from

$$Z(j\omega) = R_s(\omega) - jX_s(\omega) \qquad (11.8.d.19)$$

where

$$R_s(\omega) = \frac{\sigma'/D}{(\sigma')^2 + (\sigma'')^2} \qquad (11.8.d.20)$$

$$-X_s(\omega) = \frac{\sigma''/D}{(\sigma')^2 + (\sigma'')^2}. \qquad (11.8.d.21)$$

and D is the assumed skin-dimensions correction factor.

If all this is actually done, however, we find that the results predicted by the model, although pleasing in some respects, are still a little disappointing in that at low frequencies they are not as close as might have been hoped to predictions based on a Cole equation fitted to the high-frequency behaviour. I began to suspect that this effect at low frequencies might be attributable to the assumption made at the beginning of subsection 11.8.b, since although bandtails do not extend over arbitrarily large ranges of activation energy, neither are they truncated after the manner of (11.8.b.1). In fact at sufficiently high ΔE they tend

to meet not truncation, but another bandtail extending into the bandgap from the opposite band. Such "pairing" of bandtails is for example shown schematically by Mott and Davis (1971, Fig.2.14) and Taylor (1978, Fig.1b), and for a particular material (amorphous silicon) by Spear et al., (1978, Fig.1).

It would seem then that in order to correspond more closely with physical reality, what we actually need is a shunted CTRW model involving *two* bandtails, with one facing the other across the bandgap. In the next subsection we will find that this concept leads to a very successful model, in that it predicts results which can be closely fitted to a Cole equation over the whole complex impedance locus.

11.8.e A shunted CTRW-double-bandtail model

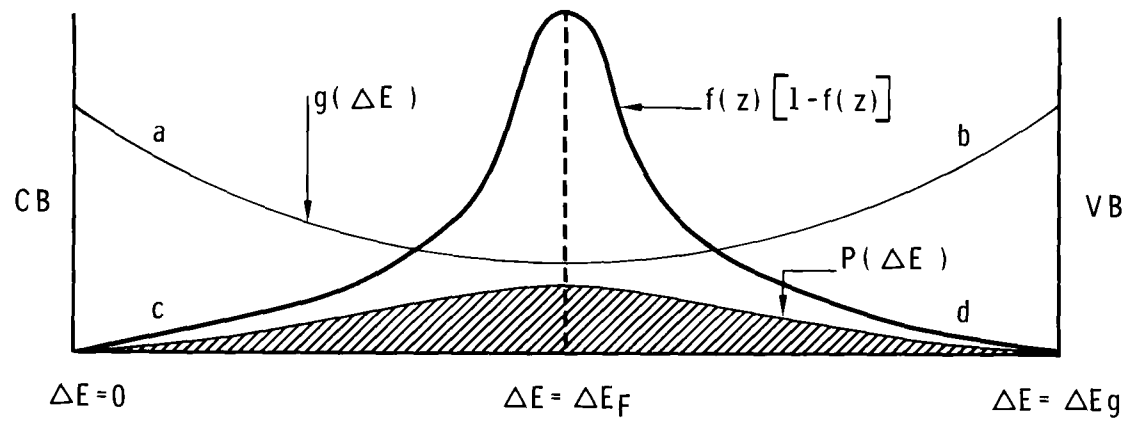


Fig. 11.8.e.I

Figure 11.8.e.I is a schematic illustration of a bandgap containing within it a density of localized states having the form we saw to be necessary in the last subsection. The Figure has been drawn assuming the Fermi energy to be in the middle of the bandgap. Let us also assume that near the point "a", the density-of-states function relevant to the multi-phonon-activated hopping of electrons can be described approximately by

$$g\left(\frac{\Delta E}{kT}\right) = B \exp\left[-\frac{\alpha}{2} \frac{(\Delta E - \Delta E_F)}{kT} \right] \qquad (11.8.e.1)$$

cf. (11.8.a.2)

and near the point "b" by

$$g(\frac{\Delta E}{kT}) = B \exp \cdot \left[\frac{\alpha}{2} \frac{(\Delta E - \Delta E_F)}{kT} \right] \qquad (11.8.e.2)$$

where B is some constant. This ensures that we are still dealing with Lewis-type bandtails.

Considering now the hopping possibility factor f(z)[1-f(z)] which was first mentioned in subsection 11.8.a, we assume again that near the point "c" it can be approximated by a pure exponential.

$$f(z)\ [1-f(z)] \simeq \exp\ [- \frac{(E - E_F)}{kT}\ ] \qquad (11.8.e.3)$$

and similarly near point "d" by the expression

$$f(z)\ [1-f(z)] \simeq \exp\ [\frac{(E - E_F)}{kT}\ ] \qquad (11.8.e.4)$$

Then near the conduction band the distribution of hopping activation energies

$$P(\Delta E) = g^2(\Delta E)\ f(z)\ [1-f(z)] \qquad (11.8.e.5)$$

will take the form

$$P(\Delta E) = Bl \exp\ [(1-\alpha) \frac{(\Delta E - \Delta E_F)}{kT}] \qquad (11.8.e.6)$$

where Bl is some new constant, and near the valence band P(Δ E) will take the form

$$P(\Delta E) = Bl \exp\ [(\alpha-1) \frac{(\Delta E - \Delta E_F)}{kT}] \qquad (11.8.e.7)$$

Consequently using

$$s = (\Delta E - \Delta E_F) / kT = \ln(\tau/\tau_F) \qquad (11.8.e.8)$$

P(ΔE) can be approximated over the whole bandgap by

$$P(\Delta E) = B2 \cdot \frac{2 \cosh(\alpha s)}{[1 + \exp(s)]\,[1 + \exp(-s)]},\quad s_{min} \leq s \leq s_{max} \qquad (11.8.e.9)$$

and by simplifying this and noting that

$$F(s) = \frac{1}{kT} P(\Delta E) \qquad (11.8.e.10)$$

we find that we have a DRT

$$F(s) = B3 \quad \frac{\cosh(\alpha s)}{1 + \cosh(s)} \quad s_{min} \leq s \leq s_{max} \qquad (11.8.e.11)$$

with

$$s_{min} = \frac{-\Delta E_F}{kT} \qquad (11.8.e.12)$$

$$s_{max} = \frac{\Delta E_g - \Delta E_F}{kT} \qquad (11.8.e.13)$$

and

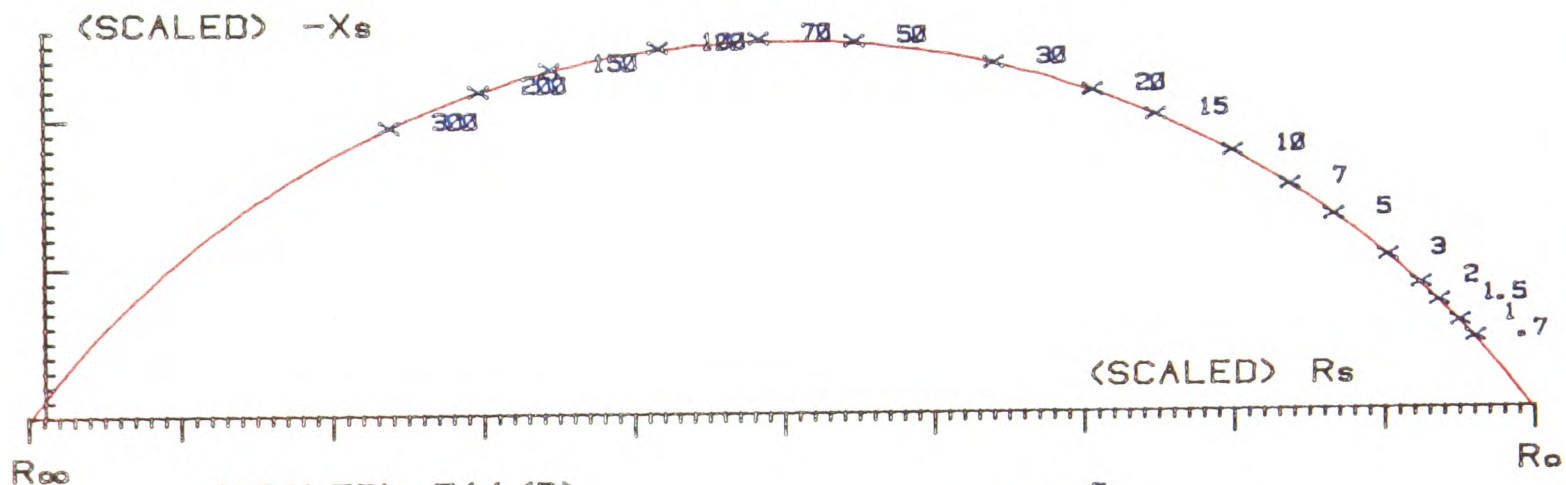
$$\frac{1}{B3} = \int_{s_{min}}^{s_{max}} \frac{\cosh(\alpha s)}{1 + \cosh(s)}\, ds \qquad (11.8.e.14)$$

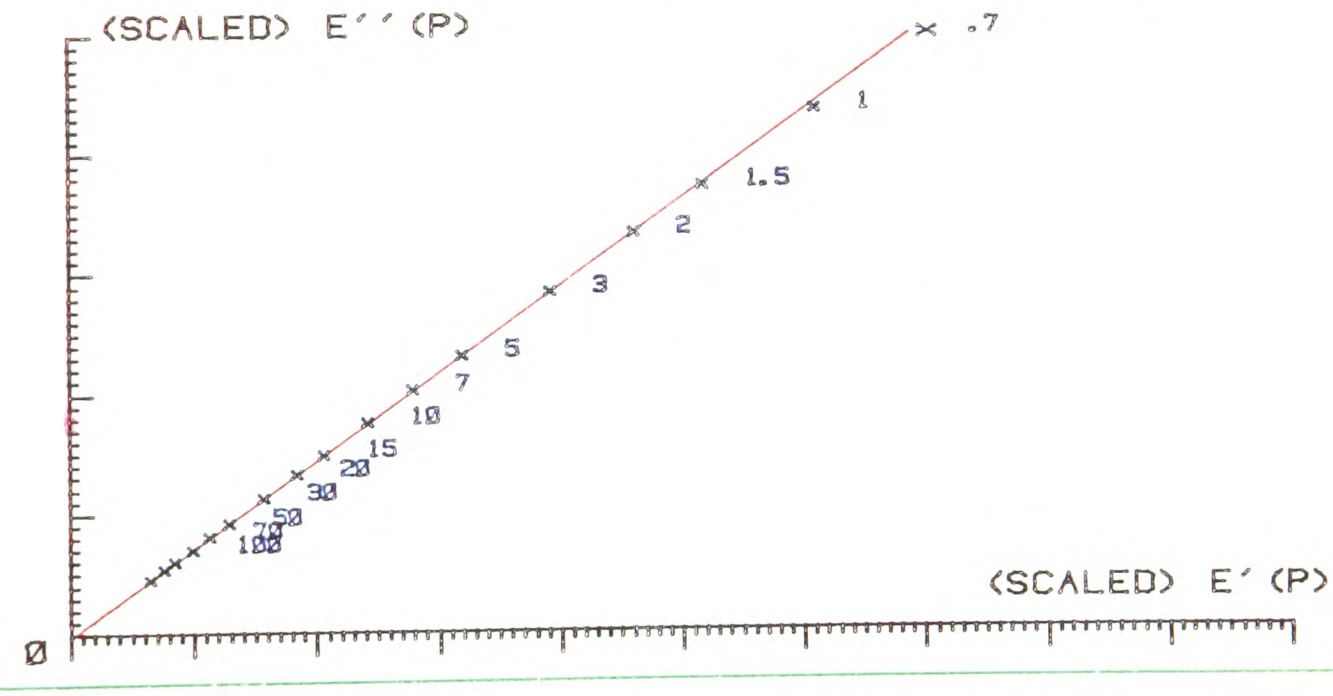
We may now combine this double bandtail model with the CTRW formalism by using equations (11.8.e.11) to (11.8.e.14) in equations (11.7.c.17) to (11.7.c.23), and then repeating the procedure used before in equations (11.8.d.) to (11.8.d.). The shunted CTRW-double bandtail model we then obtain in fact produces results which may be excellently fitted by a Cole equation, even despite the truncation of the DRT imposed by a finite ΔE_g. The model is very much better at fitting the form of clinical data than any we have yet reviewed, and Fig. 11.8.e.II may serve to illustrate what must be admitted to be a very good fit to an arc of a circle on the complex impedance plane. The Figure was produced by a graph plotter to show the results of a computer simulation of the shunted CTRW double bandtail model. (The fact that in the list of parameters the DRT (11.8.e.11)

BEHAVIOUR OF THE SHUNTED LOCALIZED-STATES MODEL WHEN

F(S)	=	SALTER
(1 - ALPHA)	=	.37
DELTA E(G)	=	1.5
DELTA E(F)	=	.75
TEMPERATURE	=	300
C(ZERO)	=	.00001
C1	=	5.00000E-09

Fig. 11.8.e.II





		+PSE	+/-SE	-PSE
NO. OF DATA PAIRS	= 17			
R(ZERO)	= 99886.8		206.982	
R(INFINITY)	= -1110.42		206.982	
F(PEAK) [USING M1]	= 64.0005	4.1924		3.93467
F(PEAK) [USING M2]	= 64.0069	.343933		.342102
E'' [E'=Ø]	= -4.55013E-10		2.99160E-10	
'U'	= 2.07016E-07	3.59337E-09		3.53206E-09
M1 FROM Z LOCUS	= .398565		1.92009E-03	
M2 FROM V/U PLOT	= .396417		7.65593E-04	
M3 FROM E* LOCUS	= .40132		5.04793E-03	
M4 FROM LN E'' PLOT	= .399282		2.62213E-03	
& WEIGHTED MEAN M	= .396968		6.49018E-04	

SINCE COMPARING M1 WITH M2, M3 AND M4 RESPECTIVELY,
THE SIGNIFICANCE OF THE DIFFERENCE BETWEEN THE MEANS IS
Ø.1Ø < P Ø.1Ø < P AND Ø.1Ø < P

COEFF. DET. OF (UNWEIGHTED) Z ARC FIT = .999988
COEFF. DET. OF (WEIGHTED) V/U PLOT = .999976
COEFF. DET. OF (WEIGHTED) E* LINE FIT = 1

has rather immodestly been labelled with my own name is due to the fact that the computer simulation was run with a number of different DRTs (as will be described in Section 11.9), and it was a convenient way of labelling equation (11.8.e.11), since so far as I know this particular DRT has not been used by anyone else but myself.) The other parameters will not be discussed at the moment.

The excellence of the fit of the model can perhaps be better understood as follows. Within its limits of truncation, the distribution (11.8.e.11) produces a very similar dF(s)/ds to that given by the Cole-Cole distribution (Cole and Cole, 1941)

$$F(s) = \frac{1}{2\pi} \frac{\sin(\alpha\pi)}{\cosh[(1-\alpha)s] - \cos(\alpha\pi)} \qquad (11.8.e.15)$$

and the Cole-Cole distribution may therefore serve as a close approximation to (11.8.e.11) for reasonable values of ΔE_g. Now, substituting (11.8.e.15) into (11.7.c.2) produces

$$\psi(j\omega) = \frac{1}{1 + (j\omega\tau_F)^{1-\alpha}} \qquad (11.8.e.16)$$

where τ_F is a time constant associated with changes hopping from the Fermi level, and using (11.8.e.16) in (11.7.b.3) and (11.7.b.4) then gives

$$\sigma^*_{CTRW}(j\omega) = B4 \cdot (j\omega\tau_F)^{\alpha} \qquad (11.8.e.17)$$

where

$$B4 = \frac{nq^2}{kT} \cdot \frac{1}{6} d^2_{rms} \cdot \frac{1}{\tau_F} \qquad (11.8.e.18)$$

and (11.8.e.17) is valid over an unlimited frequency range. This means that if we add in as usual an arbitrary, purely real shunt conductance σ_{shunts} to represent the effect of the skin appendages, thus obtaining a complex conductivity

$$\sigma^*(j\omega) = \sigma_{shunts} + B4\ (j\omega\tau_F)^{\alpha} \qquad (11.8.e.19)$$

then the corresponding complex impedance will have EXACTLY the form of the Cole equation over an unlimited frequency range. In fact using a skin-dimensions correction factor D, the model predicts

$$Z = \frac{R_o}{1 + (j\omega\tau_p)^{1-m}} \qquad (11.8.e.20)$$

with

$$R_o = 1/D.\ \sigma_{shunts} \qquad (11.8.e.21)$$

$$\tau_p = \tau_F\ .\ (D.\ R_o\ .\ B4)^{\frac{1}{\alpha}} \qquad (11.8.e.22)$$

and

$$m = 1-\alpha \qquad (11.8.e.23)$$

Now of course the distribution (11.8.e.11) will not produce exactly the perfect fit to the form of the clinical data which we have just seen is given by the Cole-Cole distribution, but it certainly does produce at least an excellent fit. Therefore we will now consider some advantages and disadvantages of this particular model of the linear electrical properties of human skin.

11.8.f Advantages and disadvantages of the shunted CTRW-double-bandtail model

The first advantage of this model is that it produces results extremely close to those predicted by the Cole equation, which we know to be exactly what we want (Section 9.5), on the basis of a plausible theory derived from the known properties of those materials, proteins, which largely compose the cell membranes and cell interiors of the stratum corneum. Pethig for example (1979, p.301) has pointed out that proteins tend to have real components of complex conductivity corresponding to the form (11.8.e.19), and since we know that the proteins of the corneum are semiconductive, and that some of them are amorphous, the applicability of the present theory seems to be well-founded.

We noted in subsection 9.3.c that applying physiological saline to the skin not only reduces R_o as would be expected, but also increases m, the reverse of what would be expected from the hydration gradient models reviewed in Section 11.5, and, so far as I can tell, from all other previously available theories. The effect can however be interpreted on the basis of the present model. Rather generally, in fact, the alpha power dependence of conductivity decreases, and $m = (1-\alpha)$ increases, as the hydration of proteins increases, and the present theory would interpret this as resulting from a "filling-out" of the neo-exponential bandtails towards a flatter density-of-states across the bandgap.

The model can also readily interpret the obedience of each cell layer in the corneum to a Cole equation with a non-zero value of m which changes little or not at all with depth. This is an experimental finding resulting from tape-stripping the skin, as we saw in subsection 9.3.d, and the interpretation is simply that the proteins of one cell layer in the corneum are

much the same as those of other cell layers in the corneum, which seems to be a reasonable hypothesis.

The theory implies that the value of m depends upon the disorder, the ionization of the side groups, and the molecular environment of the proteins of the cell membranes and cell interiors of the stratum corneum. It therefore predicts that m can be expected to change with local pH and with cell protein composition. This agrees with what was noted in subsection 10.3.a, that m is usually considerably increased in psoriatic plaques, since it is well known that the proteins of the corneocyte membrane and interior are altered in this case (see e.g. Skerrow, 1978).

Now to disadvantages. Firstly, although in subsection 9.2.c we saw that altering R_o through changing the degree of appendageal shunting had no effect upon the value of m, we know from hydration studies (subsection 9.3.c) that in general when appendageal changes are not dominating the results, then changes in R_o do tend to be associated with changes in m. In the model however they are completely independent; the particular form of the distribution (11.8.e.11) is such that it produces a vanishingly small D.C. conductivity (11.6.b.5), (unlike for example the Davidson-Cole distribution, cf. (11.6.c.16)), and thus R_o reflects only the state of the assumed appendageal shunting. This however does not agree with common sense, and implies that the form of the DRT should be altered somewhat.

Secondly, but again pertaining to the DRT, the model is partially ad hoc in that it is based upon an apparently rather arbitrary form of DRT. This was based in turn upon the idea of using two Lewis-type neo-exponential bandtails. Actually this neo-exponential form of density-of-localized-states dates back at least as far as Rose (1955), who introduced it in order to interpret certain phenomenological aspects of space-change limited conduction in solids, and its presence in the literature of solid-state

physics has been perpetuated by an assumed association with the mechanism underlying Urbach's rule for optical absorption edges (see e.g. Mott and Davis, 1971, p.240 ff). However, this association is now questioned (e.g. Mott and Davis, 1971, p.243), indeed, even by those who once strongly supported the idea (see e.g. Tauc, 1970, p.298), and there consequently now seems to be much less evidence supporting the existence of the neo-exponential form of bandtail than there once was. Since the success of the present model is critically dependent upon this form of density-of-localized-states, such a lack of evidence for it is a serious disadvantage.

Finally, the model is also totally dependent upon conduction taking place by means of electrons or holes, since band theory does not apply to ions. Since conduction in skin is likely to be at least partially and possibly predominantly ionic (see subsection 11.4.e), this too is a disadvantage.

Fortunately, the final model we shall consider in this review avoids all these disadvantages, and yet still has the same (or equivalent) advantages. Indeed, we shall see that it has some more as well.

11.9 A model of the Cole equation assuming conduction by ions, electrons or holes

11.9.a Allowing for the possibility of ionic conduction

We have seen in subsections 11.4.c., d and e that the presently available evidence favours the concept that electric charge may be transported through the corneum by ions as well as by electrons or holes. However, the problem has been that although it is fairly easy to suggest mechanisms whereby a conductivity having the form

$$\sigma^* = \sigma_1 + \sigma_2 (j\omega\tau)^{\alpha} \qquad (11.9.a.1)$$

may arise due to conduction involving electrons or holes, it is very difficult to suggest ways in which ionic mechanisms could produce the same, at least over a sufficient number of decades of frequency. The greatest progress has been made by those theorists modelling conduction in vitreous systems, but the models either produce values of the quantity α which are too close to unity, or α is not found to be sufficiently independent of frequency to fit the observations. Such restrictions even apply to the very elaborate theory produced by Macdonald (1974), which for example is only capable of generating complex impedance arcs with m less than about 0.14, as Macdonald himself has admitted (1976).

However, in this Section a model will be developed which, although founded upon the work of those who were interested in materials in which conduction is electronic, is applicable also if conduction is ionic, because it is not dependent upon the assumption of quantum-mechanical tunnelling, nor of the existence of delocalized conduction and valence bands, certain forms of bandtail, or any such thing. It is consequently all the more powerful and general, and I expect that it may be found to be useful to

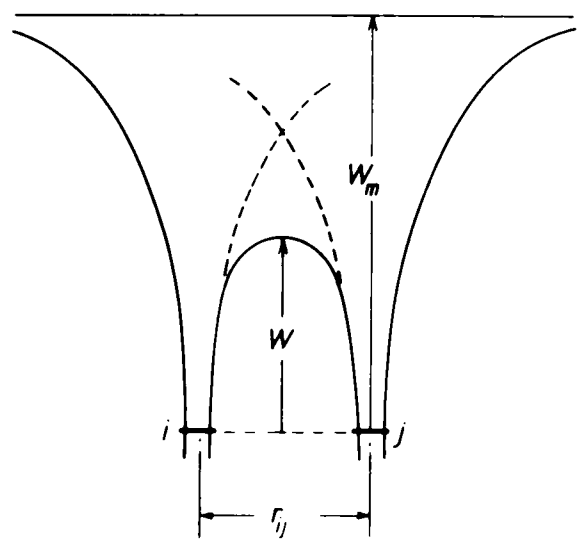
interpret the behaviour of many materials besides that of human stratum corneum, for example, that of solid ionic conductors (subsection 11.3.d), and also of amorphous semiconductors (subsection 11.3.e) when α is not approximately 0.8.

To construct this new model, we must firstly consider some work of Pike (1972).

11.9.b Some work of Pike

One of Debye's classical models of dielectric relaxation involved isolated pairs of potential wells (see e.g. Kauzmann, 1942; Daniel, 1967, p.20 ff). Within each pair of potential wells, there was assumed to be a single charge carrier, which by absorbing the energy of many phonons could hop over the top of the potential barrier separating the two potential wells and thereby reverse the electric dipole moment of the system. The relaxation time for this process depends of course upon the height of the potential barrier.

In 1972 Pike, presumably following earlier workers (see e.g. Mott and Davis, 1971, p.111), suggested that a distribution of the distances between each potential well of the pair would produce an associated distribution in the height of the potential barrier separating these wells, and thus a distribution of relaxation times in an assembly of such pairs.



The potential energy diagram for the pair element adopted by Pike and involving overlapping Coulombic potential functions

Fig. 11.9.b.I

Consider two identical sites, a distance r apart, which are capable of temporarily trapping a charge carrier. Also let each site have associated with it a potential well of the Coulomb form such as would be expected around for example an ionized impurity, or outside a structural vacancy. Then the potential wells of the two sites will interact and form a saddle-point between them, such that the activation energy W required for a charge carrier to move from one well over this saddle point and into the other well, will depend upon the separation between the sites, r, according to

$$W = W_m - \frac{4q^2}{\varepsilon r} \qquad (11.9.b.1)$$

(in this Section CGS units are used in order to facilitate reference to the work of Pike.) Here q is the charge on the charge carrier measured in e.s.u., ε is the effective local permittivity, and W_m is the activation energy required to ionize a site if it were isolated (see Fig. 11.9.b.I).

Equation (11.9.b.1) produces

$$W_m - W = \frac{4q^2}{\varepsilon r} \qquad (11.9.b.2)$$

and

$$r = \frac{4q^2}{\varepsilon (W_m - W)} \qquad (11.9.b.3)$$

so

$$\frac{dr}{dW} = \frac{4q^2}{\varepsilon (W_m - W)^2} = \frac{r}{(W_m - W)} \qquad (11.9.b.4)$$

We now assume for simplicity that the spatial distribution of sites throughout the material can be considered to be random, and that charge carrier movement will only take place between sites which are nearest neighbours.

Then if n is the number of sites per unit volume, the probability that any one site has its nearest neighbour at a distance betwen r and (r + dr) is (see e.g. Chandrasekhar, 1943, p.86)

$$P(r)dr = 4\pi n\, r^2 \exp\left(-\frac{4}{3}\pi n\, r^3\right) dr \qquad (11.9.b.5)$$

so using (11.9.b.4) we have the distribution of activation energies in the material

$$G(W)dW = \frac{dr}{dW} \cdot P(r) \cdot dW$$

$$= \frac{r}{(W_m - W)} \cdot 4\pi n\, r^2 \exp\left(-\frac{4}{3}\pi n\, r^3\right) dW \qquad (11.9.b.6)$$

or

$$G(W)dW = 4\pi n (W_m - W)^3 r^3 \frac{1}{(W_m - W)^4} \exp\left(-\frac{4}{3}\pi n\, r^3\right) dW \qquad (11.9.b.7)$$

which upon substituting (11.9.b.3) becomes

$$G(W)dW = 4\pi n \left(\frac{4q^2}{\varepsilon}\right)^3 \frac{1}{(W_m - W)^4} \exp\left[-\frac{4}{3}\pi n \left(\frac{4q^2}{\varepsilon}\right)^3 \frac{1}{(W_m - W)^3}\right] dW \qquad (11.9.b.8)$$

or

$$G(W)dW = C \frac{1}{(W_m - W)^4} \exp\left[-\frac{1}{3} C \frac{1}{(W_m - W)^3}\right] dW \qquad (11.9.b.9)$$

using

$$C = 4\pi n \left(\frac{4q^2}{\varepsilon}\right)^3 \qquad (11.9.b.10)$$

Now assuming that the time constant τ associated with jumping from each site to its nearest neighbour is of the form

$$\tau = \frac{1}{\nu_o} \exp\left(\frac{E}{kT}\right) = \frac{1}{\nu_o} \exp\left(\frac{-T\Delta S}{kT}\right) \exp\left(\frac{W}{kT}\right) = \tau_1 \exp\left(\frac{W}{kT}\right) \qquad (11.9.b.11)$$

where ν_o is some jump-attempt frequency, E is the free energy of activation, ΔS is the entropy of activation, W is the energy (enthalpy) of activation, k is Boltzmann's constant and T is the absolute temperature, we can define

$$s = \ln(\tau/\tau_m) = (W-W_m)/kT \text{ for } 0 \leq W \leq W_m \qquad (11.9.b.12)$$

Then

$$kTs = W-W_m \qquad (11.9.b.13)$$

$$W_m-W = -kTs \qquad (11.9.b.14)$$

and

$$\frac{1}{(W_m-W)^n} = \frac{1}{(-kTs)^n} = (-kTs)^{-n} \qquad (11.9.b.15)$$

so (11.9.b.9) becomes

$$G(W)dW = C(-kTs)^{-4} \exp\left[-\frac{C}{3}(-kTs)^{-3}\right] dW = F(s)ds \qquad (11.9.b.16)$$

or, using $\frac{ds}{dW} = \frac{1}{kT}$,

$$F(s) = \frac{kTC}{A}(-kTs)^{-4} \exp\left[-\frac{C}{3}(-kTs)^{-3}\right] \qquad (11.9.b.17)$$

the constant A being introduced for purposes of normalization, i.e. so that

$$\int_{-\infty}^{\infty} F(s)ds = 1 \qquad (11.9.b.18).$$

Thus A is given by

$$A = \int_{-\infty}^{\infty} kTC(-kTs)^{-4} \exp\left[-\frac{C}{3}(-kTs)^{-3}\right] ds \qquad (11.9.b.19)$$

The form of the Pike F(s) is shown below in Fig. 11.9.b.II.

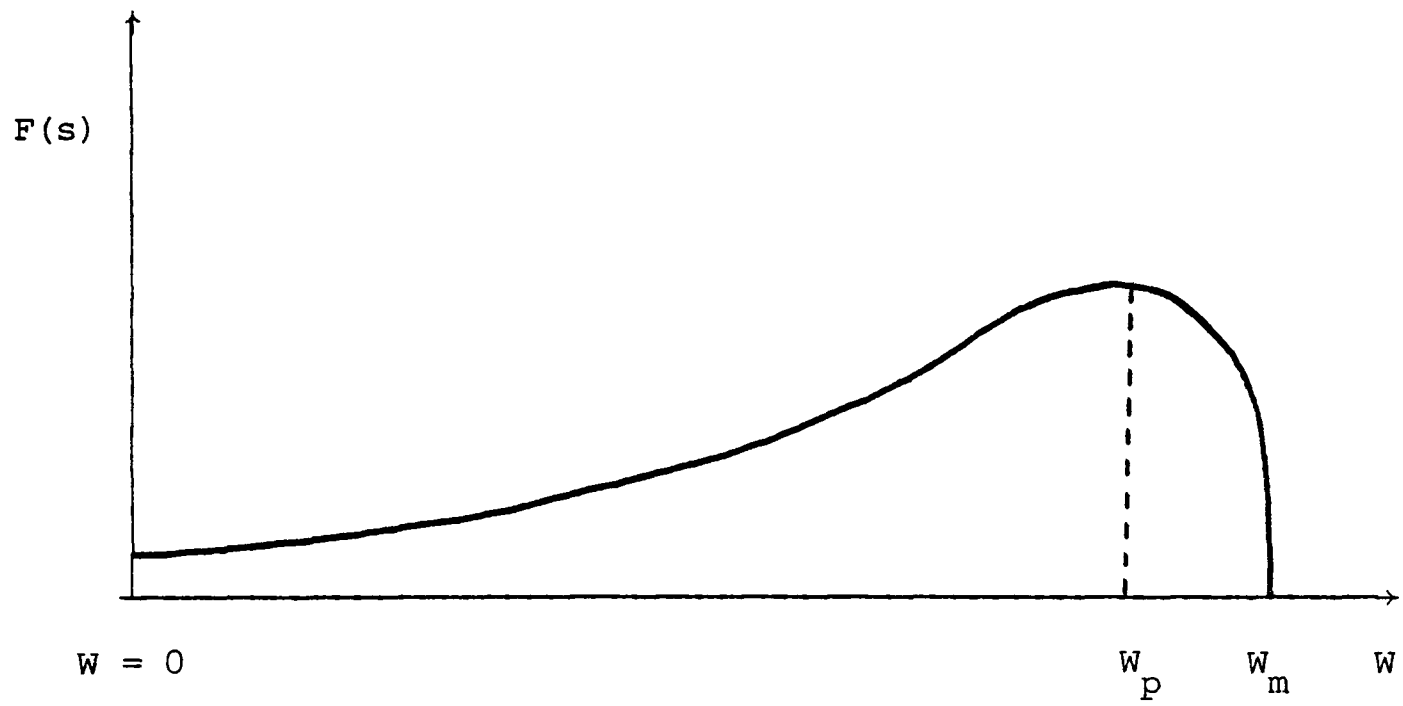


Fig. 11.9.b.II

The peak value of F(s) is at

$$W = W_p = W_m - \left(\frac{C}{4}\right)^{\frac{1}{3}} \qquad (11.9.b.20)$$

and as we shall see later (in subsection 11.9.f) this means that $W_p \simeq W_m$ for physically reasonable values of C. Thus in the tail region $0 \leq W << W_p$, the function is approximately given by

$$F(s) \simeq \frac{kTC}{A} \frac{1}{(W_m - W)^4}, \qquad 0 \leq W << W_m \qquad (11.9.b.21)$$

and Pike (1972) stated that this can be further approximated as

$$F(s) \simeq \frac{kTC}{A} \frac{1}{W_m^4} \exp(4W/W_m), \quad \frac{W}{W_m} < 0.5 \qquad (11.9.b.22)$$

an approximation which will be improved in a moment. Proceeding temporarily on the basis of Pike's approximation we may however compare with (11.9.b.22) the Davidson-Cole F(s)

$$F(s)_{D-C} = \frac{\sin(1-\alpha)\pi}{\pi} \exp[(1-\alpha)s] [1 - \exp(s)]^{\alpha-1} \qquad (11.9.b.23)$$

which in its tail region reduces to

$$F(s)_{D-C} \simeq \frac{\sin(1-\alpha)\pi}{\pi} \exp[\frac{(\alpha-1)W_m}{kT}] \exp[(1-\alpha)\frac{W}{kT}] \qquad (11.9.b.24)$$

and thus at frequencies sufficiently high for the response to be dominated by the tail, we may expect from the Pike F(s) similar behaviour to that produced by the Davidson-Cole, with

$$\frac{(1-\alpha)}{kT} = \frac{4}{W_m} \qquad (11.9.b.25)$$

i.e.

$$m = (1-\alpha) = \frac{4kT}{W_m} \qquad (11.9.b.26)$$

This is interesting because if we can use a physically plausible model which produces something close to a Davidson-Cole DRT, combining this with the CTRW formalism will then simulate the conductance behaviour of the skin (see Example 2 in subsection 11.7.c).

Let us therefore examine the expression (11.9.b.22) introduced by Pike. Both Pike (1972) and Elliott (1977), whose work will be considered again briefly in the next subsection, made use of the approximation

$$\frac{1}{(W_m - W)^i} \simeq \frac{1}{(W_m)^i} \exp\,(iW/W_m), \qquad i = \text{small integer} \qquad (11.9.b.27)$$

in deriving their parameter

$$\beta = \frac{i\ kT}{W_m} \qquad (11.9.b.28)$$

which is proportional to my parameter "m". Pike felt that the approximation was "quite good for our purposes" so long as $(W/W_m) < 0.5$. However, this may be questioned, given that the accuracy of the approximation is important because it has a large effect upon the accuracy of the expression deduced for β (and also m).

We can examine the accuracy of the Pike approximation by writing

$$\frac{1}{(W_m - W)^i} = \frac{1}{(W_m)^i} \exp\left[i.\ \frac{W}{W_m}.\ p\ \right] \qquad (11.9.b.29)$$

the difference between this equation and the Pike approximation (11.9.b.27) being the "correction factor" p. Solving for p,

$$p = -\frac{\ln(1-x)}{x}, \qquad x = W/W_m \qquad (11.9.b.30)$$

giving

$$p = 1 + \frac{x}{2} + \frac{x^2}{3} + \frac{x^3}{4} + \ldots \qquad (11.9.b.31)$$

Now although p is indeed a fairly slowly varying function of x, it can be seen from the graph (Fig. 11.9.b.III) that the Pike approximation, corresponding to putting p = 1, is a poor one across most of the range of x. In fact the "average" value of p will certainly be greater than unity, even at frequencies sufficiently high to ensure that the response is dominated by the tail region. Consequently, in practice β will exceed the value

calculated from (11.9.b.28) and m the value calculated from (11.9.b.26). Pike did not allow for this.

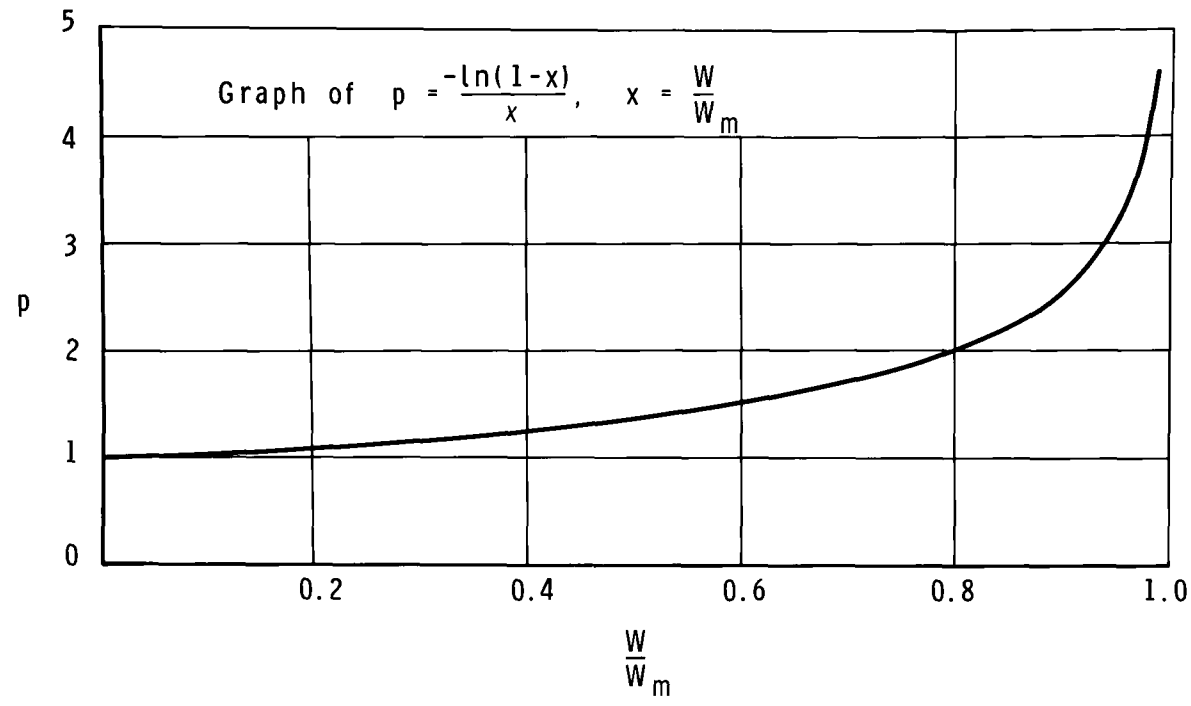


Fig. 11.9.b.III

It is however possible to improve the Pike approximation considerably. To accomplish this, we combine equations (11.9.b.29) to (11.9.b.31) into

$$\frac{1}{(W_m - W)^i} = \frac{1}{(W_m)^i} \exp\left[ix + \frac{i}{2}x^2 + \frac{i}{3}x^3 + \ldots \right] \qquad (11.9.b.32)$$

and using

$$\beta = \frac{kT\, d\,[\ln F(s)]}{dW} \qquad (11.9.b.33)$$

as may be derived from Lewis (1977), equations (43) to (44), or deduced by inspection of equations (11.9.b.21) to (11.9.b.28), we have

$$\beta = \frac{kTi}{W_m}\left[1 + x + x^2 + \ldots\right] \qquad (11.9.b.34)$$

Now Elliott (1977) included up to the second term of this series as a means of improving the Pike approximation, but ideally we should of course use more. It may therefore be useful to note that in the limited range $|x| < 1$, equation (11.9.b.34) has a finite sum, making it possible to replace the expressions derived using the Pike approximation by

$$\beta = \frac{kT.i}{W_m(1-x)} \qquad (11.9.b.35)$$

and $$m = \frac{4kT}{W_m(1-x)} \qquad (11.9.b.36)$$

However, in general we will here employ

$$m = \frac{4kT}{W_m}\ [1 + x + x^2 + \ldots\ ] \qquad (11.9.b.37)$$

and what must now be done is to relate $x = W/W_m$ to frequency, since there can be expected to be a relationship of some sort between the applied field frequency ω and the trap depth W of those charge carriers which respond. Moreover, experimental observations are better fitted if the expressions for β and m are slightly dependent upon frequency, and this would presumably have to occur through a frequency dependence of x.

Consequently Elliott (1977) made the assumption

$$\omega = 1/\tau \qquad (11.9.b.38)$$

and rearranged (11.9.b.11) to produce

$$x = \frac{W}{W_m} = \frac{kT}{W_m} \ln\left(\frac{1}{\omega\tau_1}\right) \qquad (11.9.b.39)$$

which is acceptable as a first approximation, although the assumption (11.9.b.38) is probably too simple given that a field oscillating at a single frequency ω will produce a response by carriers having a range of time constants, not just the single value $\tau = 1/\omega$.

11.9.c Some work of Elliott

In 1977 Elliott adapted Pike's theory to apply to electronic conduction in chalcogenide glasses, having found available theories to be inadequate. (Long and Balkan, 1980, have for the same reason recently adapted Pike's theory to apply to conduction in amorphous germanium.)

As we have seen, Elliott began the process of improving the Pike approximation, a process which was continued in the last subsection. However, he made two serious approximations of his own which were neither declared at the time, nor, so far as I know, corrected in any subsequent papers. They should therefore be brought to the attention of people consulting his work. The first approximation was to drop or forget the exponential part of (11.9.b.5), thus in effect producing an incorrect Pike F(s), the error being more significant the lower the field frequency. The second approximation was to use an infinite rather than a finite range of integration in his equation (10) and the one before it, which has the effect of producing power-law conductivity over a wider frequency range than is actually justifiable. *This latter approximation is very serious.*

11.9.d A shunted CTRW-Pike model : the model and the program

The model to be described here is based upon combining the CTRW formalism outlined in Section 11.7 with the Pike DRT discussed in subsection 11.9.b. However, three preliminary things should be considered.

Firstly, Pike used the DRT he derived to model the dielectric relaxation and the consequent complex conductivity of a system of potential wells associated with charge carrier trapping sites. To keep his algebra acceptably simple however he was forced to assume that charge carriers only moved between nearest-neighbour wells, and so found that he was modelling dielectric relaxation in a system of wells with zero D.C. conductivity. The complex conductivity he derived for the system was therefore that of a particular type of non-Debye dielectric.

In the present model however I have made the physically more reasonable assumption that jumps are not invariably between nearest neighbours, but that there is a finite through relatively very small chance of jumps taking place between wells which are second-, third- etc. nearest neighbours. It is very desirable to include this option in the theory because if jumps may at least sometimes occur into wells other than the nearest neighbour, a charge carrier may in the course of time percolate entirely through the material, i.e. the D.C. conductivity of the system will be non-zero. Moreover, as we have seen, the CTRW formalism can be used to derive both this D.C. conductivity and the (complex) conductivity at non-zero frequencies, provided that the DRT is known. In the present case, rather than attempting to derive the relevant DRT exactly, I have made use of the fact that so long as non-nearest-neighbour jumps are very much less likely than nearest-neighbour jumps, the effective DRT will not be significantly different from the Pike DRT. These then are the assumptions which underlie our combining the Pike DRT with the CTRW formalism to model what is basically a semiconductor, not a dielectric.

The second preliminary consideration is simpler. When applying the CTRW-Pike model to the case of skin, which as we have seen already (e.g. subsection 11.4.a) effectively means the stratum corneum, it should be remembered that the physical structure of this particular system is such that there are conductances in parallel with it; anatomically we could say that the skin appendages pierce through the corneum, and physiologically we could say that they provide shunts (i.e. alternative pathways) to diffusion through it. Consequently for the case of skin, we should employ a SHUNTED CTRW-Pike model, by adding to whatever complex conductance is predicted an arbitrary real conductance to simulate the electrical contribution of the skin appendages.

Thirdly, note that we must also somehow try to approximate the effect of a co-existent distribution of the prefactor τ_1 in (11.9.b.11), since it is unreasonable to expect ΔS to have only a single value within the material. However, no details of such a distribution are known, and so the following procedure was adopted as an admittedly improvable first approximation. Let us assume a normal distribution for the values of the activation entropy ΔS. Since we have already assumed a Pike distribution (11.9.b.8) for the values of the activation enthalpy W, the distribution of E in (11.9.b.11) will then be of a Pike form somewhat smeared-out by the action of the distribution of ΔS. Over most of the range of W this smearing-out will matter very little because any Pike distribution is fairly "flat" over this range when $W_p \simeq W_m$. However, for large values of W such that $W \simeq W_m$, corresponding to frequencies near $1/(\tau_1 \exp (W_m/kT))$, the smearing out will be noticeable, but nevertheless will not substantially affect the results predicted by the model because the shunting of the model means that its low-frequency behaviour has very little effect upon the form of the complex impedance locus. Thus for our present purposes the smearing-out

at large values of W (corresponding to low frequencies) can be and will be neglected. At the other end of the distribution of E, in the region of the cutoff of the distribution of W at W = 0 (see Fig. 11.9.b.II), the E distribution will have a Gaussian tail extending towards smaller values of E, and the corresponding DRT will be well approximated by a log-normal (Wagner-Yager) distribution. This is sufficiently similar to a Cole-Cole distribution to ensure that at frequencies high enough for $\omega > 1/\tau_1$, the tail of the E distribution will produce frequency-domain behaviour almost indistinguishable from that of a polarization impedance, with the m value of the polarization impedance deriving smoothly from that obtaining in the cutoff region of the W distribution, since the E distribution will remain continuous in this region and an equation like (11.9.b.33) can be applied to it there.

Now let us proceed to examine the actual program which was used to calculate the behaviour of the shunted Pike-CTRW model. The program is called PIKE, it is written in BASIC, and it may be referred to in Appendix F. However, if one does consult Appendix F, it will be seen that the program has a small number of features which are not discussed in the description below. These were originally included either to help in the development of the program, or to accommodate it to the restrictions of the particular version of the BASIC language usable with the main hospital computer at the time. These features are therefore no longer important, but the program has nevertheless not been tidied up, in case any mistakes present in it during the simulations reported later were thereby hidden. However, before being employed with the Pike DRT, the whole program was thoroughly tested qualitatively using the Davidson-Cole and the Cole-Cole DRTs, since for these DRTs the expected behaviour of the model could be derived algebraically, and the predictions of the program could therefore be checked for correspondence with this algebraic behaviour.

The program operates as follows. Firstly, various model parameters are set: W1 represents W_m, the ionization energy shown in Fig. 11.9.b.I, and it is given a value in electron volts (eV). Next the temperature of the system, T, is assigned a value in degrees Kelvin (K). Then C, the factor in (11.9.b.10) is set and the value of Boltzmann's constant k is stored as K in units of eV/K, and as K1 in units of erg/K. Next S1 = S(min) and S2 = S(max) are calculated following (11.9.b.12), although for the sake of the BASIC used by the computer, S2 is approximated by S1/100 rather than being set equal to zero. Then W6 is assigned the value of h/kT where h is Planck's constant, (e.g. W6 = 1.5997×10^{-13}s at 300k), and W3 is set equal to the assumed mean value of ΔS in entopy units, where 1 entropy unit = 1 calorie/^{o}C/mole, in order to calculate an "attempt time" prefactor T1 = τ_1 for use in (11.9.b.11). This Section is concluded by calculating W2 = W_p from (11.9.b.20).

The program continues by storing a value CO for the additional conductivity assumed to result from the skin appendages, and setting

$$P1 = \frac{nq^2}{k} \cdot \frac{1}{6} d^2_{rms} \qquad (11.9.d.1)$$

and C1 = P1/T for use in (11.7.c.22) and (11.7.c.23). Next, 43 logarithmically-spaced frequencies are set at which the behaviour of the model is to be calculated, and this completes the set of quantities which need to be chosen or calculated before the simulation can be used.

At each of the chosen frequencies the program proceeds to calculate normalized values of ψ' and ψ'' following (11.7.c.19) and (11.7.c.20), but approximating the integrals by series with 400 terms. These values are then used to derive σ' and σ'' according to (11.7.c.22) and (11.7.c.23), making use of the value of C1, and adding in the contribution of CO to σ'. Finally, the equivalent series resistance R_s at each frequency, and the equivalent series reactance X_s at each frequency, are calculated from

$$R_s = \frac{\sigma'/D}{(\sigma')^2 + (\sigma'')^2} \qquad (11.9.d.2)$$

$$\text{and} \quad -X_s = \frac{\sigma''/D}{(\sigma')^2 + (\sigma'')^2} \qquad (11.9.d.3)$$

The division by D, a "skin dimensions correction factor", is required in the conversion from conductivity to impedance, and D = 1000 centimetres on the assumption that conductivity is given in units of $ohm^{-1}cm^{-1}$ and that the associated impedance refers to 1 cm^2 of corneum taken to be 10μm (1×10^{-3}cm) thick. (For example, for a conductivity $\sigma = 1 \times 10^{-8}$ $ohm^{-1}cm^{-1}$, the corresponding resulting ρ would be 1×10^8 ohm cm, and the resistance of the skin site would be

$$R = \rho L/A = (1 \times 10^8 \text{ ohm cm} \times 1 \times 10^{-3}\text{cm})/1 \text{ cm}^2 = 1 \times 10^5 \text{ ohms}) \qquad (11.9.d.4)$$

Lastly, the program stores the results of these various calculations made for the different frequencies in a file which can be acted upon by modified versions of the programs RESULTS and CLINPLOT. These programs produce via a graph-plotter suitable charts showing the behaviour of the model, together with the results of the same statistical procedures as are applied to data obtained directly in vivo. Such charts thereby facilitate the comparison of theory with experiment, and such comparisons will be made in the next subsection.

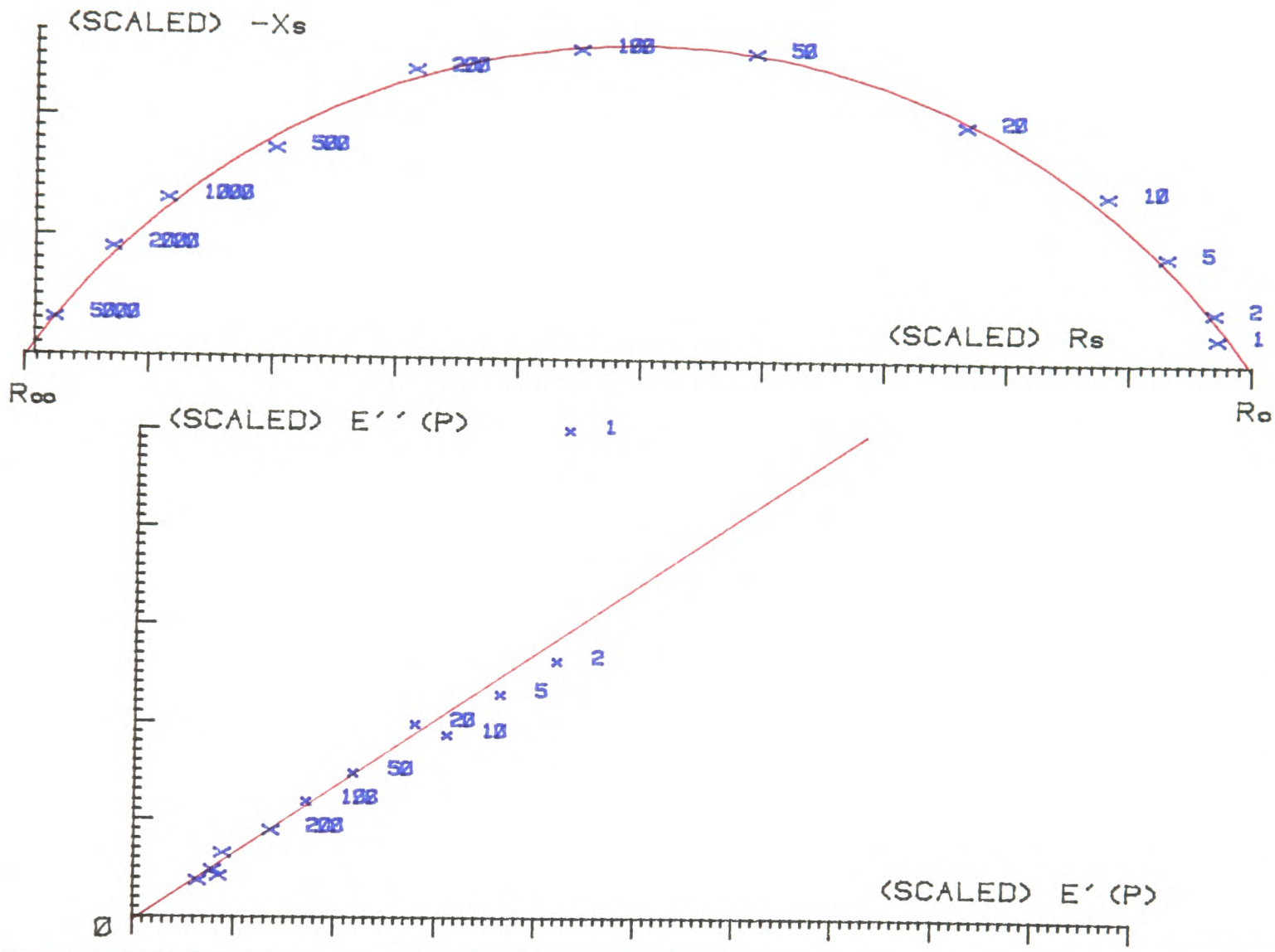
11.9.e A shunted CTRW-Pike model: simulation of clinical data

The first problem in simulating clinical data is to choose a set of clinical data to simulate. For the example to be given in this subsection, I chose the data shown in Fig.11.9.e.I, not because it was particularly accurate, but because it required an unusually large value of m to describe it, and as we have been already, the larger the value of m it is required to simulate, the fewer are the theories which can do so over an acceptably large frequency range. In other words, *this particular set of clinical data is especially difficult to simulate accurately on the complex impedance plane*, and if with even this set of data a measure of success can be obtained, then the theoretical model is that much more promising.

Fig. 11.9.e.II shows the results of a simulation of the clinical data obtained by using the shunted CTRW-Pike model with the parameter values given at the top of the chart. These values will be dicsussed in the next sub-section. For the present it is sufficient to observe how close a fit can be achieved to the clinical data of Fig. 11.9.e.I, both qualitatively and quantitatively. In my opinion at least, the fit is excellent, and no doubt it could be improved still further by minor alterations to the parameter values.

NAME = DAVID SALTER
AGE = 25
DATE = 8TH FEB 1979
TIME = 3.00 P.M.
BODY SITE = LEFT DORSAL FOREARM
SKIN TEMP. = 28 C
AMBIENT R.H. = 63 %
P-P CURRENT = 5 MICROAMPS

Fig. 11.9.e.I



			+PSE	+/-SE	-PSE
NO. OF DATA PAIRS	=	12			
R(ZERO)	=	72092.4		1121.58	
R(INFINITY)	=	-553.55		1121.58	
F(PEAK) [USING M1]	=	78.3823	28.5034		20.9023
F(PEAK) [USING M2]	=	78.5961	3.64027		3.47914
E'' [E'=0]	=	-3.23316E-10		5.70021E-10	
'U'	=	2.30839E--07	1.44502E-08		1.35989E-08
M1 FROM Z LOCUS	=	.380089		1.55443E-02	
M2 FROM V/U PLOT	=	.349183		6.62444E-03	
M3 FROM E* LOCUS	=	.383382		8.45561E-03	
M4 FROM LN E'' PLOT	=	.375912		8.83680E-03	
& WEIGHTED MEAN M	=	.36684		8.88143E-03	

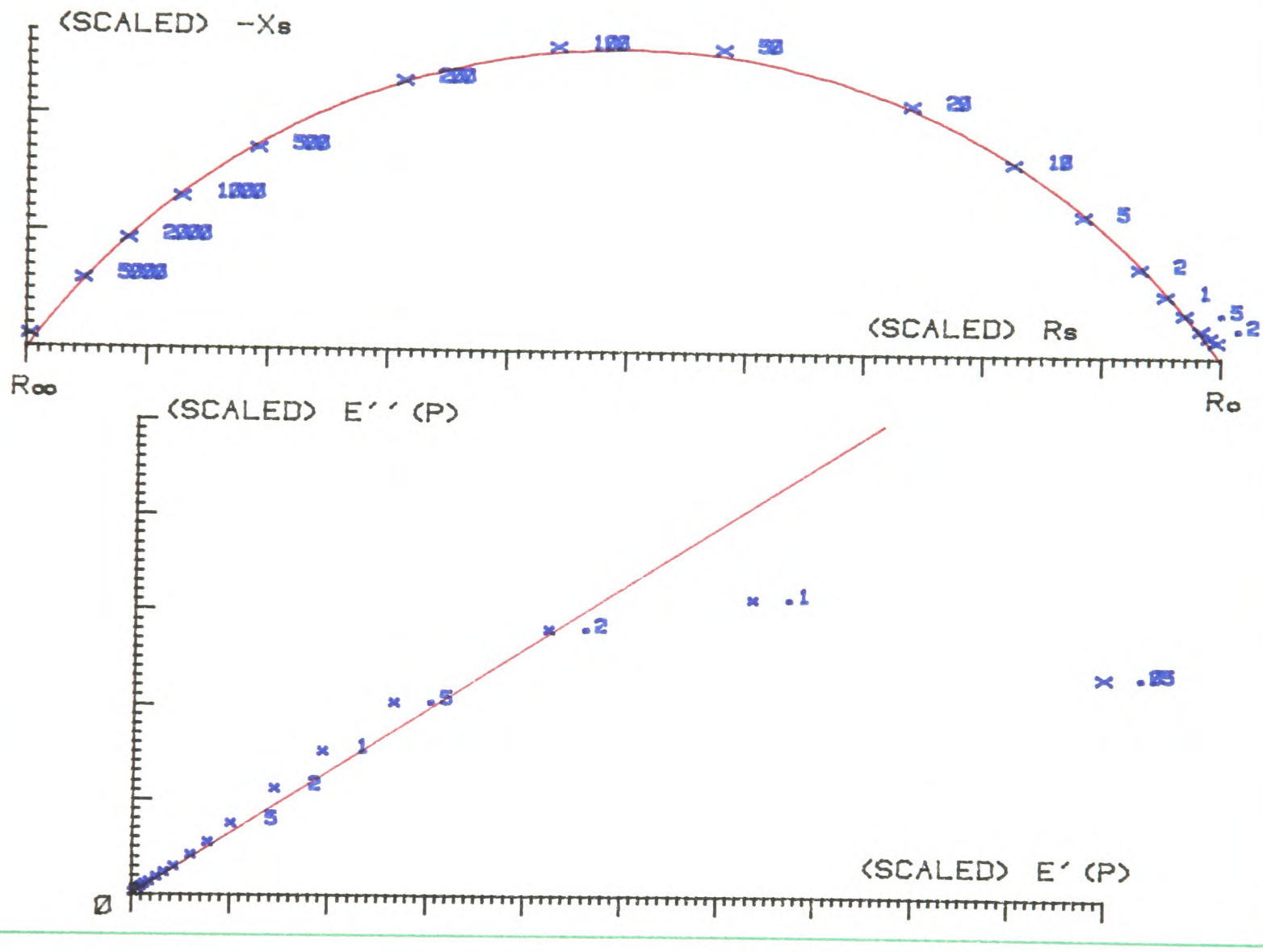
SINCE COMPARING M1 WITH M2, M3 AND M4 RESPECTIVELY,
THE SIGNIFICANCE OF THE DIFFERENCE BETWEEN THE MEANS IS
0.05 < P <= 0.10 0.10 < P AND 0.10 < P

COEFF. DET. OF (UNWEIGHTED) Z ARC FIT = .999609
COEFF. DET. OF (WEIGHTED) V/U PLOT = .998965
COEFF. DET. OF (WEIGHTED) E* LINE FIT = .983156

BEHAVIOUR OF THE SHUNTED C.T.R.W.- PIKE MODEL FOR

ENTROPY UNITS	=	36
W(MAX)	=	.45
W(PEAK)	=	.436429
PREFACTOR C	=	.00001
TEMPERATURE	=	300
C(ZERO)	=	1.20000E-09
P1	=	.0001

Fig. 11.9.e.II



			+PSE	+/-SE	-PSE
NO. OF DATA PAIRS	=	17			
R(ZERO)	=	71683.4		497.279	
R(INFINITY)	=	476.76		497.279	
F(PEAK) [USING M1]	=	74.0944	14.3999		12.0568
F(PEAK) [USING M2]	=	74.1852	.849979		.844348
E'' [E'=0]	=	1.04736E-09		1.27552E-10	
'U'	=	2.31513E-07	7.46865E-10		7.44462E-10
M1 FROM Z LOCUS	=	.387881		6.93333E-03	
M2 FROM V/U PLOT	=	.3722		1.25141E-03	
M3 FROM E* LOCUS	=	.385727		1.79907E-03	
M4 FROM LN E'' PLOT	=	.382951		4.71898E-04	
& WEIGHTED MEAN M	=	.384285		1.91773E-03	

SINCE COMPARING M1 WITH M2, M3 AND M4 RESPECTIVELY,
THE SIGNIFICANCE OF THE DIFFERENCE BETWEEN THE MEANS IS
0.02 < P <= 0.05 0.10 < P AND 0.10 < P

COEFF. DET. OF (UNWEIGHTED) Z ARC FIT	=	.999891
COEFF. DET. OF (WEIGHTED) V/U PLOT	=	.99994
COEFF. DET. OF (WEIGHTED) E* LINE FIT	=	.998628

11.9.f A shunted CTRW-Pike model: discussion of parameter values

A temperature of 300K was assumed for this and most other simulations, corresponding to 27°C which is a reasonable average temperature for the stratum corneum of an unclothed body site in a room which feels neither hot nor cold. Although the present set of clinical data were obtained at a skin temperature of 28°C, this 0.3% difference (on the Absolute scale) was ignored in view of the uncertainty in the other parameter values.

It can also be seen from Fig. 11.9.e.II that the simulation used a value of 1×10^{-5} for the prefactor C. Now from (11.9.b.10) which defines C, one may expect that its numerical value should be very small, indeed smaller than 1×10^{-5}, since although the carrier density n will be large, the cube of q^2/ε will be an extremely small number. However, it was expected from (11.9.b.17), and also shown by computation, that the results of the simulation program are very little affected by the particular value chosen for C once this is less than about 1×10^{-4}. Consequently the present value was decided upon in order to avoid the problems with BASIC which would have arisen if a realistically small value had been used.

The smallness of C means that according to (11.9.b.20) the most likely value of activation enthalpy, W_p, written W(PEAK) in Fig. 11.9.e.II, will be very close to the maximum value W_m, as in fact was assumed already in the illustration of the Pike DRT (Fig. 11.9.b.II). Thus the observed activation energy (enthalpy) for D.C. conduction through the system can be expected to be very similar to both W_m and W_p.

A value of 0.45 eV was chosen for W_m, written W(MAX) in Fig.11.9.e.II. This is considered to be quite feasible in view of two values for the activation energy for D.C. conduction through skin which we have encountered already. In subsection 9.2.c it was noted that Allenby et al. (1969) measured the activation energy of the electrical impedance at 1.5 Hz of

human skin in vitro as 14.6 k cal/mole, corresponding to 0.633 eV, which implies that the activation energy for D.C. conduction through this skin would be approximately the same. Also in subsection 9.2.c, an activation energy of 0.289 eV was derived from the in vivo measurements of D.C. skin resistance by Edelberg and Burch (1962). The average of these two values is 0.461 eV, and so the use of a value of 0.45 eV should meet with no objection.

The quantity P1 defined by (11.9.d.1) was assumed to equal 1×10^{-4}. Now if d_{rms} (see subsection 11.7.b) equals for example $3\mathring{A}$, then if each charge carrier has only a single charge such that $q = e = 4.803 \times 10^{-10}$ e.s.u., the charge carrier density n associated with the assumed value of P1 comes out at $3.9894 \times 10^{14} cm^{-3}$, corresponding to about 400 carriers in a cube of side 1μm. Such a value of n is quite acceptable; indeed materials classed as semiconductors generally have charge carrier densities in the range $10^{13} - 10^{19}$ cm^{-3} (e.g. see Wright, 1979, p.5).

The assumed conductivity contribution of the skin appendages was $CO = 1.2 \times 10^{-8}$ ohm^{-1} cm^{-1}. This order of magnitude was taken to be reasonable (the effect of altering it is examined within the next subsection), and the exact value was chosen simply on the basis of maximizing the numerical correspondence between the simulated data of Fig. 11.9.e.II and the clinical data of Fig. 11.9.e.I.

The objective of maximizing the numerical correspondence between theory and experiment was also paramount in the choice of the value of 36 entropy units for ΔS in (11.9.b.11). Although this is sufficient to reduce the attempt time to $T1 = 1.1871 \times 10^{-5}$ s, it is not at all an unlikely value in a partially hydrated polymeric system such as the stratum corneum. One may for example compare the value of 74 entropy units found by Garton and Parkman (1976) in a system of the same type, and Kauzmann also quotes

similar values (1942, Table I). Broadhurst (1972) found values of about 0.55 eV and 20 entropy units for the activation enthalpy and entropy respectively of methyl stearate which he termed "a model crystalline polymer". More recently, Long and Balkan (1980) applied in fact Pike's theory to interpret their measurements of A.C. loss in amorphous germanium, finding experimentally that attempt frequencies were as low as 10^7 to 10^{11} Hz, and were considerable affected by annealing. This again implies a large ΔS value. Garton and Parkman (1976) inferred that the charge carrier traps involved in their polymeric system must involve many bonds. It would of course be interesting to speculate what processes of bond rearrangement might be requiring a value of around 36 entropy units, corresponding to 10.8 k cal/mole at 300 k. Dawber and Moore (1980, p.26) for example note that covalent bonds usually have bond energies of 50 - 100 k cal/mole and the strength of hydrogen bonds is about 3 - 7 k cal/mole, but the effective values will of course be affected by the local permittivity, a quantity which is hydration-dependent and whose value is still in some doubt for the case of the stratum corneum. Thus it would be unwarranted to speculate further at present.

11.9.g A shunted CTRW-Pike model: the effects of altering the parameters

We will now examine the effects of altering those parameter values which were used to produce Fig. 11.9.e.II, the simulation of the set of clinical data shown in Fig. 11.9.e.I. These effects may of course be illustrated in a number of ways. Here we will begin with graphical ones and then move on to analytical ones, insofar that is as analytical descriptions have been worked out so far.

Firstly, then, consider Figures 11.9.g.I - V, which present the results of five program runs in which only one of the parameters has had its value changed from that used in the "basic" simulation, Fig. 11.9.e.II. The first two charts show the results of increasing the activation energy W_m. The third shows the effects of increasing the appendageal shunt conductivity CO, the fourth illustrates the result of decreasing P1, for example by reducing the charge carrier density, and the fifth shows the consequences of increasing the entropy unit value.

The effects of these changes upon the values of R_o, f_p and m to be used in the best-fit Cole equation for each simulation have been abstracted in Table 11.9.g.A for convenience, since in fact it will probably be best only to examine the charts cursorily until the remainder of this subsection has been read.

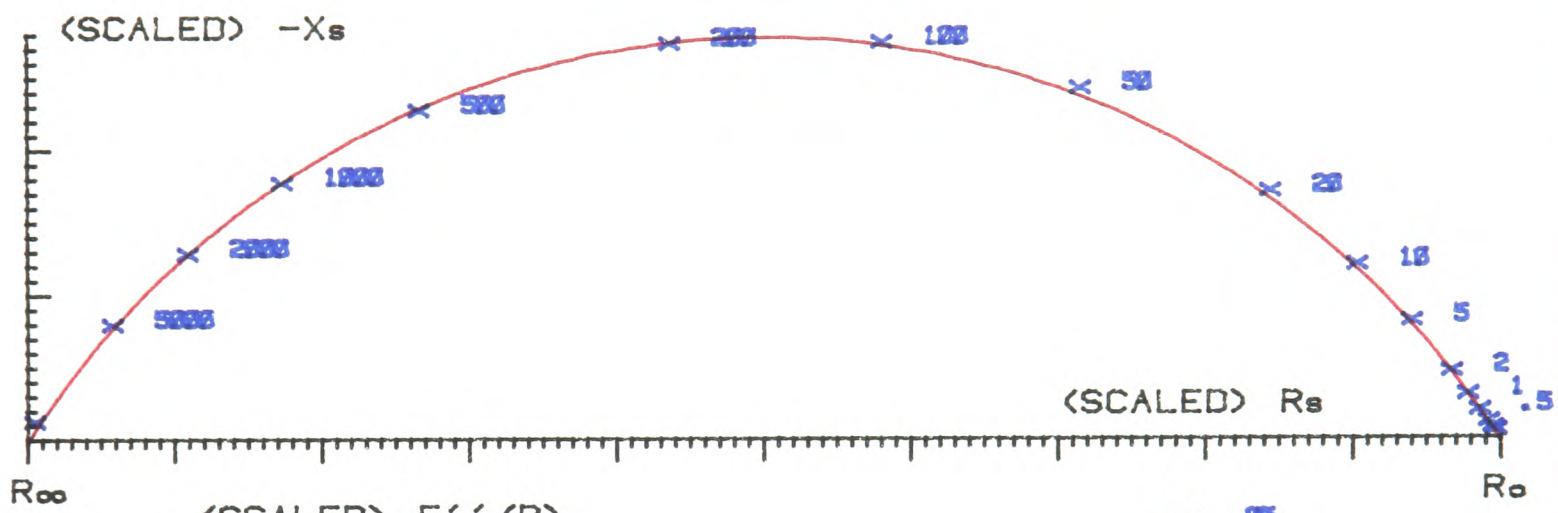
Now let us proceed to derive equations which predict the effects illustrated by the charts and by the Table.

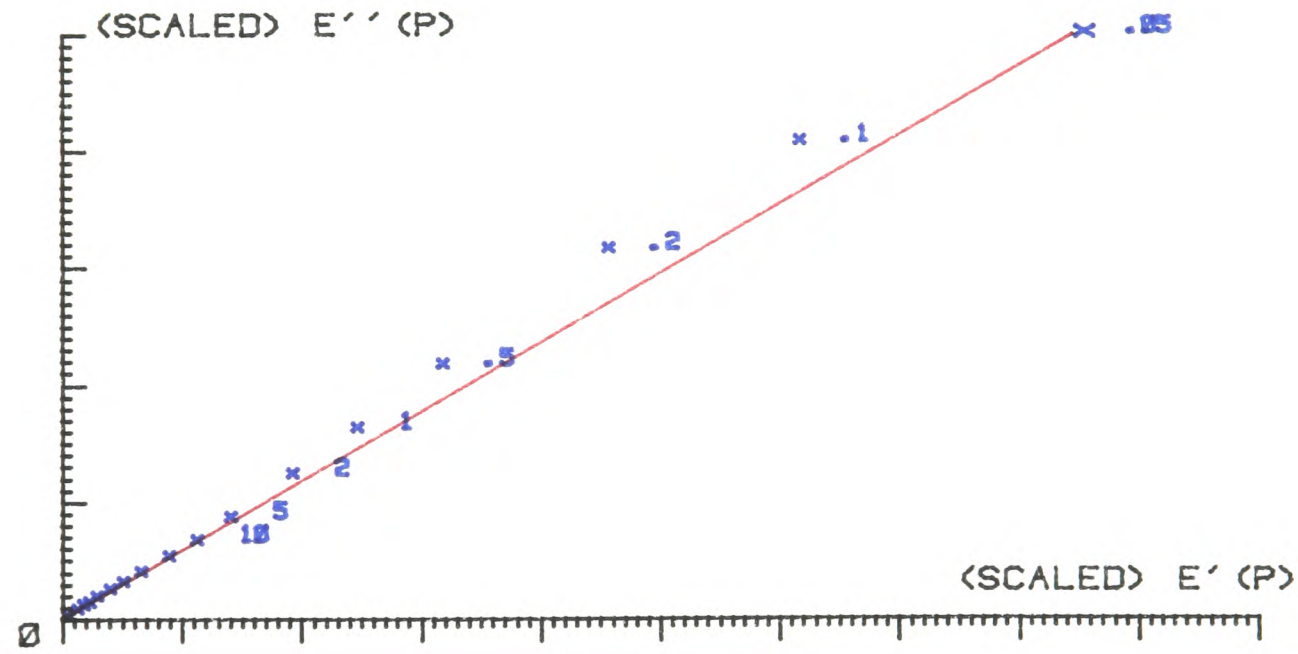
Firstly, we may expect that the D.C. conductivity of the model, σ_o, will be the sum of the conductivity of shunt pathways, σ_{shunts}, plus the conductivity which results from charge carriers percolating all the way across the system by means of the continuous-time random walk, $\sigma_{CTRW\ percolation}$. Thus

BEHAVIOUR OF THE SHUNTED C.T.R.W.- PIKE MODEL FOR

ENTROPY UNITS	=	36
W(MAX)	=	.5
W(PEAK)	=	.486428
PREFACTOR C	=	.00001
TEMPERATURE	=	300
C(ZERO)	=	1.20000E-08
P1	=	.0001

Fig. 11.9.g.I





			+PSE	+/-SE	-PSE
NO. OF DATA PAIRS	=	17			
R(ZERO)	=	81359.8		256.322	
R(INFINITY)	=	328.398		256.322	
F(PEAK) [USING M1]	=	147.042	17.2105		15.4072
F(PEAK) [USING M2]	=	147.077	1.29569		1.28439
E'' [E'=0]	=	3.49898E-10		4.10066E-11	
'U'	=	1.17189E-07	8.64457E-10		8.58128E-10
M1 FROM Z LOCUS	=	.350177		3.30344E-03	
M2 FROM V/U PLOT	=	.355364		1.13322E-03	
M3 FROM E* LOCUS	=	.338884		1.19075E-03	
M4 FROM LN E'' PLOT	=	.347234		9.79198E-04	
& WEIGHTED MEAN M	=	.347506		3.59005E-03	

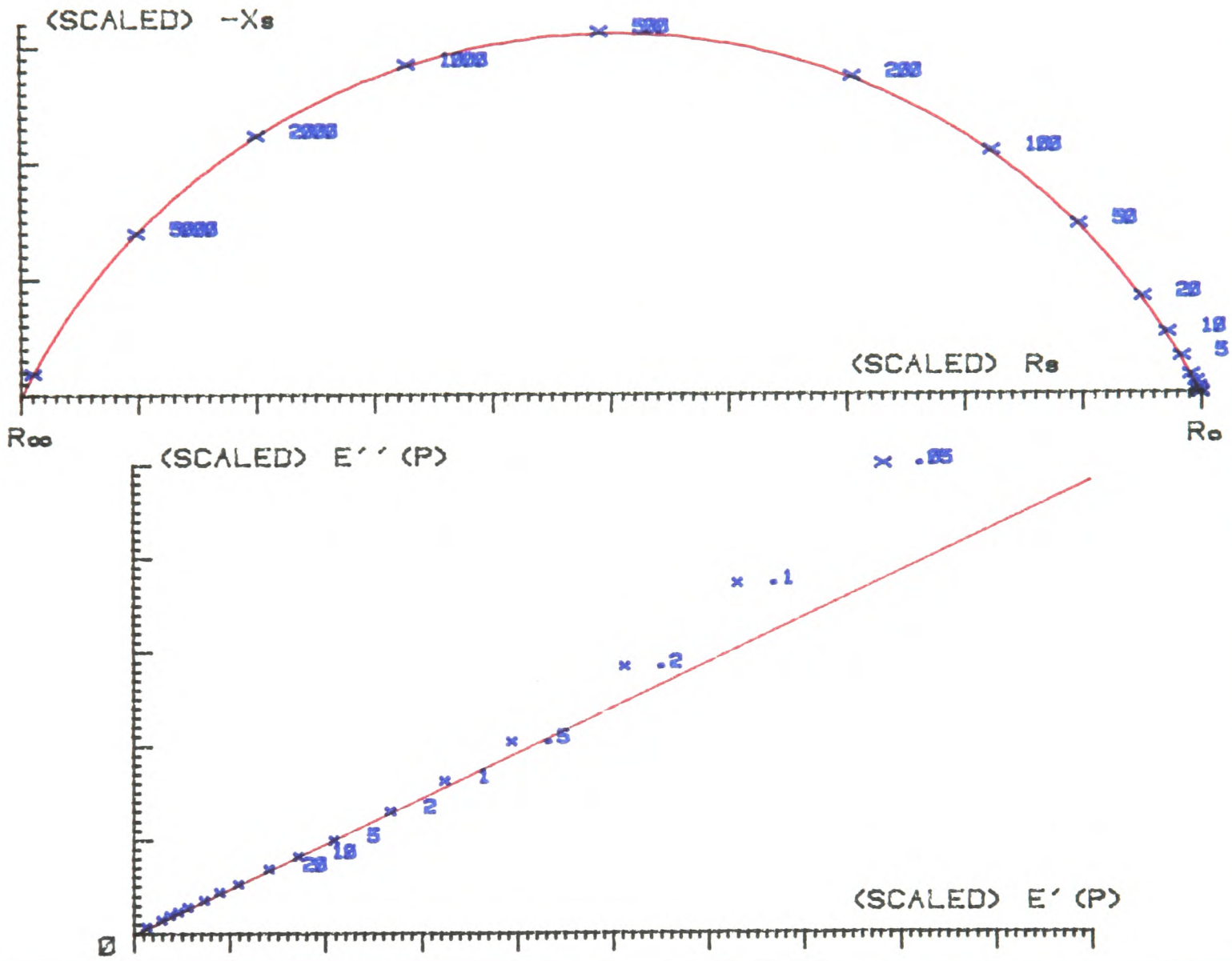
SINCE COMPARING M1 WITH M2, M3 AND M4 RESPECTIVELY,
THE SIGNIFICANCE OF THE DIFFERENCE BETWEEN THE MEANS IS
0.10 < P 0.10 < P AND 0.10 < P

COEFF. DET. OF (UNWEIGHTED) Z ARC FIT	=	.999968
COEFF. DET. OF (WEIGHTED) V/U PLOT	=	.999954
COEFF. DET. OF (WEIGHTED) E* LINE FIT	=	.99921

BEHAVIOUR OF THE SHUNTED C.T.R.W.- PIKE MODEL FOR

ENTROPY UNITS	=	38
W(MAX)	=	.6
W(PEAK)	=	.586428
PREFACTOR C	=	.00001
TEMPERATURE	=	300
C(ZERO)	=	1.20000E-08
P1	=	.0001

Fig. 11.9.g.II



			+PSE	+/-SE	-PSE
NO. OF DATA PAIRS	=	17			
R(ZERO)	=	83296.6		11.4837	
R(INFINITY)	=	15.3386		11.4837	
F(PEAK) [USING M1]	=	481.214	17.2073		16.6133
F(PEAK) [USING M2]	=	481.2	4.02307		3.98975
E'' [E'=0]	=	2.90537E-12		6.09876E-10	
'U'	=	3.43683E-08	8.11398E-10		7.92684E-10
M1 FROM Z LOCUS	=	.286455		1.50911E-04	
M2 FROM V/U PLOT	=	.286797		9.49485E-04	
M3 FROM E* LOCUS	=	.286341		4.90006E-02	
M4 FROM LN E'' PLOT	=	.286589		2.70618E-03	
& WEIGHTED MEAN M	=	.286464		3.07819E-05	

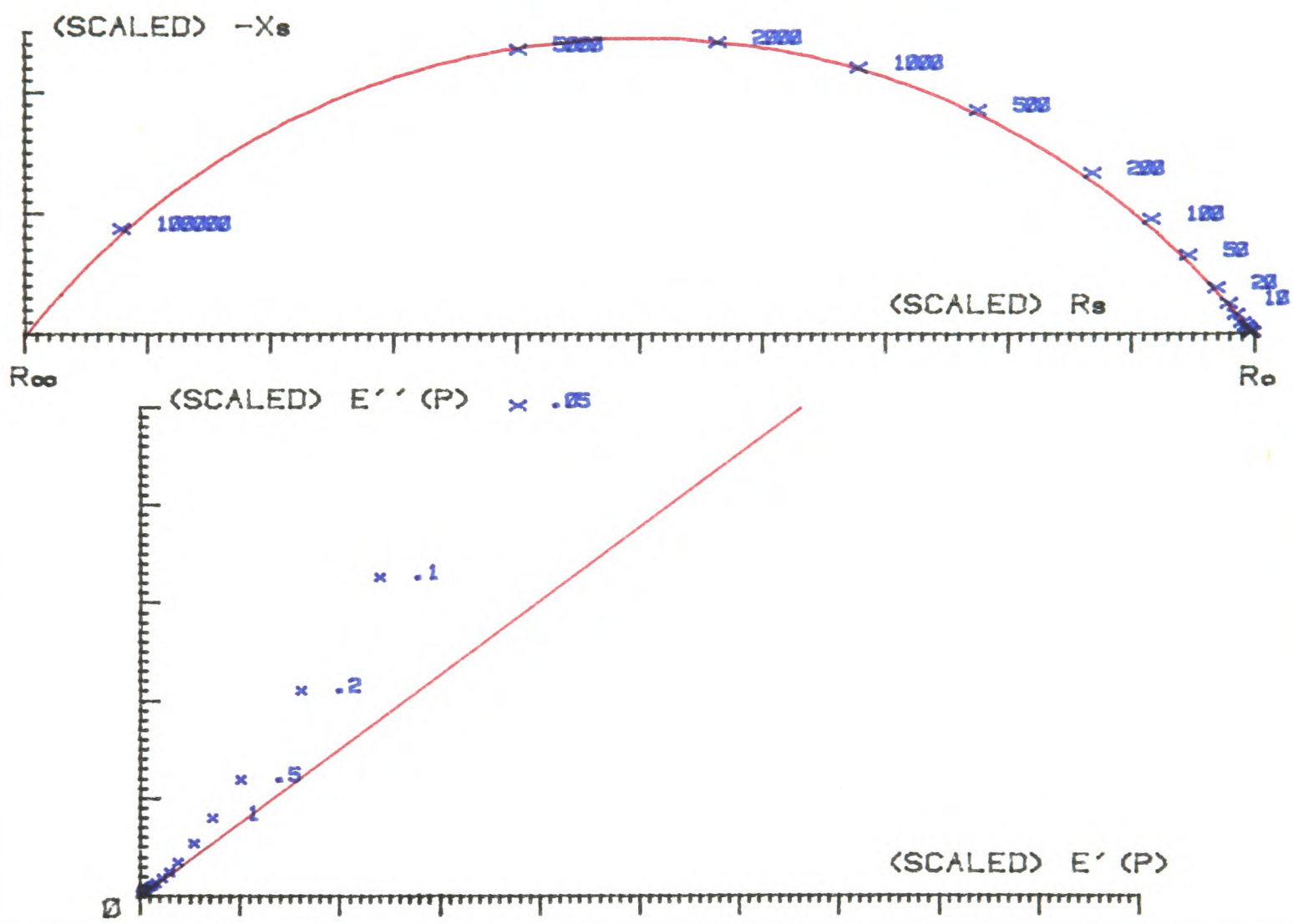
SINCE COMPARING M1 WITH M2, M3 AND M4 RESPECTIVELY,
THE SIGNIFICANCE OF THE DIFFERENCE BETWEEN THE MEANS IS
0.10 < P 0.10 < P AND 0.10 < P

COEFF. DET. OF (UNWEIGHTED) Z ARC FIT	=	1
COEFF. DET. OF (WEIGHTED) V/U PLOT	=	1
COEFF. DET. OF (WEIGHTED) E* LINE FIT	=	.999988

BEHAVIOUR OF THE SHUNTED C.T.R.W.- PIKE MODEL FOR

ENTROPY UNITS	=	36
W(MAX)	=	.45
W(PEAK)	=	.436428
PREFACTOR C	=	.00001
TEMPERATURE	=	300
C(ZERO)	=	1.20000E-07
P1	=	.0001

Fig. 11.9.g.III



			+PSE	+/-SE	-PSE
NO. OF DATA PAIRS	=	17			
R(ZERO)	=	8215.55		61.2267	
R(INFINITY)	=	60.8818		61.2267	
F(PEAK) [USING M1]	=	2841.39	761.208		600.369
F(PEAK) [USING M2]	=	2847.37	40.0806		39.5249
E''[E'=0]	=	1.59885E-10		1.68339E-11	
'U'	=	3.00721E-07	7.29018E-09		7.11764E-09
M1 FROM Z LOCUS	=	.415051		6.74410E-03	
M2 FROM V/U PLOT	=	.423797		1.02793E-03	
M3 FROM E* LOCUS	=	.412042		9.90576E-04	
M4 FROM LN E'' PLOT	=	.418116		2.39754E-03	
& WEIGHTED MEAN M	=	.417709		3.23816E-03	

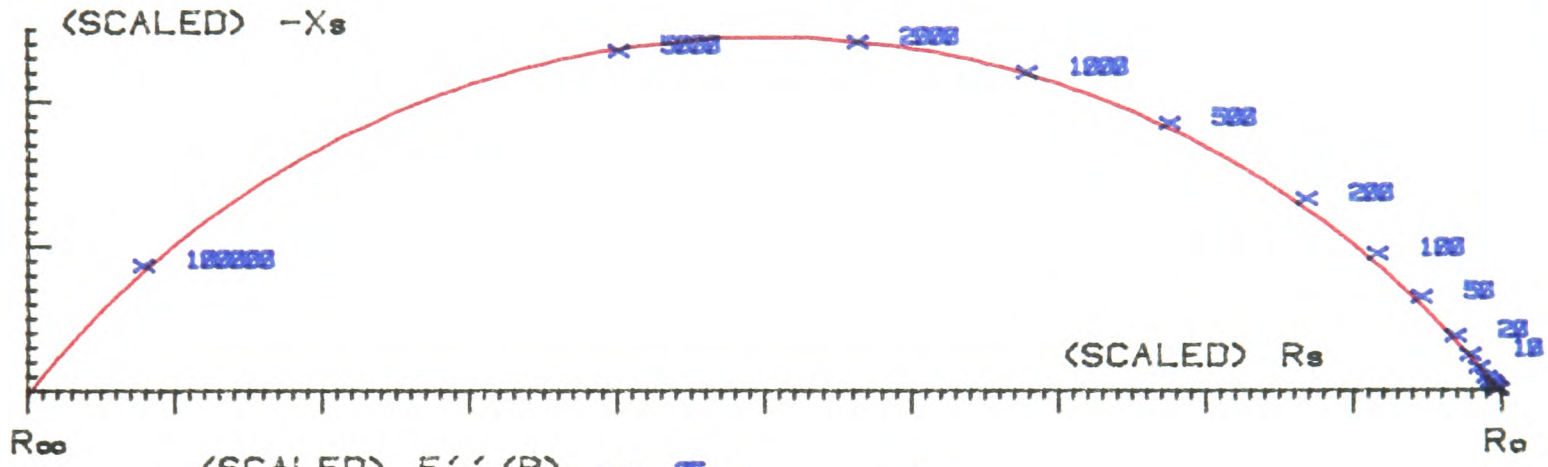
SINCE COMPARING M1 WITH M2, M3 AND M4 RESPECTIVELY,
THE SIGNIFICANCE OF THE DIFFERENCE BETWEEN THE MEANS IS
0.10 < P 0.10 < P AND 0.10 < P

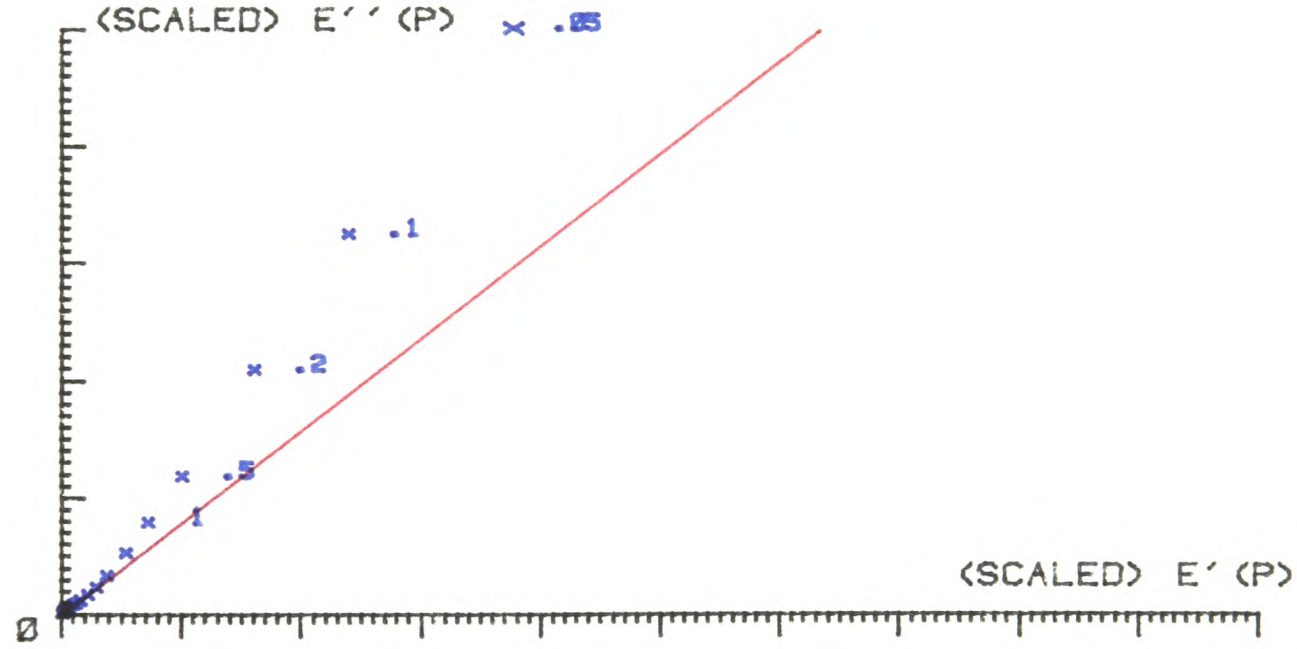
COEFF. DET. OF (UNWEIGHTED) Z ARC FIT	=	.999812
COEFF. DET. OF (WEIGHTED) V/U PLOT	=	.999952
COEFF. DET. OF (WEIGHTED) E* LINE FIT	=	.999725

BEHAVIOUR OF THE SHUNTED C.T.R.W.- PIKE MODEL FOR

ENTROPY UNITS	=	36
W(MAX)	=	.45
W(PEAK)	=	.436428
PREFACTOR C	=	.00001
TEMPERATURE	=	300
C(ZERO)	=	1.20000E-08
P1	=	.00001

Fig. 11.9.g.IV





			+PSE	+/-SE	-PSE
NO. OF DATA PAIRS	=	17			
R(ZERO)	=	82155.5		612.224	
R(INFINITY)	=	608.813		612.224	
F(PEAK) [USING M1]	=	2841.39	761.161		600.34
F(PEAK) [USING M2]	=	2847.38	52.1787		51.2397
E'' [E'=0]	=	0		0	
'U'	=	3.00566E-08	1.06748E-09		1.03087E-09
M1 FROM Z LOCUS	=	.415051		6.74364E-03	
M2 FROM V/U PLOT	=	.423815		1.33534E-03	
M3 FROM E* LOCUS	=	.424723		1.00000E-08	
M4 FROM LN E'' PLOT	=	.418035		3.49318E-03	
& WEIGHTED MEAN M	=	.424723		1.43592E-08	

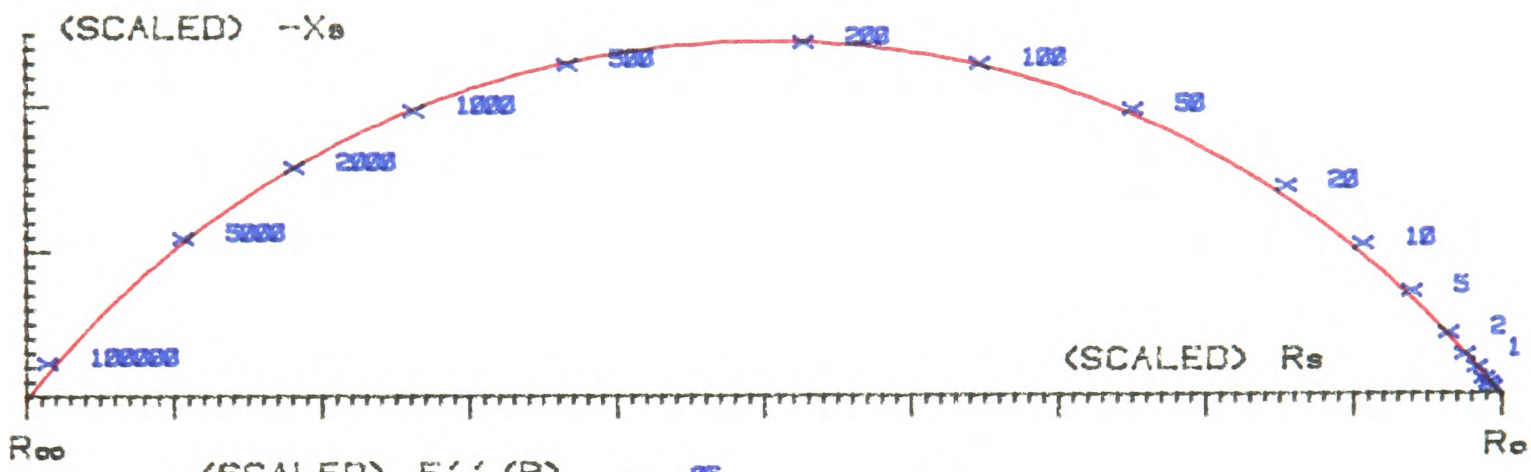
SINCE COMPARING M1 WITH M2, M3 AND M4 RESPECTIVELY,
THE SIGNIFICANCE OF THE DIFFERENCE BETWEEN THE MEANS IS
0.10 < P 0.10 < P AND 0.10 < P

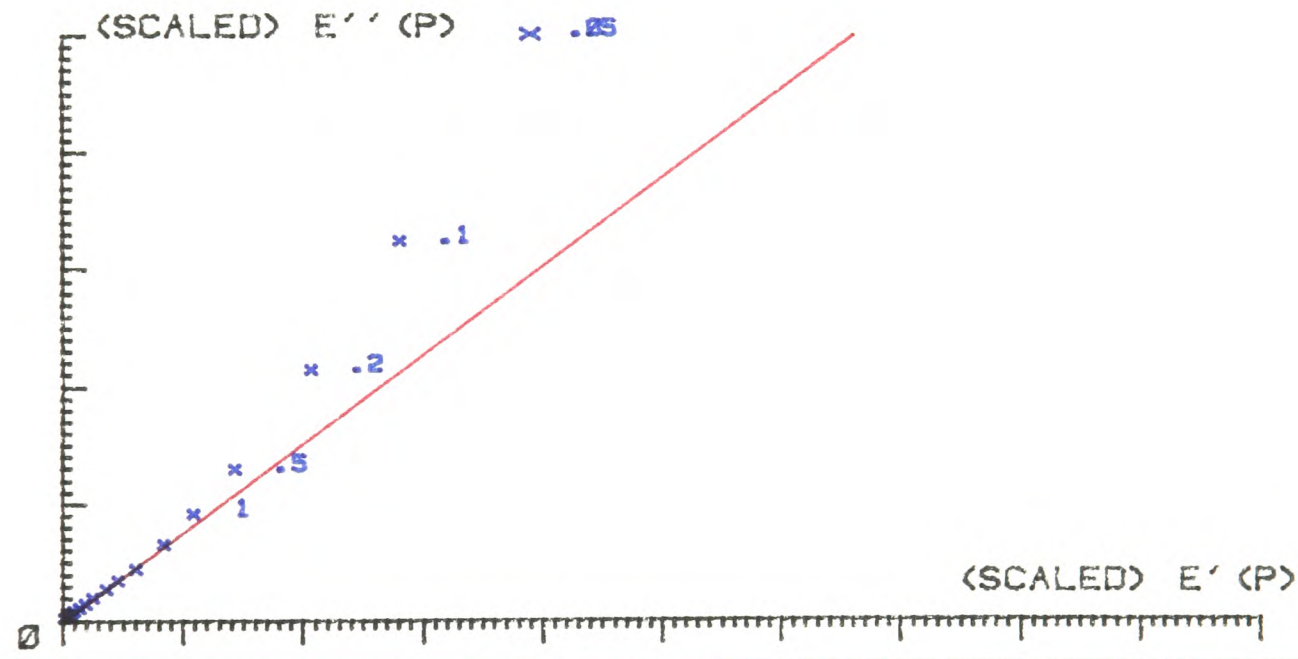
COEFF. DET. OF (UNWEIGHTED) Z ARC FIT	=	.999812
COEFF. DET. OF (WEIGHTED) V/U PLOT	=	.999919
COEFF. DET. OF (WEIGHTED) E* LINE FIT	=	1

BEHAVIOUR OF THE SHUNTED C.T.R.W.- PIKE MODEL FOR

ENTROPY UNITS	=	40
W(MAX)	=	.45
W(PEAK)	=	.436428
PREFACTOR C	=	.00001
TEMPERATURE	=	300
C(ZERO)	=	1.20000E-08
P1	=	.0001

Fig. 11.9.g.V





			+PSE	+/-SE	-PSE
NO. OF DATA PAIRS	=	17			
R(ZERO)	=	81798		593.167	
R(INFINITY)	=	482.46		593.167	
F(PEAK) [USING M1]	=	230.838	39.232	33.5329	
F(PEAK) [USING M2]	=	231.033	1.51193	1.50211	
E'' [E'=0]	=	1.50568E-10		2.24335E-11	
'U'	=	1.30513E-07	5.03482E-09	4.84780E-09	
M1 FROM Z LOCUS	=	.414851		6.78968E-03	
M2 FROM V/U PLOT	=	.422834		6.95050E-04	
M3 FROM E* LOCUS	=	.412124		1.24926E-03	
M4 FROM LN E'' PLOT	=	.419224		4.70539E-03	
& WEIGHTED MEAN M	=	.420242		2.61131E-03	

SINCE COMPARING M1 WITH M2, M3 AND M4 RESPECTIVELY,
THE SIGNIFICANCE OF THE DIFFERENCE BETWEEN THE MEANS IS
0.10 < P 0.10 < P AND 0.10 < P

COEFF. DET. OF (UNWEIGHTED) Z ARC FIT	=	.999882
COEFF. DET. OF (WEIGHTED) V/U PLOT	=	.999978
COEFF. DET. OF (WEIGHTED) E* LINE FIT	=	.999564

Table 11.9.g.A

Fig.	11.9.e.II	11.9.g.I	11.9.g.II	11.9.g.III	11.9.g.IV	11.9.g.V
E.U.	36	36	36	36	36	40
W_m	0.45	0.5	0.6	0.45	0.45	0.45
C0	$1.2x10^{-8}$	$1.2x10^{-8}$	$1.2x10^{-8}$	$1.2x10^{-7}$	$1.2x10^{-8}$	$1.2x10^{-8}$
P1	$1.0x10^{-4}$	$1.0x10^{-4}$	$1.0x10^{-4}$	$1.0x10^{-4}$	$1.0x10^{-5}$	$1.0x10^{-4}$
RESULTS:						
R_o	71,683	81,360	83,297	8,215.6	82,156	81,798
f_p	74.185	147.08	481.20	2847.4	2847.4	231.03
M1	0.3879	0.3502	0.2865	0.4151	0.4151	0.4149

$$\sigma_o = \sigma_{shunts} + \sigma_{CTRW\ percolation} \qquad (11.9.g.1)$$

and this turns out to be given in terms of the model parameters by

$$\sigma_o = CO + A1.\ \frac{P1}{T}\ [T1.\ \exp\ (W_p/kT)]^{-1} \qquad (11.9.g.2)$$

where A1 must be determined numerically, but is usually of the order of unity.

At non-zero frequencies the total conductivity will be increased by the contribution of charge carriers relaxing between the temporary trapping sites of the CTRW system; this corresponds of course to dielectric relaxation. Indeed the model predicts a dielectric loss peak as can be seen from the lower graphs on the series of charts presenting the "processed" complex permittivity locus ("processed" such that the effect of D.C. conductivity has been subtracted off). For sets of model parameters which will give results acceptably close to the Cole equation, the extra conductivity contribution $\sigma_{CTRW\ percolation}$ must come from carriers in the low-activation-energy tail of the Pike distribution, and we may then write the entire complex conductivity of the model as

$$\sigma^* = \sigma_o + j\omega\ .\ A2.\ \frac{P1}{T}\ [j\omega.\ T1.\ \exp\ (W_p/kT)]^{\alpha-1} \qquad (11.9.g.3)$$

where A2 and α are approximately independent of frequency, and σ_o can be obtained from the previous equation. Consequently if we make use of the "skin dimensions correction factor" D ≐ 1000 to convert conductivity into conductance (cf. subsection 11.9.d), we may write the complex impedance of the model as

$$Z = \frac{\frac{1}{D.\sigma_o}}{1 + \frac{A2.P1}{\sigma_o.T}\ [T1.\exp\ (W_p/kT)]^{\alpha-1}\ (j\omega)^{\alpha}} \qquad (11.9.g.4)$$

which corresponds to the Cole equation with

$$m = 1 - \alpha \qquad (11.9.g.5)$$

$$R_\infty = 0 \qquad (11.9.g.6)$$

$$R_o = \frac{1}{D.\sigma_o} \qquad (11.9.g.7)$$

and

$$\omega_{peak} = \left[\frac{\sigma_o.T}{A2.P1\ [T1.\ \exp\ (W_p/kT)]^{\alpha-1}} \right]^{\frac{1}{\alpha}} \qquad (11.9.g.8)$$

or using $\omega_{peak} = 2\pi f_p$, (11.9.g.2) and (11.9.g.5),

$$f_p = \frac{1}{2\pi}\left[\frac{CO.T}{A2.P1} [T1.\ \exp\ (W_p/kT)]^m + \frac{A1}{A2} [T1.\exp\ (W_p/kT)]^{\ m-1} \right]^{\frac{1}{1-m}} \qquad (11.9.g.9)$$

By differentiating this we can see that f_p will increase as W_m is decreased if

$$CO < \frac{(1-m)}{m} A1.\ \frac{P1}{T}\ [T1.\ \exp\ (W_p/kT)]^{-1} \qquad (11.9.g.10)$$

or using (11.9.g.2) and (11.9.g.7), if

$$CO < \frac{(1-m)}{D.R_o} \qquad (11.9.g.11)$$

Conversely of course if CO is greater than the right-hand-side of (11.9.g.11) then f_p will decrease as W_m is decreased.

We may estimate the goodness-of-fit to the Cole equation produced by any particular set of model parameters by calculating the value of an empirical "shape index" S, since it is found that in general the goodness-of-fit increases with increase in S, where

$$S = \frac{T.\ CO.\ Tl.\ \exp\ (W_p/kT)}{Al.\ Pl} = \frac{D.\ R_o.\ CO}{(1-\ D.R_o.CO)} \qquad (11.9.g.12)$$

and to obtain a close fit it is usually advisable to require that

$$S \geq 7 \qquad (11.9.g.13)$$

For those sets of model parameters which give a close fit to the Cole equation, the value of m (corresponding to the value of Ml on the charts) is given by

$$m = \frac{4akT}{W_m} \qquad (11.9.g.14)$$

where a is an approximately constant multiplying factor related to some average value of x in (11.9.b.37); such an averaging process is inherent in fitting the simulation results by a circular arc on the complex impedance plane, but it has not yet been possible to define the process analytically. For example however, with the model parameters employed in the "basic" simulation, Fig. 11.9.e.II, but using W_m = 0.45, 0.5, 0.55 ... 0.7 eV, it was found that

$$a = 1.6731 \pm 0.0115 \quad (n = 6) \qquad (11.9.g.15)$$

where the quoted non-zero standard error of "a" results from the non-zero standard errors of the Ml values obtained from least-squares fitting of the R, X data pairs to a circular arc on the complex impedance plane.

11.9.h The quantity "m" as an index of skin hydration

We have already had frequent cause to remember the observation, discussed in subsection 9.3.c, that m tends to increase with increase in the hydration of the corneum. This subsection has been written to point out how simply the shunted CTRW-Pike model can interpret this phenomenon.

In subsection 11.4.d we reviewed theories of the increase in conductivity of proteins caused by hydration, and concluded that hydration probably affected the keratins of the corneum according to a modified version of the theory of Rosenberg (1962), whereby the activation energy for semiconduction through the corneum is reduced by an increase in the effective dielectric permittivity in the corneum. This increase in permittivity is a result of an increase in water content together with the fact that the permittivity of water is much higher than that of dry protein.

Applying these ideas to the CTRW-Pike theory leads us to expect something of the form

$$W_{mw} = W_{md} - \frac{q^2}{kTR}\left[\frac{1}{\varepsilon_d} - \frac{1}{\varepsilon_d + h\,(\varepsilon_{sat} - \varepsilon_d)}\right] \qquad (11.9.h.1)$$

following the same type of notation as was used earlier in my semi-empirical equation (11.4.d.5). We can at least begin to construct a hydration-dependent shunted CTRW-Pike model by replacing every use of W_m in the old model with W_{mw} instead, representing the value of W_m in maximally hydrated conditions. This would then predict a new equation for m

$$m = \frac{4akT}{W_{mw}} \qquad (11.9.h.2)$$

from which it can be seen that *as hydration increases the denominator will decrease and m will increase, as is observed experimentally.*

I think that this interpretation of the increase of m with increase in hydration is physically more plausible than that offered in subsection 11.8.e, requiring as it does the "filling out" of the bandtail in just the right manner.

Finally, we noted in subsection 10.3.a that m tends to be very significantly increased in active psoriatic lesions, and so does trans-epidermal water loss (see e.g. Grice, 1980), and therefore presumably corneum water content too. Perhaps we may now be in a position to understand why this potentially very useful correlation occurs, and perhaps also people will begin to use it. As I have noted before (e.g. Salter, 1981), it will certainly be clinically beneficial if m can serve as a non-invasive index of some epidermal cell kinetic parameter.

11.9.i Conclusions

This Chapter has presented what so far as I know is by far the most extensive theoretical review of the linear electrical properties of skin that has been written to date. Its purpose has been to show that all the previously available models of these properties of skin were inadequate, but that it is however possible to develop an adequate model if one begins from a more rigorous foundation, namely the CTRW formalism, and then makes use of some of the recent developments in solid-state physics. Indeed this approach led to not one but two very interesting models, the shunted CTRW-double-bandtail model and the shunted CTRW-Pike model. For both of these, we may conclude the following.

Firstly, using these models it is possible to produce results which are very well fitted by the Cole equation, and this we know already (see Section 9.5) is an excellently accurate description of the linear electrical properties of skin.

Secondly, such a good fit is moreover obtainable from these models up to **higher** values of m than can be obtained from all others, excepting only the entirely ad hoc Clar model. Such higher values of m are necessary in order to fit clinical data.

Thirdly, all the model parameters required to achieve a close *quantitative* fit to clinical data have quite reasonable values.

Fourthly, both theories underlying these models provide simple interpretations of the observation that m increases as the hydration of the corneum increases (see subsections 11.8.f and 11.9.h for these interpretations).

Fifthly, the other general advantages of the shunted CTRW-double-bandtail model (which were discussed in subsection 11.8.f) are shared by the CTRW-Pike model, namely the obedience of each cell layer of the corneum to the Cole

equation, the apparent independence of m and R_o when shunting is appreciable, e.g. if (11.9.g.13) is obeyed, with the further advantage in the latter model that R_o and m need not always be independent - altering W_m, for example by hydration, will reduce R_o (see (11.9.g.2) and (11.9.g.7)) while also increasing m (see (11.9.g.14). Finally, there is the finding that m is significantly different in psoriatic skin (subsection 10.3.a), a fact that on the basis of the shunted CTRW-Pike model would be attributable to the greater transepidermal water loss and thus corneum water content in such skin (see subsection 11.9.h).

These considerations, which summarize the evidence we have examined at some length in this Chapter, should consequently be sufficient to establish both the shunted CTRW-double-bandtail model and the shunted CTRW-Pike model as being *very much better than any other available theoretical model of the linear electrical properties of skin.*

However, there are further considerations which should I believe lead us to prefer the shunted CTRW-Pike model to the shunted CTRW-double-bandtail model. These further advantages of the shunted CTRW-Pike model are as follows.

Sixthly, the applicability of the CTRW-Pike theory is independent of the type of charge carrier in the skin, and this lack of restriction is very desirable (see subsection 11.9.a).

Seventhly, the CTRW-Pike model does not depend upon an empirical DRT, but one which is entirely derivable from known physical principles.

Eightly, the Pike theory provides a simple interpretation of why in skin it is always found that

$$1 > m > 0 \qquad (11.9.i.1)$$

namely, that

$$4akT \; < \; W_m \; < \; \infty \qquad (11.9.i.2)$$

which I think is more likely than that neo-experimental bandtails should always have a density-of-states g which stays between the limits

$$C \; > \; g\ (\Delta E/kT) \; > \; C \exp\ (-\tfrac{1}{2}\ \Delta E/kT) \qquad (11.9.i.3)$$

since the right-hand one (corresponding to m = o) seems especially arbitrary. (Of course in some systems other than skin, values of α greater than unity have been reported (see e.g. Lewis, 1977, p.186), and this might follow either from the relaxation of the right-hand limit in (11.9.i.3), or, on the basis of the CTRW-Pike theory, if $W_m < 4akT$).

Thus, taking all these points into consideration, the shunted CTRW-Pike model is likely to be a substantial step forward in the search for an accurate and yet physically fundamental model with which to interpret the linear electrical properties of human skin.